CALIFORNIA INSTITUTE OF TECHNOLOGY

DANIEL AND FLORENCE GUGGENHEIM JET PROPULSION CENTER

NONLINEAR BEHAVIOR OF ACOUSTIC WAVES IN COMBUSTON CHAMBERS

F. E. C. Culick

April 1975

NONLINEAR BEHAVIOR OF ACOUSTIC WAVES IN COMBUSTION CHAMBERS

by

F. E. C. Culick

Professor of Engineering

This work was supported partly by Hercules, Inc., Magna, Utah; by Aerojet General Solic Propulsion Co., Sacramento, California; and by the National Aeronautics and Space Administration under the Jet Propulsion Laboratory Contract NAS 7-100.

JPL W.O. 614496

April 1975

Daniel and Florence Guggenheim Jet Propulsion Center

California Institute of Technology

Pasadena, California

TABLE OF CONTENTS

NOMENCLATURE

Some symbols defined in the text and used but briefly are not included here.

a^2	$\bar{\gamma}p/\rho$ speed of sound for the mixture
$\bar{a}^2$	$\bar{\gamma}p_o/\rho_o$ average speed of sound for the mixture
a_{ij}	equation (4.31a)
A_n	equation (4.3)
A_{nij}	equations (3.47) and (3.58)
G_n	amplitude defined by equation (4.4a)
b_{ij}	equation (4.31b)
B_n	equation (4.3)
B_{nij}	equations (3.48) and (3.59)
c_{ij}	equation (4.31c)
C	specific heat of particulate material
C_p, C_v	specific heats of gases
$\bar{C}_p, \bar{C}_v$	specific heats of gas/particle mixture, equation (2.3)
C_{nij}	equation (4.32)
d_{ij}	equation (4.31d)
D_{ni}	equation (4.2)
D_{nij}	equation (4.33)
e_o	stagnation internal energy of gases
e_{po}	stagnation internal energy of particulate material
E_ℓ^2	equation (3.18)
E_n^2	equation (3.16)
f_s	equation (3.4)
f_μ	equation (3.5)
f_ϵ	equation (3.6)

f_v	equation (3.7)
f_{ls}	equation (3.22)
$f_{l\mu}$	equation (3.23)
$f_{l\epsilon}$	equation (3.24)
f_{lw}	equation (3.25)
f_{ni}	equation (4.20)
$F_n^{(c)}$	equations (7.1) and (7.8)
$F_n^{(p)}$	equation (8.1)
$\vec{F}_p$	equations (2.5) and (8.2)
$\delta\vec{F}_p$	equation (2.8)
g_{ni}	equation (4.21)
h_μ	equation (3.1)
h_ϵ	equation (3.2)
h_v	equation (3.3)
$h_{l\mu}$	equation (3.19)
$h_{l\epsilon}$	equation (3.20)
h_{lw}	equation (3.21)
h_{ni}	equation (4.22)
H	equation (3.30)
H_l	equation (3.31)
I_ϵ	equation (3.43)
I_{nij}	equation (3.52)
k	complex wavenumber $k = (\omega - i\alpha)/a_o$
k_ℓ	wavenumber for longitudinal or axial modes
k_n	wavenumber for three-dimensional normal modes

ℓ_{ni}	equation (4.23)
L	length of chamber
L_1	equation (3.32)
m_b	mass flux of gases inward at the burning surface
$m_b^{(p)}$	mass flux of particulate material inward at the burning surface
M_b	Mach number of the gases at the edge of the combustion zone, $\bar{u}_b/a_o$
p	pressure
p_o	average pressure
P	equation (2.11)
P_1	equation (2.14)
q	perimeter of the chamber cross section
Q	heat release by homogeneous reactions
Q_p	equations (2.6) and (8.3)
δQ_p	equation (2.9)
R	mass averaged gas constant
$\bar{R}$	mass averaged gas constant for the gas/particle mixture
R_b	response function, equation (7.4)
$\mathcal{R}$	equations (3.42), (7.2), and (7.7)
S_b	total area of burning surface
S_c	cross section area
S_1	equation (2.15)
T	temperature of gases in the chamber
T_p	temperature of particulate material
T_s	temperature of gases at the edge of the combustion zone
ΔT	$T-T_s$

$T_{1\pm}^{n_{ij}}$, $T_{2\pm}^{n_{ij}}$, $T_{3\pm}^{n_{ij}}$, $T_{4\pm}^{n_{ij}}$	equations (4.26) - (4.29)
$\vec{u}$	velocity of the gases
$\vec{u}_p$	velocity of the particulate material
u_b	speed of gases entering at the burning surface
v	volume
w_p	rate of conversion of particulate material to gas (mass/vol-sec)
α	attenuation or growth constant
β	equation (6.13)
γ	ratio of specific heats for the gases, C_p/C_v
$\bar{\gamma}$	ratio of specific heats for the gas/particle mixture, $\bar{C}_p/\bar{C}_v$
$\varkappa$	mass fraction of particulate material, ρ_p/ρ_g
η_n	equations (1.6) and (4.3)
ρ	density of the gas/particle mixture, $\rho = \rho_g+\rho_p$
ρ_g	density of the gases
ρ_p	density of the particulate material
ρ_o	average density of the gas/particle mixture
σ	diameter of particles
Σ_l	equation (2.13)
τ_d	equation (8.9)
τ_t	equation (8.10)
ϕ_n	equation (4.2)
ψ_l	normal mode shapes for one-dimensional problems
ψ_n	normal mode shapes for three-dimensional problems
ω_l	angular frequency for one-dimensional normal modes
ω_n	angular frequency for three-dimensional normal modes

NONLINEAR BEHAVIOR OF ACOUSTIC WAVES IN COMBUSTION CHAMBERS

F. E. C. Culick

ABSTRACT

This report is concerned with the general problem of the nonlinear growth and limiting amplitude of acoustic waves in a combustion chamber. The analysis is intended to provide a formal framework within which practical problems can be treated with a minimum of effort and expense. There are broadly three parts. First, the general conservation equations are expanded in two small parameters, one characterizing the mean flow field and one measuring the amplitude of oscillations, and then combined to yield a nonlinear inhomogeneous wave equation. Second, the unsteady pressure and velocity fields are expressed as syntheses of the normal modes of the chamber, but with unknown time-varying amplitudes. This procedure yields a representation of a general unsteady field as a system of coupled nonlinear oscillators. Finally, the system of nonlinear equations is treated by the method of averaging to produce a set of coupled nonlinear first order differential equations for the amplitudes and phases of the modes. These must be solved numerically, but results can be obtained quite inexpensively.

Subject to the approximations used, the analysis is applicable to any combustion chamber. The most interesting applications are probably to solid rockets, liquid rockets, or thrust augmentors on jet engines. The discussion of this report is oriented towards solid propellant rockets.

I. INTRODUCTION

The purpose of this analysis is to develop a suitable framework for studying the growth and limiting amplitude of acoustic waves driven mainly by interactions with combustion processes. Although the emphasis here is on the problem as it arises in solid propellant rocket motors, other cases can be treated in the same way. For example, since sources of mass and energy within the volume are accounted for, unstable waves in liquid rocket motors and engine thrust augmentors may be regarded as special cases. The principal distinguishing features of the solid propellant motor are the source of mass and energy at the boundary, and the non-uniform flow field.

A primary motivation is to produce analytical results which may be used to interpret data. For many practical situations, elaborate numerical computations based on the governing differential equations are inappropriate owing to uncertainties in the required input information. The essential idea pursued here is to convert the governing partial differential equations to a set of ordinary nonlinear differential equations in time, for the amplitudes of the normal modes of the chamber. The way in which this is done is very strongly conditioned by previous work on the linear stability of the normal modes [Culick (1973-1975)] and constitutes a development and extension of recent work on nonlinear behavior, Culick (1971). The precursor of this work was based on the observation that an oscillatory motion in a solid propellant motor very often exhibits quite clean sinusoidal behavior even when the amplitude attains a limiting value much larger than those at which nonlinear effects are clearly evident in, for example, acoustic resonance tubes driven at room temperature. This suggested that the acoustic field might be represented approximately in the form of a standing wave having time-dependent amplitude,

$$\frac{p'}{p_o} \approx \eta(t)\psi(\vec{r}) \tag{1.1}$$

$$\vec{u}' \approx \frac{\dot{\eta}(t)}{\bar{\gamma}k^2} \nabla\psi(\vec{r}) \tag{1.2}$$

where $k = \omega/\bar{a}$ is the wavenumber. The true wave structure in space is distorted by fractional amounts of the order of the Mach number of the mean flow, which, as shown by Culick (1971), need not be explicitly determined within the approximations used. The problem comes down to finding the amplitude $\eta(t)$. Thus, the unstable wave is regarded as one having a fixed shape in space, but the amplitude varies in time. For example, if one examines the fundamental mode of a T-burner, $\psi = \cos(z/L)$ and the mid-plane of the chamber is always a nodal plane.

The argument in the earlier work led to the nonlinear equation for η,

$$\ddot{\eta} + \omega^2\eta + \dot{\eta}f(\eta, \dot{\eta}) = 0 \tag{1.3}$$

where, partly by assumption and partly from the analysis

$$f(\eta, \dot{\eta}) = -2\alpha + \beta_1|\eta| + \beta_2\eta^2 + \gamma_1|\dot{\eta}| + \gamma_2|\dot{\eta}|^2 \tag{1.4}$$

Equation (1.3) describes, as one would anticipate on physical grounds, a nonlinear oscillator, and it is often possible to attach a physical interpretation to the coefficients α, β_1, β_2, γ_1, γ_2.

Approximate solutions to Equation (1.3) have been constructed both by the method of averaging, Krylov and Bogoliubov (1947), Bogoliubov and Mitropolsky (1961), and by expansion in two time variables, Kevorkian (1966). Although differing in certain details - for example, higher approximations are more easily constructed by using two time variables - the results obtained by the two methods are equivalent. In either case, the first approximation has the form

$$\eta(t) = \mathcal{A}(t)\sin(\omega t + \varphi(t)) \tag{1.5}$$

The amplitude $\mathcal{A}(t)$ exhibits the correct gross behavior; during growth, $\mathcal{A}(t)$ increases from an arbitrarily small value, progressing through a period of linear behavior ($\mathcal{A} \sim \exp(\alpha t)$), and ultimately leveling off at some limiting value determined by the coefficients in $f(\eta, \dot{\eta})$.

However, the approach just described fails in what appears to be an important respect. That is, even to second order in some small parameter characterizing f, no even harmonics are generated. This is not only contrary to observations in solid propellant rockets, and expecially in T-burners, but it cannot be correct if nonlinear effects associated with convection (i.e., those represented mainly by the term $\vec{u} \cdot \nabla\vec{u}$) are present.

It is therefore necessary to construct a new analysis. Because the results based on the simple analysis just described do in fact exhibit some important features of the behavior, it is reasonable to examine modifications and extensions of that approach.

The basic idea here is to permit explicitly, from the beginning, the presence of all possible standing waves. This really amounts to stating that an arbitrary unsteady field can be synthesized of its Fourier components. Equations (1.1) and (1.2) are replaced by the expansions *

$$\frac{p'}{P_o} = \sum_{i=0}^{\infty} \eta_i(t)\psi_j(\vec{r}) \tag{1.6}$$

$$\vec{u}' = \sum_{i=1}^{\infty} \frac{\dot{\eta}_i(t)}{\nabla k_i^2} \nabla\psi_i(\vec{r}) \tag{1.7}$$

The total pressure density and velocity fields are of course average plus fluctuation fields

$$p = \overline{p} + \epsilon p' \tag{1.8}$$

$$\rho = \overline{\rho} + \epsilon \rho' \tag{1.9}$$

$$\vec{u} = \mu\vec{\overline{u}} + \epsilon\vec{u}' \tag{1.10}$$

* The term i=0 in (1.6) is simply $\eta_o(t)$ representing a shift of the average pressure. There is no corresponding velocity fluctuation, so a term i=0 does not appear in (1.7). Only in §10 will the influence of $\eta_o \neq 0$ be accounted for.

where μ is introduced as a dimensionless quantity measuring the magnitude of the near flow speed, and ϵ is similarly a measure of the amplitude of the oscillations. Both μ and ϵ are essentially parameters for bookkeeping (see § 2).

In § 2 the procedure for constructing the nonlinear wave equation is outlined. Mainly the three-dimensional problem is discussed, but some contributions arising from the corresponding one-dimensional analysis will be incorporated. There are two features distinguishing this analysis from previous works treating nonlinear motions in liquid propellant rockets: sources of mass, momentum, and energy at the burning surfaces are included; and the mean flow field is non-uniform.*

The expansions (1.6) and (1.7) are introduced in the nonlinear wave equation, and in § 3 a set of equations for the time-dependent coefficients $\eta_n(t)$. Each equation of this system represents the motion of a simple forced oscillator, where the force F_n depends both linearly and nonlinearly on all the η_i:

$$\frac{d^2\eta_n}{dt^2} + \omega_n^2 \eta_n = F_n(\eta_1, \eta_2, \ldots) \qquad (1.11)$$

If only the linear terms are retained, then one can extract from (1.11) all known results for linear stability analysis. The nonlinear terms arise from the gasdynamics in the chamber, the combustion, and other processes. Only the contribution from the gasdynamics can presently be given simple explicit forms. Owing to the manner in which the problem has been formulated here, many of the nonlinear terms represent coupling between the modes. It should be noted also that terms representing linear coupling arise as well, both from the gasdynamics and from the combustion processes.

*The average pressure, density, and temperature are assumed to be uniform, a realistic approximation to the situation in rocket motors. To treat certain types of thrust augmentors, one must account for nonuniform average temperatures and densities, which can be done within the framework developed in this report.

In §4 an approximate means of solving the set (1.11) is discussed. While it is true that if F_n is given, the coupled equations can be solved numerically, this may be a relatively expensive procedure. The purpose here is to provide a considerably faster and cheaper means of obtaining the information desired. Here the technique used is essentially that termed generically the "method of averaging." It is based on the assumption -- almost always valid for the unstable motions encountered in practice-- that the motions exhibit relatively slowly varying amplitude and phase. Thus, the functions $\eta_n(t)$ are represented as

$$\eta_n(t) = \alpha_n(t)\sin(\omega_n t + \varphi_n(t)) = A_n(t)\sin\omega_n t + B_n(t)\cos\omega_n t \qquad (1.12)$$

According to the basic assumption used, the quantities α_n, φ_n, A_n, B_n suffer only small fractional changes during one period of the oscillation. The analysis then produces coupled first order ordinary differential equations, a system which is cheaper to solve than the system of second order equations.

The system of first order equations is valid for problems in which the frequencies of the higher modes are not necessarily integral multiples of the fundamental frequency. In §4 the general equations are given. As an elementary example, the motions of two coupled pendula is analyzed in §5· this shows the familiar beating of the oscillations, a feature which seems not to have been accommodated by previous applications of the method of averaging.

Many practical problems involve purely longitudinal ("organ pipe") modes, for which the frequencies are integral multiples of the fundamental. The system of nonlinear first order equations simplifies considerably for this case, treated in §6. For applications, it is necessary to incorporate representations of processes responsible for the loss and gain of energy

by the waves. An approximation to the interactions between pressure waves and surface combustion is described in §7. One way of handling the loss of energy due to particles suspended in the gas is covered in §8; the results show favorable comparison with more exact numerical calculations reported elsewhere. In §9, linear and nonlinear viscous losses on an inert surface are examired. Associated with the nonlinear unsteady motions there is also a change in the average pressure; this is discussed in §10.

Several examples of unstable motions in motors and T-burners are covered in §11. The cases have been chosen for comparison with numerical results previously reported; again, the agreement appears to be quite good.

As noted above, the analysis has been strongly motivated by previous work on the linear stability of motions. In §12 the connection is discussed. One of the attractive features of the formulation of the nonlinear behavior is that the more familiar linear results are not merely accommodated, but explicitly incorporated and used. An interesting and important unsolved problem concerns the influence of coefficients characterizing linear behavior on the nonlinear behavior. The coefficients are proportional to the real and imaginary parts of the complex wavenumber computed in the linear analysis. Nonlinear behavior appears to be quite sensitive to their values; a few examples are included in the brief discussion given in §12.2.

Analysis based on expansion in normal modes with time-dependent coefficients have earlier been reported for unsteady motions in liquid propellant rocket motors [e.g. Zinn and Powell (1970), Lores and Zinn (1973) and other works cited there]. Results were obtained for specific problems by solving the second order equations for the amplitudes. Reduction to a set of first order equations was not effected. Thus, the computational costs must be substantially greater. Moreover, interpretation of the formal rep-

sentation, and incorporation of processes such as particle damping and surface heat losses appears to be somewhat more difficult than for the analysis developed here. It is likely that the techniques discussed in the references cited above and those discussed in this report should produce the same second order equations for the same problem. This has not been verified.

II. CONSTRUCTION OF THE NONLINEAR WAVE EQUATION.

The nonlinear wave equation for the pressure is constructed by suitably combining the conservation equations and the equation of state. For applications to solid propellant rocket motors, it is necessary to treat the medium in the chamber as a two-phase mixture of gas and particles. Culick (1974) has outlined the steps necessary to produce the equations for the velocity and pressure

$$\rho \frac{\partial \vec{u}}{\partial t} + \rho \vec{u} \cdot \nabla \vec{u} + \nabla p = \delta \vec{F}_p - \vec{\sigma} \tag{2.1}$$

$$\frac{\partial p}{\partial t} + \vec{u} \cdot \nabla p + \bar{\gamma} p \nabla \cdot \vec{u} = \frac{\bar{R}}{\bar{C}_v} \left[(\vec{u}_p - \vec{u}) \cdot \vec{F}_p + \vec{u} \cdot \vec{\sigma} + (e_{po} - e_o) w_p \right.$$

$$\left. + (Q + \delta Q_p) + (1 + \kappa) \bar{C}_v T w_p \right] \tag{2.2}$$

Here, ρ is the density of the mixture, $\rho = \rho_p + \rho_g$, and κ is the ratio of the mass of particulate matter to the mass of gas in a unit volume of chamber: $\kappa = \rho_p / \rho_g$. It will be assumed throughout that κ is a constant in both space and time. With C the specific heat of the particulate material, the properties of the mixture are:

$$\bar{C}_v = \frac{C_v + \kappa C}{1 + \kappa} \qquad \bar{C}_p = \frac{C_p + \kappa C}{1 + \kappa} \qquad \bar{\gamma} = \frac{\bar{C}_p}{\bar{C}_v}$$

$$\rho = \rho_g (1 + \kappa) \qquad \bar{a}^2 = \bar{\gamma} \bar{R} T = \frac{\bar{\gamma} p}{\rho} \tag{2.3}$$

The equation of state is

$$p = \bar{R}\rho T = \frac{R\rho_g T}{1+\kappa} \tag{2.4}$$

where R is the gas constant for the gas only, and $\bar{R} = \bar{C}_p - \bar{C}_v = R/(1+\kappa)$. Note that $(\bar{\ })$ is used in (2.3) and (2.4) to denote certain material properties of the mixture. Later the same notation will be used to denote time averages of variables.

The force of interaction and heat transfer between the gas and particles is represented by

$$\vec{F}_p = -\left[\rho_p \frac{\partial \vec{u}_p}{\partial t} + \rho_p \vec{u}_p \cdot \nabla \vec{u}_p\right] \tag{2.5}$$

$$Q_p = -\left[\rho_p \frac{\partial e_p}{\partial t} + \rho_p \vec{u}_p \cdot \nabla e_p\right] \approx -\rho_p C\left[\frac{\partial T_p}{\partial t} + \vec{u}_p \cdot \nabla T_p\right] \tag{2.6}$$

The differences between the local values of velocity and temperature are

$$\delta\vec{u}_p = \vec{u}_p - \vec{u} \qquad \delta T_p = T_p - T \tag{2.7}$$

Then the differential force and heat transfer are

$$\delta\vec{F}_p = -\rho_p\left[\frac{\partial \delta\vec{u}_p}{\partial t} + (\vec{u}_p \cdot \nabla\vec{u}_p - \vec{u} \cdot \nabla\vec{u})\right] \tag{2.8}$$

$$\delta Q_p = -\rho_p C\left[\frac{\partial \delta T_p}{\partial t} + (\vec{u}_p \cdot \nabla T_p - \vec{u} \cdot \nabla T)\right] \tag{2.9}$$

All symbols are defined in the list of the end of the report; additional details leading to the forms quoted here may be found in Culick (1974).

The nonlinear wave equation is found from (2.1) and (2.2) as

$$\frac{\partial^2 p}{\partial t^2} - \bar{\gamma}p\nabla \cdot \frac{\nabla p}{\rho} - \bar{\gamma}p\nabla \cdot (\vec{u} \cdot \nabla\vec{u}) - \left[\bar{\gamma}\frac{\partial p}{\partial t}\nabla \cdot \vec{u} + \frac{\partial}{\partial t}(\vec{u} \cdot \nabla p)\right] - \bar{\gamma}p\nabla \cdot \left(\frac{\delta\vec{F}_p - \vec{\sigma}}{\rho}\right) + \frac{\partial P}{\partial t} \tag{2.10}$$

where

$$P = \frac{\bar{R}}{\bar{C}_v}\left[(\vec{u}_p - \vec{u}) \cdot \vec{F}_p + \vec{u} \cdot \vec{\sigma} + (e_{po} - e_o)\, w_p + (Q + \delta Q_p) + (1+\kappa)\bar{C}_v T w_p\right] \tag{2.11}$$

The corresponding results for purely one-dimensional problems [see Culick

(1973, 1974) for further details of the formulation] is

$$\frac{\partial^2 p}{\partial t^2} - \frac{\bar{\gamma} p}{S_c}\frac{\partial}{\partial z}\left(\frac{S_c}{\rho}\frac{\partial p}{\partial z}\right) = \bar{\gamma} p \frac{1}{S_c}\frac{\partial}{\partial z}\left(S_c u \frac{\partial u}{\partial z}\right)$$
$$- \left[\bar{\gamma}\frac{\partial p}{\partial t}\frac{1}{S_c}\frac{\partial}{\partial z}(uS_c) + \frac{\partial}{\partial t}\left(u\frac{\partial p}{\partial z}\right)\right]$$
$$- \gamma p \frac{1}{S_c}\frac{\partial}{\partial z}\left(S_c \frac{\delta F_p - \Sigma_1}{\rho}\right) \qquad (2.12)$$
$$+ \frac{\partial P_1}{\partial t} + \frac{\partial S_1}{\partial t}$$

with

$$\Sigma_1 = (u-u_p)w_p + \frac{1}{S_c}\left[u\int m_b dq + u_p \int m_b^{(p)} dq\right] \qquad (2.13)$$

$$P_1 = \frac{\bar{R}}{\bar{C}_v}\left[(u_p - u)F_p + u\Sigma_1 + (e_{po}-e_o)w_p + (Q+\delta Q_p)\right.$$
$$\left. + (1+\varkappa)\bar{C}_v T w_p\right] \qquad (2.14)$$

$$S_1 = \frac{1}{S_c}\int\left[(1+\varkappa)\bar{\gamma}\bar{R}(T+\Delta T) + \frac{\bar{R}}{2\bar{C}_v}\{u_b^2 - u^2 + \varkappa(u_{pb}^2 - u_p^2)\right]m_b dq$$
$$+ \frac{1}{S_c}\int\left[C\Delta T + \frac{\bar{R}}{2\bar{C}_v}(u_{pb}^2 - u_p^2)\right]\rho_p \delta u_p dq \qquad (2.15)$$

It has been assumed, to obtain the form shown for S_1, that ΔT, the difference between the temperature of the material at the edge of the combustion zone and the average value in the chamber, is the same for both gas and particles. This is not an essential assumption, but is done here to simplify the formulas somewhat. Note that except for extra terms in Σ_1 and S_1, there is a one-to-one correspondence between the terms of (2.10) and (2.12).

There are two ways of proceeding towards soluble problems. A formal expansion procedure can be applied directly to the complete wave equations, (2.10) and (2.11); or the first order equations (2.1) and (2.2)

can be expanded, and the wave equation formed. The results are identical, but because the second calculation is somewhat simpler, it is given here.

Substitute the expansions (1.8) - (1.10) into (2.1) and retain only terms to second order in ϵ to find:

$$\frac{\partial \vec{u}'}{\partial t} + \frac{1}{\bar{\rho}} \nabla p' = -\mu[\vec{\bar{u}} \cdot \nabla \vec{u}' + \vec{u}' \cdot \nabla \vec{\bar{u}}] - \epsilon[\vec{u}' \cdot \nabla \vec{u}' + \frac{\rho'}{\bar{\rho}} \frac{\partial \vec{u}'}{\partial t}] + \frac{1}{\epsilon \bar{\rho}} (\delta \vec{F}_p' - \vec{\sigma}') \qquad (2.16)$$

$$\frac{\partial p'}{\partial t} + \bar{\gamma}\bar{p} \nabla \cdot \vec{u}' = -\mu[\vec{\bar{u}} \cdot \nabla p' + \bar{\gamma} p' \nabla \cdot \vec{\bar{u}}] - \epsilon[\bar{\gamma} p' \nabla \cdot \vec{u}' + \vec{u}' \cdot \nabla p'] + \frac{1}{\epsilon} P' \qquad (2.17)$$

where P' is the fluctuation of P. To this point terms to all orders of μ have been retained, and no assumption has been made about the ordering of $\delta \vec{F}_p'$, $\vec{\sigma}'$ and P'. Eventually only terms to first order in the mean flow speed will be retained, so the mean pressure and density will be constant. For simplicity, use that fact now and write* $\bar{p} = p_o$, $\bar{\rho} = \rho_o$, $\bar{a}^2 = \bar{\gamma} p_o / \rho_o$.

The nonlinear wave equation may be formed now by differentiating (2.17) with respect to time, and substituting (2.16) into the second term on the left hand side. Some rearrangement gives

$$\begin{aligned} \nabla^2 p' - \frac{1}{\bar{a}^2} \frac{\partial^2 p'}{\partial t^2} = & -\mu \left\{ \rho_o \nabla \cdot (\vec{\bar{u}} \cdot \nabla \vec{u}' + \vec{u}' \cdot \nabla \vec{\bar{u}}) - \frac{1}{\bar{a}^2} \vec{\bar{u}} \cdot \nabla \frac{\partial p'}{\partial t} - \frac{\bar{\gamma}}{\bar{a}^2} \frac{\partial p'}{\partial t} \nabla \cdot \vec{\bar{u}} \right\} \\ & - \epsilon \left\{ \rho_o \nabla \cdot (\vec{u}' \cdot \nabla \vec{u}') - \frac{\bar{\gamma}}{\bar{a}^2} \frac{\partial}{\partial t} (p' \nabla \cdot \vec{u}') - \frac{1}{\bar{a}^2} \frac{\partial}{\partial t} (\vec{u}' \cdot \nabla p') + \nabla \cdot (\rho' \frac{\partial \vec{u}'}{\partial t}) \right\} \\ & - \frac{1}{\epsilon} \left\{ \frac{1}{\bar{a}^2} \frac{\partial P'}{\partial t} - \bar{a}^2 \nabla \cdot (\delta \vec{F}_p' - \vec{\sigma}') \right\} \end{aligned} \qquad (2.18)$$

The boundary condition accompanying (2.18) is found by taking the component of (2.16) normal to the boundary:

$$\begin{aligned} \hat{n} \cdot \nabla p' = & -\rho_o \frac{\partial \vec{u}'}{\partial t} \cdot \hat{n} - \mu \rho_o (\vec{\bar{u}} \cdot \nabla \vec{u}' + \vec{u}' \cdot \nabla \vec{\bar{u}}) \cdot \hat{n} - \epsilon (\rho_o \vec{u}' \cdot \nabla \vec{u}' + \rho' \frac{\partial \vec{u}'}{\partial t}) \cdot \hat{n} \\ & + \frac{1}{\epsilon} (\delta \vec{F}_p' - \vec{\sigma}') \cdot \hat{n} \end{aligned} \qquad (2.19)$$

The one-dimensional counterparts of (2.17) and (2.18) are easily deduced by replacing ∇ by $\partial/\partial z$, and the divergence $\nabla \cdot \vec{v}$ of a vector $\vec{v}$ by

*Note that ρ_o stands for the average value of the density of the mixture: $\rho_o = \rho_{po} + \rho_{go} = \rho_{go}(1+\kappa)$.

$S_c^{-1}\partial/\partial z(S_c v_z)$. Also, $\vec{\sigma}$ is replaced by Σ_1 and P by $P_1 + S_1$.

For computations of linear stability, only terms of order μ appear on the right hand sides of both (2.18) and (2.19). The solution for the n^{th} mode then has the form (1.1), with $\eta(t)$ a simple exponential,

$$p_n' = p_o e^{\alpha_n t} \psi_n(\vec{r}) \tag{2.20}$$

Thus, the first influence of the perturbation produces a growth or decay; α_n is proportional to the average flow speed, characterized by μ. There is a small change of the frequency, but the spatial structure of the mode, ψ_n, is undistorted in first approximation. Calculations of-that-sort can be extended: the next approximation provides a formula for α_n correct to second order in the mean flow speed, and the first order distortion of the mode shape.

The purpose here is to develop a description of nonlinear temporal behavior associated with second order acoustics. The perturbations associated with combustion and mean flow are the same as those accounted for in the treatment of linear stability. In order that only linear terms in μ should appear in (2.18) and (2.19), it is necessary that the undistorted mode shapes should be used on the right hand sides. Formally, this step implies that terms of order μ^2, $\epsilon\mu$ and higher are neglected compared with those of order μ and ϵ. This corresponds to the following limit process applied to the small parameter μ and ϵ.

Consider, for example, only the two terms on the right hand side of (2.18),

$$\mu\left\{\rho_o \nabla\cdot(\vec{u}\cdot\nabla\vec{u}')\right\} + \epsilon\left\{\rho_o\nabla\cdot(\vec{u}'\cdot\nabla\vec{u}')\right\}$$

The acoustic velocity field with first order distortion is

$$\vec{u}' = \vec{u}_a' + \mu\vec{u}_1'$$

where $\vec{u}_a'$ is the classical acoustic field. Substitution gives

$$\mu\Big[\Big\{\rho_o\nabla\cdot(\vec{\bar{u}}\cdot\nabla\vec{u}_a')\Big\} + \frac{\epsilon}{\mu}\Big\{\rho_o\nabla\cdot(\vec{u}_a'\cdot\nabla\vec{u}_a')\Big\}$$

$$\mu\Big\{\rho_o\nabla\cdot(\vec{\bar{u}}\cdot\nabla\vec{u}_1')\Big\} + \epsilon\Big\{\rho_o\nabla\cdot(\vec{u}_a'\cdot\nabla\vec{u}_1' + \vec{u}_1'\cdot\nabla\vec{u}_a')\Big\}$$

$$+\mu\epsilon\Big\{\rho_o\nabla\cdot(\vec{u}_1'\cdot\nabla\vec{u}_1')\Big\}\Big]$$

Now let $\mu, \epsilon \to 0$ but $\epsilon/\mu \sim 0(1)$. Only the first terms survive, containing the undistorted parts of the acoustic field. Similar reasoning applies to the other terms on the right hand sides of (2.18) and (2.19). The procedure can be extended to higher order in both μ and ϵ.

The expansions (1.6) and (1.7) are therefore appropriate. How they are used to give a coupled set of equations for the amplitudes $\eta_n(t)$ is described in the next section.

III. ORDINARY NONLINEAR EQUATIONS FOR THE AMPLITUDES

3.1 Construction of the Equations

Define the functions

$$h_\mu = -\rho_o\nabla\cdot(\vec{\bar{u}}\cdot\nabla\vec{u}' + \vec{u}'\cdot\nabla\vec{\bar{u}}) + \frac{1}{\bar{a}^2}\vec{\bar{u}}\cdot\nabla\frac{\partial p'}{\partial t} + \frac{\bar{\gamma}}{\bar{a}^2}\frac{\partial p'}{\partial t}\nabla\cdot\vec{\bar{u}} \tag{3.1}$$

$$h_\epsilon = -\rho_o\nabla\cdot(\vec{u}'\cdot\nabla\vec{u}') + \frac{\bar{\gamma}}{\bar{a}^2}\frac{\partial}{\partial t}(p'\nabla\cdot\vec{u}') + \frac{1}{\bar{a}^2}\frac{\partial}{\partial t}(\vec{u}'\cdot\nabla p') - \nabla\cdot(\rho'\frac{\partial\vec{u}'}{\partial t}) \tag{3.2}$$

$$h_v = -\frac{1}{\epsilon}\Big[\frac{1}{\bar{a}^2}\frac{\partial P'}{\partial t} - \nabla\cdot(\delta\vec{F}_p' - \vec{\sigma}')\Big] \tag{3.3}$$

$$f_s = \rho_o\frac{\partial\vec{u}'}{\partial t}\cdot\hat{n} \tag{3.4}$$

$$f_\mu = \rho_o(\vec{\bar{u}}\cdot\nabla\vec{u}' + \vec{u}'\cdot\nabla\vec{\bar{u}})\cdot\hat{n} \tag{3.5}$$

$$f_\epsilon = (\rho_o\vec{u}'\cdot\nabla\vec{u}' + \rho'\frac{\partial\vec{u}'}{\partial t})\cdot\hat{n} \tag{3.6}$$

$$f_v = -\frac{1}{\epsilon}(\delta\vec{F}_p' - \vec{\sigma}')\cdot\hat{n} \tag{3.7}$$

Then the nonlinear wave equation (2.18) and boundary condition (2.19) become*

*The ordering parameters are hereafter suppressed except in h_v and f_v.

$$\frac{1}{\bar{a}^2}\frac{\partial^2 p'}{\partial t^2} - \nabla^2 p' = -(h_\mu + h_\epsilon + h_v) \tag{3.8}$$

$$\hat{n} \cdot \nabla p' = -f_s - f_\mu - f_\epsilon - f_v \tag{3.9}$$

Multiply (3.8) by the mode shape ψ_n for the nth mode and integrate over the volume of the chamber. The first term on the left hand side can be re-written using Green's theorem, and (3.9) is then substituted. Some use must be made of the following properties of the ψ_n:

$$\nabla^2 \psi_n + k_n^2 \psi_n = 0 \tag{3.10}$$

$$\hat{n} \cdot \nabla \psi_n = 0 \tag{3.11}$$

$$\int \psi_i \psi_n dV = \delta_{ni} E_n^2 \tag{3.12}$$

$$k_n^2 = \omega_n^2 / \bar{a}^2 \tag{3.13}$$

These operations lead to

$$\int \psi_n \frac{\partial^2 p'}{\partial t^2} dV + \omega_n^2 \int \psi_n p' dV = -\bar{a}^2 \int \psi_n [h_\mu + h_\epsilon + h_v] dV - \bar{a}^2 \oiint \psi_n [f_s + f_\mu + f_\epsilon + f_v] dS \tag{3.14}$$

Because of the orthogonality (3.12) of the ψ_n, substitution of (1.7) in the left hand side of (3.14) gives

$$p_o E_n^2 [\ddot{\eta}_n + \omega_n^2 \eta_n] = -\bar{a}^2 \int \psi_n [h_\mu + h_\epsilon + h_v] dV - \bar{a}^2 \oiint \psi_n [f_s + f_\mu + f_\epsilon + f_v] dS \tag{3.15}$$

where

$$E_n^2 = \int \psi_n^2 dV \tag{3.16}$$

For the one-dimensional formulation, the equation corresponding to (3.15) is

$$p_o E_e^{\,2}[\ddot{\eta}_\ell + \omega_\ell^{\,2}\eta_\ell] = -\bar{a}^{-2}\int_o^L \psi_\ell [h_{1\mu}+h_{1\epsilon}+h_{1w}]\, S_c dz$$

$$-\bar{a}^{-2}[\, S_c \psi_\ell (f_{1s}+f_{1\mu}+f_{1\epsilon}+f_{1w}]_o^L \tag{3.17}$$

where

$$E_\ell^{\,2} = \int_o^L \psi_\ell^{\,2} S_c dz \tag{3.18}$$

$$h_{1\mu} = -\rho_o \frac{1}{S_c}\frac{\partial}{\partial z}\left(S_c \frac{\partial}{\partial z}(\overline{uu'})\right) + \frac{\bar{u}}{\bar{a}^2}\frac{\partial^2 p'}{\partial z \partial t} + \frac{\bar{\gamma}}{S_c}\frac{\partial p'}{\partial t}\frac{d}{dz}(\bar{u}S_c) \tag{3.19}$$

$$h_{1\epsilon} = -\rho_o \frac{1}{S_c}\frac{\partial}{\partial z}(S_c u'\frac{\partial u'}{\partial z}) + \frac{\bar{\gamma}}{\bar{a}^2 S_c}\frac{\partial}{\partial t}(p'\frac{\partial}{\partial z}(S_c u')) + \frac{1}{\bar{a}^2}\frac{\partial}{\partial t}(u'\frac{\partial p'}{\partial z}) - \frac{1}{a^2 S_c}\frac{\partial}{\partial z}(S_c \rho' \frac{\partial u'}{\partial t}) \tag{3.20}$$

$$h_{1w} = -\frac{1}{\epsilon}\left\{\frac{1}{\bar{a}^2}\frac{\partial}{\partial t}(P_1' + S_1') - \frac{1}{S_c}\frac{\partial}{\partial z}[S_c(\delta F_p' - \Sigma')]\right\} \tag{3.21}$$

$$f_{1s} = \rho_o \frac{\partial u'}{\partial t} \tag{3.22}$$

$$f_{1\mu} = \rho_o \frac{\partial}{\partial z}(uu') \tag{3.23}$$

$$f_{1\epsilon} = \rho_o u' \frac{\partial u'}{\partial z} + \rho' \frac{\partial u'}{\partial t} \tag{3.24}$$

$$f_{1w} = -\frac{1}{\epsilon}(\delta F_p' - \Sigma_1') \tag{3.25}$$

3.2 Evaluating the Linear Terms

After some re-arrangement, one can establish the following identities:

$$\int \psi_n h_\mu dV + \oiint \psi_n f_\mu dS = \rho_o k_n^{\,2}\int(\vec{\bar{u}}\cdot\vec{u}')\psi_n dV - \rho_o \int[\vec{u}' \times \nabla \times \vec{\bar{u}}]\cdot\nabla\psi_n dV$$

$$+\frac{1}{\bar{a}^2}\int \psi_n [\vec{\bar{u}}\cdot\nabla\frac{\partial p'}{\partial t} + \bar{\gamma}\frac{\partial p'}{\partial t}\nabla\cdot\vec{\bar{u}}]\, dV \tag{3.26}$$

$$\int_o^L \psi_\ell h_{1\mu} S_c dz + [S_c \psi_\ell f_{1\mu}]_o^L = \rho_o \int_o^L \bar{u} u' \psi_\ell S_c dz + \frac{1}{\bar{a}^2} \int_o^L \psi_\ell \left[\bar{u} \frac{\partial^2 p'}{\partial z \partial t} + \frac{\bar{\gamma}}{S_c} \frac{\partial p'}{\partial t} \frac{d}{dz}(\bar{u} S_c)\right] S_c dz \tag{3.27}$$

$$\int \psi_n h_v dV + \oint\!\!\!\oint \psi_n f_v dS = -\frac{1}{\epsilon} \int \left[\frac{1}{\bar{a}^2} \psi_n \frac{\partial P'}{\partial t} + (\delta \vec{F}_p' - \vec{\sigma}') \cdot \nabla \psi_n\right] dV \tag{3.28}$$

$$\int_0^L \psi_\ell h_{1w} dV + [S_c \psi_\ell f_{1w}]_o^L = -\frac{1}{\epsilon} \int_o^L \left[\frac{1}{\bar{a}^2} \psi_\ell \frac{\partial}{\partial t}(P_1' + S_1') + (\delta F_p' - \Sigma_1') \frac{d\psi_\ell}{dz}\right] S_c dz \tag{3.29}$$

The terms in (3.28) and (3.29) represent the influences of both surface and residual combustion within the volume; the contributions associated with condensed material suspended in the gas; and, for the one-dimensional problem, the effects of flow entering from the lateral boundary. Later (§ 3.3) the peculiarly one-dimensional terms will be combined in the three-dimensional problem according to the prescription discussed by Culick (1975). To simplify writing, define the functions H, H_1 and L_1, which appear in (3.34) and (3.35):

$$H = \frac{1}{\epsilon}\left[\frac{1}{\bar{a}^2} \psi_n \frac{\partial P'}{\partial t} + (\delta \vec{F}_p' - \vec{\sigma}') \cdot \nabla \psi_n\right] \tag{3.30}$$

$$H_1 = \frac{1}{\epsilon}\left[\frac{1}{\bar{a}^2} \psi_\ell \frac{\partial P_1'}{\partial t} + (\delta F_p' - \sigma_1') \frac{d\psi_\ell}{dz}\right] \tag{3.31}$$

$$L_1 = \frac{1}{\epsilon}\left[\frac{1}{\bar{a}^2} \psi_\ell \frac{\partial S_1'}{\partial t} - (\Sigma_1' - \sigma_1') \frac{d\psi_\ell}{dz}\right] \tag{3.32}$$

The acoustic quantities appearing in (3.26) and (3.27) are approximated by the expansions (1.6) and (1.7) to give*

$$\int \psi_n h_\mu dv + \oint\!\!\!\oint \psi_n f_\mu dS \equiv \frac{\rho_o}{\bar{\gamma}} \sum_{i=1}^{\infty} \mathring{\eta}_i \left\{ \int \left[\frac{k_n^2}{k_i^2} \psi_n \vec{\bar{u}} \cdot \nabla \psi_i - \psi_i \vec{\bar{u}} \cdot \nabla \psi_n\right] dv \right.$$
$$- \int (\nabla \psi_i \times \nabla \times \vec{\bar{u}}) \psi_n \cdot dv$$
$$\left. + (\bar{\gamma} - 1) \int \psi_i \psi_n \nabla \cdot \vec{\bar{u}}\, dv \right\}$$
$$+ \frac{1}{\bar{a}^2} \oint\!\!\!\oint \frac{\partial p'}{\partial t} \psi_n \vec{\bar{u}} \cdot \hat{n}\, dS \tag{3.33}$$

*As noted in connection with (1.6), η_o will be assumed to be zero throughout except in § 10.

$$\int \psi_\ell \, h_{1\mu} \, dv + \left[S_c \psi_\ell f_{1\mu} \right]_o^L \equiv \frac{\rho_o}{\bar{\gamma}} \sum_{m=1}^{\infty} \dot{\eta}_m \left\{ \int \left[\frac{k_\ell^2}{k_m^2} \psi_\ell \, \bar{u} \, \frac{d\psi_m}{dz} - \psi_m \, \bar{u} \, \frac{d\psi_\ell}{dz} \right] S_c \, dz \right.$$

$$\left. + (\bar{\gamma} - 1) \int_o^L \psi_m \psi_\ell \, \frac{1}{S_c} \frac{d}{dz} (S_c \bar{u}) S_c \, dz \right\}$$

$$- \left[\psi_\ell \, \frac{\partial p'}{\partial z} \, \bar{u}_b \, S_c \right]_o^L \qquad (3.33)^*$$

The terms containing f_s and f_{1s} are conveniently combined with the last terms of (3.32) and (3.33). Then with the preceding results, Equations (3.15) and (3.17) become

$$E_n^2 \left[\ddot{\eta}_n + \omega_n^2 \eta_n \right] = - \sum_{i=1}^{\infty} \dot{\eta}_i \left\{ \int \left[\frac{k_n^2}{k_i^2} \psi_n \, \vec{\bar{u}} \cdot \nabla \psi_i - \psi_i \, \vec{\bar{u}} \cdot \nabla \psi_n \right] dv \right.$$

$$- \int (\nabla \psi_i \times \nabla \times \vec{\bar{u}}) \, \psi_n \, dv$$

$$\left. + (\bar{\gamma} - 1) \int \psi_i \psi_n \, \nabla \cdot \vec{\bar{u}} \, dv \right\}$$

$$+ \frac{\bar{\gamma}}{\rho_o} \oiint \psi_n \frac{\partial}{\partial t} \left[\rho_o \, \vec{u}_b + \frac{p' \bar{u}_b}{\bar{a}^2} \right] dS \qquad (3.34)$$

$$- \frac{\bar{\gamma}}{\rho_o} \left\{ \int \psi_n \, h_\epsilon \, dv + \oiint \psi_n \, f_\epsilon \, dS \right\}$$

$$+ \frac{\bar{\gamma}}{\rho_o} \int H \, dv$$

$$E_\ell^2 \left[\ddot{\eta}_\ell + \omega_\ell^2 \eta_\ell \right] = - \sum_{m=1}^{\infty} \dot{\eta}_m \left\{ \int \left[\frac{k_\ell^2}{k_m^2} \psi_\ell \, \bar{u} \, \frac{d\psi_m}{dz} - \psi_m \, \bar{u} \, \frac{d\psi_\ell}{dz} \right] S_c \, dz \right.$$

$$\left. + (\bar{\gamma} - 1) \int \psi_m \psi_\ell \, \frac{1}{S_c} \, \frac{d}{dz} (S_c \bar{u}) S_c \, dz \right\}$$

(Continued)

---

* The signs of [ ] and the surface integral have been changed so $\vec{u}' \cdot \hat{n} = u_b'$ and $\vec{\bar{u}} \cdot \hat{n} = \bar{u}_b$ are positive inward.

(Continued from Page 16)

$$+\frac{\bar{\gamma}}{\rho_o}\left[S_c\,\psi_\ell\,\frac{\partial}{\partial t}(\rho_o u_b' + \frac{p' u_b}{\bar{a}^2})\right]_o^L \qquad (3.34)^*$$

$$-\frac{\bar{\gamma}}{\rho_o}\left\{\int_o^L \psi_\ell\, h_{1\epsilon}\, S_c\, dz + \left[S_c \psi_\ell f_{1\epsilon}\right]_o^L\right\}$$

$$+\frac{\bar{\gamma}}{\rho_o}\int_o^L H_1 S_c\, dz + \frac{\bar{\gamma}}{\rho_o}\int_o^L L_1\, S_c\, dz$$

3.3 Surface Terms in the One-Dimensional Problem; Combining the One- and Three-Dimensional Problems

It is the function L_1 which contains the terms found in the one-dimensional approximation. Only the linear forms will be treated in this work. With the definitions (2.13) and (2.15), L_1 to first order is

$$S_c' L_1 = \psi_\ell(1+\varkappa)\frac{\partial}{\partial t}\int (m_b' + \bar{m}_b \frac{\Delta T'}{T_o})dq + \psi_\ell(1+\varkappa)\frac{\partial}{\partial t}\int \frac{T'}{T_o}\,\bar{m}_b\, dq$$

$$-\left[u'\int \bar{m}_b\, dq + u_p'\int \bar{m}_b^{(p)} dq\right]\frac{d\psi_\ell}{dz} \qquad (3.35)$$

It is readily established, Equation (3.11) of Culick (1974) that

$$\frac{(1+\varkappa)}{\rho_o}(m_b' + \bar{m}_b \frac{\Delta T'}{T_o}) = u_b' + p' \frac{\bar{u}_b}{\rho_o \bar{a}^2} \quad . \qquad (3.36)$$

Then because the integral over dz dq is the integral over the lateral surface, we can write

$$\frac{\bar{\gamma}}{\rho_o}\int L_1\, S_c\, dz = \frac{\bar{\gamma}}{\rho_o}\iint \psi_\ell \frac{\partial}{\partial t}(\rho_o u_b' + p' \frac{\bar{u}_b}{\bar{a}^2})dS$$

$$+\frac{\bar{\gamma}(1+\varkappa)}{\rho_o}\frac{\partial}{\partial t}\iint \frac{T'}{T_o}\,\psi_\ell\,\bar{m}_b\, dS - \frac{\bar{\gamma}(1+\varkappa)}{\rho_o}\iint u' \frac{d\psi_\ell}{dz}\,\bar{m}_b\, dS$$

$$-\frac{\bar{\gamma}}{\rho_o}\iint \delta u_p \frac{d\psi_\ell}{dz}\,\bar{m}_b^{(p)} dS$$

---

* The sign of u_b' in [ ] has been changed so that u_b' is positive inward at the end surfaces.

it is a good approximation for most practical problems that the temperature fluctuations within the chamber are nearly isentropic.* With this assumption, and the approximation that the composition of the material leaving the combustion zone is the same as that within the chamber (so $\rho_o = (1+\kappa)\bar{\rho}_g$), the last identity can be written

$$\frac{\bar{\gamma}}{\rho_o}\int_o^L L_1 dz = \frac{\bar{\gamma}}{\rho_o}\iint \psi_\ell \frac{\partial}{\partial t}\left(\rho_o u_b' + p'\frac{\bar{u}_b}{\bar{a}^2}\right) dS$$

$$+ (\bar{\gamma}-1)\frac{\partial}{\partial t}\iint \frac{p'}{p_o}\psi_\ell \bar{u}_b\, dS \qquad (3.37)$$

$$- \bar{\gamma}\iint u' \frac{d\psi_\ell}{dz}\bar{u}_b\, dS - \frac{\bar{\gamma}}{\rho_o}\iint \delta u_p \frac{d\psi_\ell}{dz}\bar{m}_b^{(p)}\, dS$$

The terms multiplied by $(\gamma-1)$ in (3.34) and (3.37) combine to give

$$-(\bar{\gamma}-1)\sum_{m=1}^{\infty}\dot{\eta}_m\int_o^L \psi_m\psi_\ell \frac{w_p}{\bar{\rho}_g} S_c\, dz \qquad (3.38)$$

where use has been made of the continuity equation for one-dimensional flow. Substitution of (3.37) and (3.38) into (3.34) then leads to

$$E_\ell^2[\ddot{\eta}_\ell + \omega_\ell^2 \eta_\ell] = -\sum_{m=1}^{\infty}\dot{\eta}_m\left\{\int\left[\frac{k_\ell^2}{k_m^2}\psi_\ell \bar{u}\frac{d\psi_m}{dz} - \psi_m \bar{u}\frac{d\psi_\ell}{dz}\right] S_c\, dz\right.$$

$$\left. + (\bar{\gamma}-1)\int_o^L \psi_m\psi_\ell \frac{\bar{w}_p}{\bar{\rho}_g} S_c\, dz\right\}$$

$$+\frac{\bar{\gamma}}{\rho_o}\frac{\partial}{\partial t}\left\{\iint \psi_\ell(\rho_o u_b' + p'\frac{\bar{u}_b}{\bar{a}^2})dS + \left[S_c\psi_\ell(\rho_o u_b' + p'\frac{\bar{u}_b}{\bar{a}^2}\right]_o^L\right\}$$

(Continued)

* This assumption which, at the expense of substantially more labor, can be relaxed, means that temperature or entropy waves (convected by the average flow) are not represented in the volume of the chamber. Nonisentropic temperature fluctuations at the surface are accounted for ($\Delta T \neq 0$). There is at present no evidence or calculation showing how important this inconsistency might be. Essentially what is included is the direct influence of nonisentropic surface combustion on the acoustic field, but interactions between the entropy waves and the acoustic waves are ignored.

(Continued from p. 18)

$$- \left\{ \sum_{m=1}^{\infty} \frac{\dot{\eta}_m}{k_m^2} \iint \frac{d\psi_m}{dz} \frac{d\psi_\ell}{dz} \bar{u}_b \, dS + \frac{\bar{\gamma}}{\rho_o} \iint \delta u_p \frac{d\psi_\ell}{dz} \bar{m}_b^{(p)} \, dS \right\}$$

$$+ \frac{\bar{\gamma}}{\rho_o} \int_o^L H_1 \, S_c \, dz \qquad (3.39)$$

Note that the surface integrals in (3.39) extend along the lateral boundary only, and that the velocities u_b', $\bar{u}_b$ appearing in those integrals are positive inward. The second set of brackets containing surface terms obviously correspond exactly to the surface integral in (3.34). According to the argument proposed by Culick (1974) these should be written in the general case as*

$$\bar{\gamma} \frac{\partial}{\partial t} \oiint \psi_n (u_{\parallel}' \delta_{\parallel} + u_{\perp}' \delta_{\perp}) dS \ ,$$

where $u_{\parallel}'$ and $u_{\perp}'$ both stand for the formula (3.36).

Moreover, the surface terms contained in the last brackets of (3.39) can be incorporated in the three-dimensional problems in the form

$$\sum_{i=1}^{\infty} \frac{\dot{\eta}_i}{k_i^2} \oiint (\nabla \psi_i) \cdot (\nabla \psi_n) \, \delta_{\parallel} \bar{u}_b dS + \frac{\bar{\gamma}}{\rho_o} \oiint \delta \vec{u}_b' \cdot \nabla \psi_n \, \bar{m}_b^{(p)} \delta_{\parallel} \, dS \ .$$

Consequently, with proper interpretation, all problems are represented by the equation

$$E_n^2 \left[\ddot{\eta}_n + \omega_n^2 \eta_n \right] = - E_n^2 \sum_{i=1}^{\infty} D_{ni} \dot{\eta}_i - \frac{\bar{\gamma}}{\rho_o} \oiint \delta \vec{u}_p' \cdot \nabla \psi_n \, \bar{m}_b^{(p)} \, dS$$

$$+ \frac{\bar{\gamma}}{\rho_o} \int H \, dv + \frac{\partial}{\partial t} \oint \mathcal{R} \psi_n \, dS$$

$$- \frac{\bar{\gamma}}{\rho_o} \left\{ \int \psi_n \, h_\epsilon dv + \oiint \psi_n \, f_\epsilon \, dS \right\} \qquad (3.40)$$

---

* The symbols $u_{\perp}'$, $u_{\parallel}'$, $\delta_{\perp}$, $\delta_{\parallel}$ are defined and discussed in § 4 of Culick (1975).

where

$$E_n^2 D_{ni} = \int\left[\frac{k_n^2}{k_i^2}\psi_n \vec{\bar{u}}\cdot\nabla\psi_i - \psi_i \vec{\bar{u}}\cdot\nabla\psi_n\right]dv + (\bar{\gamma}-1)\int\psi_i\psi_n\frac{\bar{w}_p}{\bar{\rho}_g}\,dv + \frac{1}{k_i^2}\oint\!\!\!\oint(\nabla\psi_i)\cdot(\nabla\psi_n)\bar{u}_b\,\delta_\parallel dS \tag{3.41}$$

$$\mathcal{R} = \rho_o(u'_\perp\delta_\perp + u'_\parallel\delta_\parallel) \tag{3.42}$$

That the nonlinear terms for the one- and three-dimensional problems correspond exactly, and therefore can be accommodated as shown in (3.40), is demonstrated in the next section.

3.4 Nonlinear Terms

To the order considered here, there are no nonlinear terms explicitly dependent on the mean flow. The representations will therefore be directly useful for the classical problem of nonlinear waves in a resonant tube. No special considerations are required for the one-dimensional problem. With the definitions (3.2) and (3.6),

$$\begin{aligned} I_\epsilon &= \frac{\bar{\gamma}}{\rho_o}\left\{\int\psi_n h_\epsilon dv + \oint\!\!\!\oint\psi_n f_\epsilon dS\right\} \\ &\equiv \frac{\bar{\gamma}}{\rho_o}\int\nabla\psi_n\cdot\left[\rho_o\vec{u}'\cdot\nabla\vec{u}' + \rho'\frac{\partial\vec{u}'}{\partial t}\right]dv \\ &\quad + \frac{\bar{\gamma}}{\rho_o\bar{a}^2}\int\psi_n\left[\bar{\gamma}\frac{\partial}{\partial t}(p'\nabla\cdot u') + \frac{\partial}{\partial t}(u'\cdot\nabla p')\right]dv \end{aligned} \tag{3.43}$$

It is within the approximations already introduced to use the zero order acoustic approximations in these integrals:

$$\frac{\partial\vec{u}'}{\partial t} \approx -\frac{1}{\rho_o}\nabla p' \qquad \frac{\partial p'}{\partial t} \approx -\bar{\gamma}p_o\nabla\cdot\vec{u}' \tag{3.44}$$

Then (3.43) may be written as

$$I_\epsilon = \bar{\gamma} \int [\nabla \psi_n \cdot (\vec{u}' \cdot \nabla \vec{u}') - \psi_n \{ \bar{\gamma} (\nabla \cdot \vec{u}')^2 + \vec{u}' \cdot \nabla (\nabla \cdot \vec{u}') \}] dv$$

$$- \frac{1}{\rho_o P_o} \int [\nabla \psi_n \cdot (p' \nabla p') + \psi_n \{ (\nabla p')^2 + \bar{\gamma} p' \nabla^2 p' \}] dv \qquad (3.45)$$

In the first term of the second integral, the approximation $\rho' \approx \bar{a}^{-2} p'$ has been used; this is consistent* with (3.44). Now substitute the expansions (1.6) and (1.7) to find, with the terms involving η_o dropped,

$$I_\epsilon = E_n^2 \sum_{i=1}^{\infty} \sum_{j=1}^{\infty} \left[A_{nij} \dot{\eta}_i \dot{\eta}_j + B_{nij} \eta_i \eta_j \right] \qquad (3.46)$$

where

$$A_{nij} = \frac{1}{\bar{\gamma} E_n^2} \frac{1}{k_i^2 k_j^2} \int [\nabla_n \cdot (\nabla \psi_i \cdot \nabla (\nabla \psi_j))$$

$$- \psi_n [\bar{\gamma} k_i^2 k_j^2 \psi_i \psi_j - k_j^2 \nabla \psi_i \cdot \nabla \psi_j] dv \qquad (3.47)$$

$$B_{nij} = - \frac{\bar{a}^2}{\bar{\gamma} E_n^2} \int [\nabla \psi_n \cdot (\psi_i \nabla \psi_j) + \psi_n \{ (\nabla \psi_i) \cdot (\nabla \psi_j) - \bar{\gamma} k_j^2 \psi_i \psi_j \}] dv \qquad (3.48)$$

Four integrals appear in these definitions:

$$I_{1n}^{ij} = \int \nabla \psi_n \cdot (\nabla \psi_i \cdot \nabla (\nabla \psi_j)] dv \qquad (3.49)$$

$$I_{2n}^{ij} = \int \nabla \psi_n \cdot (\psi_i \nabla \psi_j) dv \qquad (3.50)$$

$$I_{3n}^{ij} = \int \psi_n \nabla \psi_i \cdot \nabla \psi_j \, dv \qquad (3.51)$$

$$I_{nij} = \int \psi_n \psi_i \psi_j \, dv \qquad (3.52)$$

---

* More detailed consideration has been given by Chester (1961) to the use of acoustic approximations in the representation of finite amplitude waves.

Then (3.47) and (3.48) are

$$\bar{\gamma} E_n^2 k_i^2 k_j^2 A_{nij} = I_{1n}^{ij} + k_j^2 I_{3n}^{ij} - \gamma k_i^2 k_j^2 I_{nij} \tag{3.53}$$

$$-\frac{\bar{\gamma} E_n^2}{\bar{a}^2} B_{nij} = I_{2n}^{ij} + I_3 - \bar{\gamma} k_j^2 I_{nij} \tag{3.54}$$

One can eventually reduce (3.49)-(3.51) to multiples of I_{nij}:

$$I_{1n}^{ij} = \frac{1}{4}[k_j^4 - (k_n^2 - k_i^2)^2] I_{nij} = \frac{1}{4} k_n^2 (k_i^2 + k_j^2 - k_n^2) I_{nij} + \frac{1}{4}(k_j^2 - k_i^2)(k_i^2 + k_j^2 - k_n^2) I_{nij} \tag{3.55}$$

$$I_{2n}^{ij} = \frac{1}{2}(k_j^2 - k_i^2 + k_n^2) I_{nij} = \frac{1}{2} k_n^2 I_{nij} + \frac{1}{2}(k_j^2 - k_i^2) I_{nij} \tag{3.56}$$

$$I_{3n}^{ij} = \frac{1}{2}(k_i^2 + k_j^2 - k_n^2) I_{nij} \tag{3.57}$$

The second parts of (3.55) and (3.56) show I_{1n}^{ij} and I_{2n}^{ij} decomposed into pieces which are respectively symmetric and antisymmetric under interchange of the indices (i, j). With these results, (3.53) and (3.54) become

$$A_{nij} = \frac{I_{nij}}{4 \bar{\gamma} k_i^2 k_j^2 E_n^2} [(k_j^2 + k_i^2)^2 - k_n^4 - 4 \bar{\gamma} k_i^2 k_j^2] + \frac{I_{nij}}{2 \bar{\gamma} k_i^2 k_j^2 E_n^2} (k_j^2 - k_i^2)(k_j^2 + k_i^2 - k_n^2) \tag{3.58}$$

$$B_{nij} = \frac{(\bar{\gamma} - 1)\bar{a}^2 I_{nij}}{2 \bar{\gamma} E_n^2} (k_j^2 + k_i^2) + \frac{(\bar{\gamma} - 1)\bar{a}^2 I_{nij}}{2 \bar{\gamma} E_n^2} (k_j^2 - k_i^2) \tag{3.59}$$

Again, the two parts on the right hand sides are respectively symmetric and antisymmetric in (i, j). In § 4, Equations (4.32) and (4.33), the following combinations will arise:

$$A_{nij}\,\omega_i\omega_j \pm B_{nij} = \frac{\bar{a}^2 I_{nij}}{2\bar{\gamma}E_n^2}\left[\frac{(k_i^2+k_j^2)^2-k_n^4}{2k_ik_j} - 2\bar{\gamma}k_ik_j \pm (\bar{\gamma}-1)(k_i^2+k_j^2)\right] + \frac{\bar{a}^2 I_{nij}}{2\bar{\gamma}E_n^2}(k_j^2-k_i^2)\left[\frac{k_j^2+k_i^2-k_n^2}{2k_ik_j} \pm (\bar{\gamma}-1)\right] \tag{3.60}$$

It should be noted that there is yet no restriction to a particular geometry; the form of the chamber influences the numerical results through the values of the k_i and the integral I_{nij}. Because some terms in I_ϵ, eq. (3.45), contain p', there are non-zero values for i = 0 or j = 0. These are associated with the DC shift of mean pressure due to nonlinear processes; this is treated separately in § 10.

Finally, because the nonlinear terms (3.46) are summed over all (i, j), and the coefficients A_{nij}, B_{nij} are multiplied by functions which are symmetric in (i, j), only the terms containing the symmetric parts of A_{nij}, B_{nij} will survive. Thus, only the first brackets in (3.60) will be required for later calculations.

IV. APPLICATION OF THE METHOD OF AVERAGING

Most of the terms on the right hand side are such that (3.40) may be brought to the form

$$\ddot{\eta}_n + \omega_n^2\,\eta_n = F_n \tag{4.1}$$

with

$$F_n = -\sum_{i=1}^{\infty}\left[D_{ni}\,\dot{\eta}_i + E_{ni}\,\eta_i\right] - \sum_{i=1}^{\infty}\sum_{j=1}^{\infty}\left[A_{nij}\,\dot{\eta}_i\dot{\eta}_j + B_{nij}\eta_i\eta_j\right] \tag{4.2}$$

Other contributions (for example proportional to $|\eta_i|, \eta_i|\eta_j|, \ldots$, etc.) may arise; they are easily handled within the framework to be described now and need not be considered explicitly.

The set of coupled equations (4.1) can be solved numerically, but at considerable expense. It is the intent here to reduce the second order equations to first order equations, for which solutions may be calculated quite cheaply. The basis for the approach taken is the fact that many of the observed instabilities are essentially periodic with amplitudes slowly changing in time. Each mode may therefore be reasonably represented by the form (1.12) with $\mathcal{A}_n(t)$, $\varphi_n(t)$, $A_n(t)$ and $B_n(t)$ slowly varying functions of time. Equations for the amplitudes and phases are found by averaging (4.1) over an interval τ which will be defined later.

Accounts of the method of averaging have been given by Krylov and Bogoliubov (1947) and Bogoliubov and Mitropolsky (1961). The results are restricted by the condition that F_n must be periodic. This is true for the problems treated here if the modal frequencies are integral multiples of the fundamental, a condition which is satisfied only by purely longitudinal modes. Moreover, solutions are required here for a time interval longer than that for which the more familiar results are valid. Both difficulties are overcome--to some approximation not clarified or examined here--by the following heuristic development.

Equation (4.1) represents the behavior of a forced oscillator, for which the motion is

$$\eta_n(t) = \mathcal{A}_n(t)\sin\left(\omega_n t + \varphi_n(t)\right) = A_n \sin\omega_n t + B_n \cos\omega_n t \tag{4.3}$$

and

$$\mathcal{A}_n = [A_n^2 + B_n^2]^{\frac{1}{2}} \tag{4.4a}$$

$$\varphi_n = \arctan [B_n/A_n] \tag{4.4b}$$

The energy of the oscillator is

$$\mathcal{E}_n = \frac{1}{2}\omega_n^2 \eta_n^2 + \frac{1}{2}\dot{\eta}_n^2 \tag{4.5}$$

Because the oscillator has instantaneous velocity $\dot{\eta}_n$, the rate at which work is done on the oscillator is $\dot{\eta}_n F_n$. The values time-averaged over the interval τ at time t are

$$\langle \mathcal{E}_n \rangle = \frac{1}{\tau}\int_t^{t+\tau} \mathcal{E}_n \, dt' \qquad \langle \dot{\eta} F_n \rangle = \frac{1}{\tau}\int_t^{t+\tau} \dot{\eta}_n F_n \, dt' \tag{4.6}$$

Conservation of energy for the averaged motion requires that the rate of change of time-averaged energy of the oscillator equal the time-averaged rate of work done:

$$\frac{d}{dt}\langle \mathcal{E}_n \rangle = \langle \dot{\eta}_n F_n \rangle \tag{4.7}$$

In all that follows the essential assumption is used that the fractional changes of the amplitude and phase are small during the interval of averaging. The changes in time τ are approximately $\dot{a}_n \tau$ and $\dot{\phi}_n \tau$, so the assumption is

$$\dot{a}_n \tau << a_n, \qquad \dot{\phi}_n \tau << 2\pi \tag{4.8}$$

According to (4.2), the velocity of the oscillator is

$$\dot{\eta}_n = \omega_n a_n \cos(\omega_n t + \varphi_n) + [\dot{\phi}_n a_n \cos(\omega_n t + \varphi_n) + \dot{a}_n \sin(\omega_n t + \psi_n)]$$

The inequalities (4.8) imply that the terms in brackets are negligible compared with the first term; the stronger condition is set [see Krylov and Bogoliubov (1947), p. 10] that the combination vanishes exactly:

$$\dot{\phi}_n a_n \cos(\omega_n t + \varphi_n) + \dot{a}_n \sin(\omega_n t + \varphi_n) = 0 \tag{4.9}$$

Thus the velocity and energy are

$$\dot{\eta} = \omega_n a_n \cos(\omega_n t + \varphi_n) \tag{4.10}$$

$$\mathcal{E}_n = \omega_n^2 a_n^2 \tag{4.11}$$

A second consequence of (4.8) is that when the integrals in (4.6) are done, a_n and φ_n are taken to be constant--i.e. they do not vary significantly during the interval of averaging. Equation (4.7) therefore becomes

$$\frac{da_n}{dt} = \frac{1}{\omega_n \tau} \int_t^{t+\tau} F_n \cos(\omega_n t' + \varphi_n) dt' \tag{4.12}$$

An equation relating $\dot{\varphi}_n$ and $\dot{a}_n$ is found by substituting (4.2), (4.9), and (4.10) into (4.1). The time-averaged result is

$$\frac{d\varphi_n}{dt} = \frac{-1}{\omega_n \tau a_n} \int_t^{t+\tau} F_n \sin(\omega_n t' + \varphi_n) dt' \tag{4.13}$$

Although a_n, φ_n are approximately constant over one cycle, they may vary substantially over long periods of time. Equations (4.12) and (4.13) are then awkward to use. The difficulty is avoided by solving (4.3), (4.4), (4.12) and (4.13) for $\dot{A}_n$ and $\dot{B}_n$. It is this pair of equations which will be used as the basis for subsequent work:

$$\frac{dA_n}{dt} = \frac{1}{\omega_n \tau} \int_t^{t+\tau} F_n \cos \omega_n t' \, dt' \tag{4.14}$$

$$\frac{dB_n}{dt} = \frac{-1}{\omega_n \tau} \int_t^{t+\tau} F_n \sin \omega_n t' \, dt' \tag{4.15}$$

For F_n given by (4.2), the first order equations have the form

$$\frac{dA_n}{dt} = \left(\frac{dA_n}{dt}\right)_{linear} + \left(\frac{dA_n}{dt}\right)_{nonlinear} \tag{4.16}$$

$$\frac{dB_n}{dt} = \left(\frac{dB_n}{dt}\right)_{linear} + \left(\frac{dB_n}{dt}\right)_{nonlinear} \tag{4.17}$$

The linear contributions are:

$$\left(\frac{dA_n}{dt}\right)_{linear} = -\tfrac{1}{2}D_{nn}A_n - \tfrac{1}{2}\frac{E_{nn}}{\omega_n}B_n - \frac{1}{2\omega_n}\sum^{i\neq n}\left\{\omega_i D_{ni}\left[(f_{ni}+h_{ni})A_i-(g_{ni}+\ell_{ni})B_i\right]\right\}$$

$$-\frac{1}{2\omega_n}\sum^{i\neq n}\left\{E_{ni}\left[(g_{ni}-\ell_{ni})B_i-(f_{ni}-h_{ni})A_i\right]\right\} \tag{4.18}$$

$$\left(\frac{dB_n}{dt}\right)_{linear} = -\tfrac{1}{2}D_{nn}B_n + \tfrac{1}{2}\frac{E_{nn}}{\omega_n}A_n + \frac{1}{2\omega_n}\sum^{i\neq n}\left\{\omega_i D_{ni}\left[(f_{ni}-h_{ni})B_i+(g_{ni}-\ell_{ni})A_i\right]\right\}$$

$$+\frac{1}{2\omega_n}\sum^{i\neq n}\left\{E_{ni}\left[(g_{ni}-\ell_{ni})B_i-(f_{ni}-h_{ni})A_i\right]\right\} \tag{4.19}$$

where

$$f_{ni} = \frac{\sin(\omega_i+\omega_n)\frac{\tau}{2}}{(\omega_i+\omega_n)\frac{\tau}{2}}\cos\left[(\omega_i+\omega_n)(t+\tfrac{\tau}{2})\right] \tag{4.20}$$

$$g_{ni} = \frac{\sin(\omega_i+\omega_n)\frac{\tau}{2}}{(\omega_i+\omega_n)\frac{\tau}{2}}\sin\left[(\omega_i+\omega_n)(t+\tfrac{\tau}{2})\right] \tag{4.21}$$

$$h_{ni} = \frac{\sin(\omega_i-\omega_n)\frac{\tau}{2}}{(\omega_i-\omega_n)\frac{\tau}{2}}\cos\left[(\omega_i-\omega_n)(t+\tfrac{\tau}{2})\right] \tag{4.22}$$

$$\ell_{ni} = \frac{\sin(\omega_i-\omega_n)\frac{\tau}{2}}{(\omega_i-\omega_n)\frac{\tau}{2}}\sin\left[(\omega_i-\omega_n)(t+\tfrac{\tau}{2})\right] \tag{4.23}$$

The nonlinear contributions are

$$\left(\frac{dA_n}{dt}\right)_{nonlinear} = -\frac{1}{2\omega_n}\sum_{i=1}^{\infty}\sum_{i=1}^{\infty}\left\{C_{nij}\left[a_{ij}\,T_{1+}^{nij} - C_{ij}\,T_{3+}^{nij}\right]\right.$$

$$\left.+\,D_{nij}\left[b_{ij}\,T_{1-}^{nij} + d_{ij}\,T_{3-}^{nij}\right]\right\} \tag{4.24}$$

$$\left(\frac{dB_n}{dt}\right)_{\text{nonlinear}} = \frac{1}{2\omega_n} \sum_{i=1}^{\infty} \sum_{j=1}^{\infty} \left\{ C_{nij} \left[a_{ij} T_{2+}^{nij} - c_{ij} T_{4+}^{nij} \right] + D_{nij} \left[b_{ij} T_{2-}^{nij} + d_{ij} T_{4-}^{nij} \right] \right\} \tag{4.25}$$

where

$$T_{1\pm}^{nij} = \frac{\sin(\omega_n+\omega_\pm)\frac{\tau}{2}}{(\omega_n+\omega_\pm)\frac{\tau}{2}} \cos\left[(\omega_n+\omega_\pm)(t+\tfrac{\tau}{2})\right] + \frac{\sin(\omega_n-\omega_\pm)\frac{\tau}{2}}{(\omega_n-\omega_\pm)\frac{\tau}{2}} \cos\left[(\omega_n-\omega_\pm)(t+\tfrac{\tau}{2})\right] \tag{4.26}$$

$$T_{2\pm}^{nij} = \frac{\sin(\omega_n+\omega_\pm)\frac{\tau}{2}}{(\omega_n+\omega_\pm)\frac{\tau}{2}} \sin\left[(\omega_n+\omega_\pm)(t+\tfrac{\tau}{2})\right] - \frac{\sin(\omega_n-\omega_\pm)\frac{\tau}{2}}{(\omega_n-\omega_\pm)\frac{\tau}{2}} \sin\left[(\omega_n-\omega_\pm)(t+\tfrac{\tau}{2})\right] \tag{4.27}$$

$$T_{3\pm}^{nij} = \frac{\sin(\omega_n+\omega_\pm)\frac{\tau}{2}}{(\omega_n+\omega_\pm)\frac{\tau}{2}} \sin\left[(\omega_n+\omega_\pm)(t+\tfrac{\tau}{2})\right] - \frac{\sin(\omega_n-\omega_\pm)\frac{\tau}{2}}{(\omega_n-\omega_\pm)\frac{\tau}{2}} \sin\left[(\omega_n-\omega_\pm)(t+\tfrac{\tau}{2})\right] \tag{4.28}$$

$$T_{4\pm}^{nij} = \frac{\sin(\omega_n+\omega_\pm)\frac{\tau}{2}}{(\omega_n+\omega_\pm)\frac{\tau}{2}} \cos\left[(\omega_n+\omega_\pm)(t+\tfrac{\tau}{2})\right] - \frac{\sin(\omega_n-\omega_\pm)\frac{\tau}{2}}{(\omega_n-\omega_\pm)\frac{\tau}{2}} \cos\left[(\omega_n-\omega_\pm)(t+\tfrac{\tau}{2})\right] \tag{4.29}$$

$$\left.\begin{aligned} \omega_+ &= \omega_i + \omega_j \\ \omega_- &= \omega_i - \omega_j \end{aligned}\right\} \tag{4.30}$$

$$a_{ij} = \frac{1}{2}(A_iA_j - B_iB_j)$$

$$b_{ij} = \frac{1}{2}(A_kA_j + B_iB_j)$$

$$c_{ij} = \frac{1}{2}(A_iB_j + A_jB_i \qquad (4.31)\text{a, b, c, d}$$

$$d_{ij} = \frac{1}{2}(A_iB_j - A_jB_i)$$

$$C_{nij} = A_{nij}\,\omega_i\omega_j - B_{nij} \qquad (4.32)$$

$$D_{nij} = A_{nij}\,\omega_i\omega_j + B_{nij} \qquad (4.33)$$

The coefficients C_{nij} and D_{nij} are calculated with Equation (3.60); as noted at the end of § 3, only the symmetric parts are required.

These formulas are valid for any geometry; the modal frequencies may have any values. Considerable simplification may accompany special cases. Most of the following discussion will be concerned with problems involving purely longitudinal modes, for which $\omega_n = n\omega_1$.

The interval of averaging remains unspecified. Two possible ties are fairly obvious: $\tau = \tau_1$, the period of the fundamental oscillation; and $\tau = \tau_n$, the period of the n^{th} mode. In the first case, each equation is averaged over the same interval, while if $\tau = \tau_n$, each equation is averaged over its own period. Partly because the argument leading to (4.14) and (4.15) is not rigorous, there is no wholly satisfying reason for choosing one or the other alternative. If the same interval, $\tau = \tau_1$, is used for all equations, then it is necessary, for (4.8) to be satisfied, that the amplitude and phase of the n^{th} oscillation not change much in roughly n of its own periods. This same condition must be met if $\tau = \tau_n$ in each of the n equations.

For in the equation n = 1, a_n and φ_n can be taken outside the integral only if they are nearly constant over the interval $\tau_1 = n\,\tau_n$.

In all the problems considered here, the motions are in fact dominated by the fundamental mode: the time scale of the slow changes is usually longer than τ_1, and is essentially the same for all modes. Hence, the choice $\tau = \tau_1$ is appealing and will be used here. It happens also that in some cases the equations are somewhat simpler. Comparison of numerical results for the two possibilities has not been made.

V. AN EXAMPLE OF AMPLITUDE MODULATION

It appears that applications of the method of averaging, and the procedure based on expansion in two time variables as well, have been restricted to problems for which the function F_n, Equation (4.1), is periodic. This is true, for example, if the modal frequencies ω_n are integral multiples of the fundamental, $\omega_n = n\omega_1$. Because the specific examples discussed later are, for simplicity, also based on the condition that $\omega_n = n\omega_1$, it is useful to examine a simple case in which the frequencies are not so related. This may serve not to prove but to suggest the validity of Equations (4.14) and (4.15). The practical importance of this conclusion is considerable, for one is then in a position to treat nonlinear problems involving tangential and mixed tangential/axial modes which are commonly unstable in certain kinds of combustion chambers.

Consider the simple problem of two oscillators linearly coupled and described by the equations

$$\ddot{\eta}_1 + \omega_1^2 \eta_1 = K\eta_2 \tag{5.1}$$

$$\ddot{\eta}_2 + \omega_1^2 \eta_2 = K\eta_1 \tag{5.2}$$

Equations (4.18) and (4.19) reduce to

$$\frac{dA_i}{dt} = -\frac{K}{2\omega_i}\left[(g_{ij} + \ell_{ij})A_j + (f_{ij} + h_{ij})B_j\right] \tag{5.3}$$

$$\frac{dB_i}{dt} = \frac{K}{2\omega_i}\left[(g_{ij} - \ell_{ij})B_j - (f_{ij} - h_{ij})A_j\right] \tag{5.4}$$

Here, if i = 1, then j = 2 and conversely, giving four equations. For the case when the two oscillators have nearly the same frequency, $\omega_1+\omega_2 \approx 2\omega_1$, $\omega_1-\omega_2 \approx 0$, so $h_{ij} \to 1$ and f_i, g_i, $\ell_{ij} \to 0$. It is then a simple matter to show that the A_i, B_i all satisfy the same equation,

$$\left[\frac{d^2}{dt^2} + \frac{(K/2)^2}{\omega_1\omega_2}\right]\begin{Bmatrix} A_i \\ B_i \end{Bmatrix} = 0 \tag{5.5}$$

The coefficients all oscillate at the "beat frequency," approximately equal to $K/2\omega_1$.

For example, if the initial condition is $\eta_1 = 0$, $\eta_2 \neq 0$, then a solution is

$$\eta_1 = C_1 \sin\left(\frac{K}{2\omega_1}t\right) \sin \omega_1 t \tag{5.6}$$

$$\eta_2 = C_2 \cos\left(\frac{K}{2\omega_1}t\right) \cos \omega_1 t \tag{5.7}$$

VI. LONGITUDINAL MODES: $\omega_n = n\omega_1$

This special case will serve as the basis for many of the examples discussed later. The integrands in (4.14) and (4.15) are now periodic, with period τ_1; the limits on the integrals can therefore be changed from $(t, t+\tau)$ to $(0, \tau)$. In accord with the remarks at the end of §4, $\tau = \tau_1$. Then (4.14) and (4.15) become

$$\frac{dA_n}{dt} = \frac{1}{2\pi n} \int_0^{2\pi/\omega_1} F_n(t)\cos \omega_n t \, dt \tag{6.1}$$

$$\frac{dB_n}{dt} = -\frac{1}{2\pi n} \int_0^{2\pi/\omega_1} F_n(t)\sin \omega_n t \, dt \tag{6.2}$$

The linear coupling terms (4.20) - (4.23) all vanish when $\omega_n = n\omega_1$, and the only non-zero values of (4.26) - (4.29) are

$$T_{1+}^{nij} = \delta_{n,\,i+j} \qquad T_{1-}^{nij} = \delta_{n,\,i-j} + \delta_{n,\,j-i} \tag{6.3}$$

$$T_{4+}^{nij} = \delta_{n,\,i+j} \qquad T_{4-}^{nij} = \delta_{n,\,i-j} - \delta_{n,\,i+j} \tag{6.4}$$

The equations (4.16) and (4.17) are now

$$\frac{dA_n}{dt} = -\frac{1}{2} D_{nn} A_n - \frac{1}{2} \frac{E_{nn}}{\omega_n} B_n - \frac{1}{2\omega_n} \sum_{i=1}^{\infty} \sum_{j=1}^{\infty} \left[C_{nij} a_{ij} \delta_{n,\,i+j} + D_{nij}\, b_{nij} (\delta_{n,i-j} + \delta_{n,i+j}) \right] \tag{6.5}$$

$$\frac{dB_n}{dt} = -\frac{1}{2} D_{nn} B_n + \frac{1}{2} \frac{E_{nn}}{\omega_n} A_n - \frac{1}{2\omega_n} \sum_{i=1}^{\infty} \sum_{j=1}^{\infty} \left[C_{nij}\, c_{ij}\, \delta_{n,\,i+j} - D_{nij}\, d_{ij} (\delta_{n,i-j} - \delta_{n,j-1}) \right] \tag{6.6}$$

With the mode shape $\psi_n = \cos k_n z$, the integral I_{nij} is

$$I_{nij} = \frac{v}{4} (\delta_{n,\,i+j} + \delta_{n,\,i-j} + \delta_{n,\,j-i}) \tag{6.7}$$

and the formula (3.60) gives eventually

$$C_{nij} = -\frac{\bar{\bar{\gamma}}+1}{4\bar{\gamma}} \{\omega_n^2 - (\omega_j^2 - \omega_i^2)\} \delta_{n,\,i+j} + \frac{1}{4\bar{\gamma}} \{[2\omega_n^2 - (\bar{\gamma}-1)(\omega_j+\omega_i)^2] + (3-\bar{\gamma})(\omega_j^2 - \omega_i^2)\} (\delta_{n,\,i-j} + \delta_{n,\,j-i}) \tag{6.8}$$

$$D_{nij} = -\frac{1}{4\bar{\gamma}}\{[2\omega_n^2-(\bar{\gamma}-1)(\omega_j-\omega_i)^2] + (3-\bar{\gamma})(\omega_j^2-\omega_i^2)\}\delta_{n,\,i+j}$$

$$+\frac{\bar{\gamma}+1}{4\bar{\gamma}}\{\omega_n^2 + (\omega_j^2 - \omega_i^2)\}(\delta_{n,i-j} + \delta_{n,j-i}) \tag{6.9}$$

Let

$$\alpha_n = -\frac{1}{2}D_{nn} \qquad \theta_n = -\frac{1}{2\omega_n}E_{nn} \tag{6.10}$$

and after some arithmetic, Equations (6.5) and (6.6) can be put in the form:

$$\frac{dA_n}{dt} = \alpha_n A_n + \theta_n B_n + \frac{\beta_n}{2}\sum_{i=1}^{\infty}[A_i(A_{n-i}-A_{i-n}-A_{n+i}) - B_i(B_{n-i}+B_{i-n}+B_{n-i})]$$

$$+\frac{\beta_n}{2}\sum_{i=1}^{\infty}\left\{\frac{1}{\omega_n^2}A_i[(\omega_{n-i}^2-\omega_i^2)A_{n-i}-(\omega_{i-n}^2-\omega_i^2)A_{i-n}-(\omega_{n+i}^2-\omega_i^2)A_{n+i}]\right. \tag{6.11}$$

$$\left.-\frac{1}{\omega_n^2}B_i[(\omega_{n-i}^2-\omega_i^2)B_{n-i}+(\omega_{i-n}^2-\omega_i^2)B_{i-n}+(\omega_{n+i}^2-\omega_i^2)B_{n+i}]\right\}$$

$$\frac{dB_n}{dt} = \alpha_n B_n - \theta_n A_n + \frac{\beta_n}{2}\sum_{i=1}^{\infty}[A_i(B_{n-i}+B_{i-n}-B_{n+i}) + B_i(A_{n-i}-A_{i-n}+A_{n+i})]$$

$$+\frac{\beta_n}{2}\sum_{i=1}^{\infty}\left\{\frac{1}{\omega_n^2}A_i[(\omega_{n-i}^2-\omega_i^2)B_{n-i}+(\omega_{i-n}^2-\omega_i^2)B_{i-n}-(\omega_{n+i}^2-\omega_i^2)B_{n+i}]\right. \tag{6.12}$$

$$\left.+\frac{1}{\omega_n^2}B_i[(\omega_{n-i}^2-\omega_i^2)A_{n-i}-(\omega_{i-n}^2-\omega_i^2)A_{i-n}+(\omega_{n+i}^2-\omega_i^2)A_{n+i}]\right\}$$

where

$$\beta = \frac{\bar{\gamma}+1}{8\bar{\gamma}} \tag{6.13}$$

The first series in (6.11) and (6.12) arise from the symmetric parts of C_{nij} and D_{nij}. One can verify directly, in accord with the remark fol-

lowing (3.60) that, because terms cancel one another by pairs, the second series in (6.10) and (6.11) vanish. Consequently, the equations to be solved for problems involving purely longitudinal modes are

$$\frac{dA_n}{dt} = \alpha_n A_n + \theta_n B_n + \frac{\beta n}{2} \sum_{i=1}^{\infty} [A_i(A_{n-i} - A_{i-n} - A_{n+i}) - B_i(B_{n-i} + B_{i-n} + B_{n+i})] \qquad (6.14)$$

$$\frac{dB_n}{dt} = \alpha_n B_n - \theta_n A_n + \frac{\beta n}{2} \sum_{i=1}^{\infty} [A_i(B_{n-i} + B_{i-n} - B_{n+i}) + B_i(A_{n-i} - A_{i-n} + A_{n+i})] \qquad (6.15)$$

Some numerical examples are given in Section 10 and 11. For most cases considered, five modes will be treated. The explicit equations, obtained from (6.14) and (6.15), are

$$\frac{dA_1}{dt} = \alpha_1 A_1 + \theta_1 B_1 - \beta(A_1A_2 + A_2A_3 + A_3A_4 + A_4A_5) - \beta(B_1B_2 + B_2B_3 + B_3B_4 + B_4B_5) \qquad (6.16a)$$

$$\frac{dB_1}{dt} = \alpha_1 B_1 - \theta_1 A_1 + \frac{\beta}{2}[(B_1A_2 - A_1B_2) + (B_2A_3 - A_2B_3) + (B_3A_4 - B_4A_3) + (B_4A_5 - B_5A_4)] \qquad (6.16b)$$

$$\frac{dA_2}{dt} = \alpha_2 A_2 + \theta_2 B_2 + \beta A_1^2 - 2\beta(A_1A_3 + A_2A_4 + A_3A_5) - \beta B_1^2 - 2\beta(B_1B_3 + B_2B_4 + B_3B_5) \qquad (6.17a)$$

$$\frac{dB_2}{dt} = \alpha_2 B_2 - \theta_2 A_2 + 2\beta[B_1A_1 + (B_1A_3 - B_3A_1) + (B_2A_4 - B_4A_2) + (B_3A_5 - B_5A_2)] \qquad (6.17b)$$

$$\frac{dA_3}{dt} = \alpha_3 A_3 + \theta_3 B_3 + 3\beta A_1A_2 - 3\beta(A_1A_4 + A_2A_5) - 3\beta(B_1B_2 + B_1B_4 + B_2B_5) \qquad (6.18a)$$

$$\frac{dB_3}{dt} = \alpha_3 B_3 - \theta_3 A_3 + 3\beta(B_1A_2 + B_1A_4 + B_2A_1 + B_2A_5) - 3\beta(A_1B_4 + A_2B_5) \qquad (6.18b)$$

$$\frac{dA_4}{dt} = \alpha_4 A_4 + \theta_4 B_4 + 4\beta(\tfrac{1}{2}A_2^2 + A_1 A_2 - A_1 A_5) - 4\beta(\tfrac{1}{2}B_2^2 + B_1 B_3 + B_1 B_5) \qquad (6.19a)$$

$$\frac{dB_4}{dt} = \alpha_4 B_4 - \theta_4 A_4 + 4\beta(A_1 B_3 + A_2 B_2 + A_3 B_1 + A_5 B_1) - 4\beta(A_1 B_5) \qquad (6.19b)$$

$$\frac{dA_5}{dt} = \alpha_5 A_5 + \theta_5 B_5 + 5\beta(A_1 A_4 + A_2 A_3) - 5\beta(B_1 B_4 + B_2 B_3 \qquad (6.20a)$$

$$\frac{dB_5}{dt} = \alpha_5 B_5 - \theta_5 A_5 + 5\beta(A_1 B_5 + B_1 A_4 + A_2 B_3 + B_3 A_2) \qquad (6.20b)$$

VII. AN APPROXIMATION TO THE INFLUENCE OF TRANSIENT SURFACE COMBUSTION

Only the simplest representation of the influence of unsteady combustion processes will be covered here. Elementary results for the linear response to harmonic pressure variations form the basis. Certain of the features of truly transient behavior will be ignored in the interest of obtaining formulas which are clear and inexpensive to use.

The influence of surface combustion is contained in $\mathcal{R}$, defined by Equation (3.42). It follows from (3.40) that the corresponding contribution to the force F_n in (4.1) is

$$F_n^{(c)} = \frac{\bar{\gamma}}{\rho_o E_n^2} \frac{\partial}{\partial t} \iint_S \mathcal{R}\, \psi_n \, dS \ . \qquad (7.1)$$

To simplify the discussion, consider only one of the pieces of $\mathcal{R}$; e.g., let $\delta_\perp = 1$, $\delta_\parallel = 0$, so (3.42) is

$$\mathcal{R} = \rho_o u_b' + \bar{u}_b \frac{p'}{a_o^2} = (1+\varkappa)\left(m_b' + \bar{m}_b \frac{\Delta T'}{T_o}\right) \ . \qquad (7.2)$$

It is best here also to avoid the complications associated with a condensed phase: set $\varkappa = 0$, so the following results apply to propellants not containing metal.

There exists a class of analysis, discussed by Culick (1968), which produces a formula for $\hat{m}_b/\bar{m}_b$, the fluctuation of mass flux due to a sinusoidal variation of pressure. This is a linear result, $\hat{m}_b/\bar{m}_b$ being proportional to the pressure fluctuation:

$$\frac{\hat{m}_b}{\bar{m}_b} = R_b \frac{\hat{p}}{p_o} = [R_b^{(r)} + iR_b^{(i)}] \frac{\hat{p}}{p_o} \quad . \tag{7.3}$$

The response function, R_b, is a complex function of frequency,

$$R_b = \frac{nAB}{\lambda + \frac{A}{\lambda} - (1+A) + AB} \quad , \tag{7.4}$$

in which A is proportional to the activation energy for the surface reaction, and B depends on both A and the heat released by the surface reaction. Out of the same analyses, one can extract the formula for $\Delta\hat{T}/T_o$ [see also Krier, et al. (1968)]:

$$\frac{\Delta\hat{T}}{T_o} = \left[\frac{\bar{T}_s}{T_o} \frac{C}{C_p} \frac{AB}{E} (R_b - n) - \frac{\gamma - 1}{\gamma} \right] \frac{\hat{p}}{p_o} \quad . \tag{7.5}$$

Consequently, if these results are used, (7.2) becomes, for sinusoidal motions,

$$\hat{R} = \rho_o \bar{u}_b \left[\left(1 + \frac{\bar{T}_s}{T_o} \frac{C}{C_p} \frac{AB}{E} \right) R_b - \left(n \frac{\bar{T}_s}{T_o} \frac{C}{C_p} \frac{AB}{E} + \frac{\gamma - 1}{\gamma} \right) \right] \frac{\hat{p}}{p_o}$$

$$= \rho_o \bar{u}_b [\mathcal{R}^{(r)} + i\mathcal{R}^{(i)}] \frac{\hat{p}}{p_o} \tag{7.6}$$

Note that $\mathcal{R}^{(r)}$ and $\mathcal{R}^{(i)}$ are dimensionless functions of the frequency and the other parameters; if nonisentropic temperature fluctuations are ignored, $\mathcal{R}_i^{(r)} = R_b^{(r)}(\omega_i)$ and $\mathcal{R}_i^{(i)} = R_b^{(i)}(\omega_i)$.

Now the formula (7.6) is, by construction, for steady sinusoidal variations only. The approximation suggested here is a means of using the formula under conditions when the amplitude and phase of the oscillations are varying in time. This is done by noting that for sinusoidal motions, i is equal to

$\omega^{-1}\,\partial/\partial t$. The replacement is made in (7.6), and assumed to apply to all modes. Thus, $\hat{p}/p_o$ stands for $\eta_i\psi_i$, and for an arbitrary pressure field expanded in the form (1.6), R in (7.1) will hereafter be taken as

$$R = \rho_o \bar{u}_b \sum_{i=1}^{\infty} \left[R_i^{(r)} + \frac{1}{\omega_i} R_i^{(i)} \frac{\partial}{\partial t} \right] \eta_i \psi_i \quad . \tag{7.7}$$

The subscript $(\ )_i$ on $R_i^{(r)}$ and $R_i^{(i)}$ means that each function is evaluated at the frequency of the i^{th} mode; these quantities can be calculated from (7.6) and (7.4).

The force (7.1) is now

$$F_n^{(c)} = \frac{\gamma \bar{u}_b}{E_n^2} \sum_{i=1}^{\infty} \left[R_i^{(r)} \dot{\eta}_i - \omega_i R_i^{(i)} \eta_i \right] \iint \psi_n \psi_i dS \quad . \tag{7.8}$$

The further approximation, $\ddot{\eta}_i \approx -\omega_i^2 \eta_i$, has been made in (7.8); this is consistent with approximations already made in deriving the equations (4.1).

Finally, the rule (6.8) gives directly the contributions from surface combustion to $\alpha_n^{(c)}$ and $\theta_n^{(c)}$ to be used in (6.12) and (6.13):

$$\alpha_n^{(c)} = \frac{\gamma \bar{u}_b}{2E_n^2} R_i^{(r)} \oint \psi_n \psi_i dS \tag{7.9}$$

$$\theta_n^{(c)} = - \frac{R_i^{(i)}}{R_i^{(r)}} \alpha_n^{(c)} \tag{7.10}$$

The same procedure can be applied to propellants containing metal; only some details are changed to account for $\varkappa \neq 0$.

A similar approximation can be used for handling combustion within the volume of a chamber as one finds in liquid rockets, thrust augmentors, and rolid rockets exhibiting residual combustion. Although other contributions will in general arise, associated with mass and momentum exchange, the direct contribution of energy release is represented by the terms con-

taining Q and w_p in eq. (2.2). The perturbations are part of P', (2.11), which appears ultimately in H, H_1, and L_1, eqs. (3.30) - (3.32). Those functions are on the right hand sides of the oscillator equations (3.39) and (3.41). The dynamical behavior of combustion within the volume may, for example, be represented by some sort of response function; the well-known n-τ model developed by Crocco and co-workers is a special form. In any case, the contributions to the individual harmonics can be approximated as surface combustion was handled above. No results for bulk combustion have been obtained.

VIII. AN APPROXIMATION TO THE LINEAR AND NONLINEAR ATTENUATION OF WAVES BY GAS/PARTICLE INTERACTIONS

Particularly in solid propellant rockets using metallized propellants, but in other systems as well, some of the combustion products appear in the form of liquid or solid particles. The viscous interacting between the particles and the gas may, under suitable conditions, provide a significant dissipation of energy. It is often the case that the Reynolds number based on the particle diameter is outside the range in which Stokes' law is valid; it is necessary to use a more realistic representation of the drag force. This introduces another nonlinear influence in the general problem.

Let $F_n^{(p)}$ denote that part of F_n in eq. (4.1), representing the influences of inert particles. The terms involved are those containing $\delta\vec{F}'_p$ and $\delta Q'_p$, the fluctuations of (2.8) and (2.9). By tracing the development from (2.10) and (2.11) to (2.18) and (2.19), to (3.8) and (3.9), to (3.40), with H defined by (3.30), one finds that the terms in question are

$$F_n^{(p)} = \frac{\bar{\gamma}}{\rho_o E_n^2} \int \frac{1}{\epsilon} \left[\frac{1}{\bar{a}^2} \frac{\bar{R}}{\bar{C}_v} \frac{\partial}{\partial t} (\delta Q'_p + \delta\vec{u}'_p \cdot \vec{F}_p)\psi_n + \delta\vec{F}'_p \cdot \nabla\psi_n \right] dV \quad . \tag{8.1}$$

The differential heat transfer and force acting, per unit volume, between the condensed phase and the gas are defined by (2.8) and (2.9); explicit formulas can be found only by solving the equations of motion (2.5) and (2.6) with the force $\vec{F}_p$ and heat transfer Q_p specified. Numerical calculations [Levine and Culick (1972, 1974)] have shown that for many practical cases, nonlinear interactions are likely to be important. The approximate analysis here will be based on the nonlinear laws used in those works:

$$\vec{F}_p = \bar{\rho}_p \frac{18\mu}{\rho_s \sigma^2} (\vec{u}_p - \vec{u})\left[1 + \frac{1}{6} \mathrm{Re}^{2/3}\right] \tag{8.2}$$

$$Q_p = \bar{\rho}_p \frac{12 C_p \mu}{Pr \rho_s \sigma^2} (T_p - T)\left[1 + .23\, Pr^{.33} Re^{.55}\right] \tag{8.3}$$

where

$$Re = \frac{\rho_{go} \sigma}{\mu} \left|\vec{u}_p - \vec{u}\right| . \tag{8.4}$$

Hereafter, the real flow will be treated only in a local approximation so that the particle motions may be treated as one-dimensional; interactions between particles are assumed to be negligible. For a single particle, with spatial variations of the motion ignored, the equations to be solved for u'_p and T'_p are

$$\frac{du'_p}{dt} = -\frac{1}{\bar{\rho}_p} F_p = -\frac{18\mu}{\rho_s \sigma^2} (u'_p - u')\left[1 + \frac{1}{6} Re^{2/3}\right] \tag{8.5}$$

$$C \frac{dT'_p}{dt} = -\frac{1}{\bar{\rho}_p} Q_p = -\frac{12 C_p \mu}{Pr \rho_s \sigma^2} (T'_p - T')\left[1 + .23\, Pr^{.33} Re^{.55}\right] \tag{8.6}$$

To evaluate $\delta F'_p$ and $\delta Q'_p$, the quantities $\delta u'_p = u'_p - u'$ and $\delta T'_p = T'_p - T'$ are required; by subtracting du'/dt from (8.5), and dT'/dt from (8.6), one finds the equations

$$\frac{d\delta u'_p}{dt} + \frac{1}{\tau_d} \delta u'_p = -\frac{du'}{dt} - K_1 \frac{\delta u'_p}{\tau_d} \left|\delta u'_p\right|^{2/3} \tag{8.7}$$

$$\frac{d\delta T'_p}{dt} + \frac{1}{\tau_t} \delta T'_p = -\frac{dT'}{dt} - K_2 \frac{\delta T'_p}{\tau_t} \left|\delta u'_p\right|^{.55} \tag{8.8}$$

with

$$\tau_d = \frac{\rho_s \sigma^2}{18\mu} \tag{8.9}$$

$$\tau_t = \frac{3}{2} \frac{C}{C_p} Pr T_d \tag{8.10}$$

$$K_1 = \frac{1}{6} \left(\frac{\rho_{go} \sigma}{\mu}\right)^{2/3} \tag{8.11}$$

$$K_2 = .459\,Pr^{.33}\left(\frac{\rho_{go}\sigma}{\mu}\right)^{.55} \tag{8.12}$$

Comparison of (8.7) and (8.8) with (2.8) and (2.9) (again with spatial variations ignored) gives the formulas

$$\delta F'_p = -\bar{\rho}_p \frac{d\delta u'_p}{dt} = \bar{\rho}_p\left[\frac{1}{\tau_d}\,\delta u'_p + \frac{du'}{dt}\right] + K_1\bar{\rho}_p \frac{\delta u'_p}{\tau_d}\,|\delta u'_p|^{2/3} \tag{8.13}$$

$$\delta Q'_p = -\bar{\rho}_p C \frac{d\delta T'_p}{dt} = \bar{\rho}_p C\left[\frac{1}{\tau_t}\,\delta T'_p + \frac{dT'}{dt}\right] + K_2\bar{\rho}_p C \frac{\delta T'_p}{\tau_t}\,|\delta u'_p|^{.55} \tag{8.14}$$

As an approximation, the nonlinear terms in (8.13) and (8.14) will be evaluated by using the linear solutions for $\delta u'_p$ and $\delta T'_p$. With $K_1 = K_2 = 0$, the linear solutions to (8.7) and (8.8), satisfying the initial conditions $\delta u'_p = \delta u'_{po}$, $\delta T'_p = \delta T'_{po}$ at $t = t_o$, are

$$\delta u'_p = \left[\frac{1}{\tau_d} e^{-t/\tau_d} \int_{t_o}^{t} e^{t'/\tau_d} u'(t')dt' - u'(t)\right] - \left[\delta u'_{po} - u'(t_o)\right] e^{-(t-t_o)/\tau_d} \tag{8.15}$$

$$\delta T'_p = \left[\frac{1}{\tau_t} e^{-t/\tau_d} \int_{t_o}^{t} e^{t'/\tau_t} T'(t')dt' - T'(t)\right] - \left[\delta T'_{po} - T'(t_o)\right] e^{-(t-t_o)/\tau_t} \tag{8.16}$$

The second parts, arising from the initial conditions, represent short term transients which are negligible for $t - t_o \gg \tau_d$. If these are retained, they will introduce in the oscillator equations (4.1) terms which depend explicitly on the history of the motions. In the interests of simplifying the analysis, these terms will be ignored. This is an approximation which is accurate only if the periods of the oscillations (all harmonics) are long compared with τ_d. For the n^{th} acoustic mode, the velocity and temperature fluctuations are

$$u' = \frac{1}{\bar{\gamma} k_n^2}\,\dot{\eta}_n \frac{d\psi_n}{dz}, \quad T' = \left(\frac{\bar{\gamma}-1}{\bar{\gamma}}\right) T_o \eta_n \psi_n \tag{8.17}$$

where η_n is given by (1. 12). Substitution into (8. 15) and (8. 16) gives

$$\delta u'_p = X_1(\eta_n - \tau_d\dot{\eta}_n)\frac{1}{\bar{\gamma}k_n^2}\frac{d\psi_n}{dz} \tag{8.18}$$

$$\delta T'_p = -\frac{X_2}{\omega_n}\left(\omega_n\tau_t\eta_n + \frac{\dot{\eta}_n}{\omega_n}\right)\frac{\bar{\gamma}-1}{\bar{\gamma}}T_o\psi_n \tag{8.19}$$

The functions A_n and B_n are taken to be constant in this part of the calculation because the results will eventually be used in the right hand sides of (4. 14) and (4. 15); because the short term transients have been ignored, the lower limit on the integrals is $t_o = 0$. Explicit dependence on frequency is contained in X_1 and X_2.

$$X_1 = (\omega_n\Omega_d)/(1+\Omega_d^2) \tag{8.20}$$

$$X_2 = (\omega_n\Omega_t)/(1+\Omega_t^2) \tag{8.21}$$

where

$$\Omega_d = \omega_n\tau_d \quad \text{and} \quad \Omega_t = \omega_n\tau_t \ . \tag{8.22}$$

Substitution of (8. 18) and (8. 19) into (8. 13) and (8. 14) gives for the linear parts only,

$$(\delta F'_p)_{lin} = \frac{\bar{\rho}_p\omega_n}{\bar{\gamma}k_n^2}\left[\left(\frac{X_1}{\omega_n\tau_d} - \omega_n\right)\eta_n - \frac{X_1}{\omega_n}\dot{\eta}_n\right]\frac{d\psi_n}{dz} \tag{8.23}$$

$$(\delta Q'_p)_{lin} = \frac{\bar{\rho}_p\omega_n}{\bar{\gamma}}CT_o(\bar{\gamma}-1)\left[-\frac{X_2}{\omega_n}\eta_n - \left(\frac{X_2}{\omega_n\tau_t} - \omega_n\right)\frac{1}{\omega_n^2}\dot{\eta}_n\right]\psi_n \tag{8.24}$$

These locally one-dimensional results can be used in (8. 1) with $d\psi_n/dz$ replaced by $\nabla\psi_n$ to give

$$[F_n^{(p)}]_{lin} = -\frac{\kappa}{1+\kappa}\left[X_1 + (\bar{\gamma}-1)\frac{C}{\bar{C}_p}X_2\right]\dot{\eta}_n - \omega_n\frac{\kappa}{1+\kappa}\left[\frac{\Omega_d^2}{1+\Omega_d^2} + (\bar{\gamma}-1)\frac{C}{\bar{C}_p}\frac{\Omega_t^2}{1+\Omega_t^2}\right] \tag{8.25}$$

Again by applying the rule (6.8), one finds for the linear contributions from gas/particle interactions:

$$\alpha_n^{(p)} = -\frac{1}{2}\left(\frac{\kappa}{1+\kappa}\right)\left[X_1+(\bar{\gamma}-1)\frac{C}{\bar{C}_p}X_2\right] \tag{8.26}$$

$$\theta_n^{(p)} = \frac{\omega_n}{2}\left(\frac{\kappa}{1+\kappa}\right)\left[\frac{\Omega_d^2}{1+\Omega_d^2}+(\bar{\gamma}-1)\frac{C}{\bar{C}_p}\frac{\Omega_t^2}{1+\Omega_t^2}\right] \tag{8.27}$$

Recent numerical results reported by Levine and Culick (1974) have shown that the result (8.24) is quite good for smaller particles, and if the frequency is not too high. Beyond limits which are presently not well-defined, the Reynolds number (8.4) becomes too large for the linear drag and heat transfer laws to be accurate. Further comments on the accuracy and some examples are given below.

The problem of analyzing nonlinear particle motions is avoided here. A correct treatment would involve solving (8.7) and (8.8), the results then being used in (8.13) and (8.14). A very much simpler course is taken here; the linear solutions are used everywhere for $\delta u_p'$ and $\delta T_p'$. The nonlinear part of the force $F_n^{(p)}$ is

$$\left[F_n^{(p)}\right]_{\text{nonlin}} = \frac{\bar{\gamma}\bar{p}}{\rho_o E_n^2}\left\{\frac{K_1}{\tau_d}\tilde{I}_1+\frac{\bar{R}/\bar{C}_v}{\bar{a}^2}\left[\frac{CK_2}{\tau_t}\tilde{I}_2+\frac{1}{\tau_d}\tilde{I}_3+\frac{K_1}{\tau_d}\tilde{I}_4\right]\right\} \tag{8.28}$$

where the integrals are:

$$\tilde{I}_1 = \int |\delta\vec{u}_p'|^{2/3}\,\delta\vec{u}_p'\cdot\nabla\psi_n\,dV \tag{8.29}$$

$$\tilde{I}_2 = \int \frac{\partial}{\partial t}\left(\delta T_p'|\delta\vec{u}_p'|^{.55}\right)\psi_n dV \tag{8.30}$$

$$\tilde{I}_3 = \int \frac{\partial}{\partial t}(\delta\vec{u}_p')^2\psi_n dV \tag{8.31}$$

$$\tilde{I}_4 = \int \frac{\partial}{\partial t}\left((\delta\vec{u}_p')^2|\delta\vec{u}_p'|^{2/3}\right)\psi_n dV \tag{8.32}$$

To evaluate these integrals, it is easier to re-write the formulas (8.18) and (8.19) for three-dimensional motions as

$$\delta\vec{u}'_p = \left(\frac{X_1}{\bar{\gamma}k_n^2}\right)(1+\Omega_d^2)^{\frac{1}{2}}(A^2+B^2)^{\frac{1}{2}}\sin(\omega_n t+\phi_n^d)\nabla\psi_n \tag{8.33}$$

$$\delta T'_p = -\left(\frac{\bar{\gamma}-1}{\bar{\gamma}}\right)T_o\left(\frac{X_2}{\omega_n^2}\right)(1+\Omega_t^2)^{\frac{1}{2}}(A^2+B^2)^{\frac{1}{2}}\cos(\omega_n t+\phi_n^t)\psi_n \tag{8.34}$$

where

$$\sin\phi_n^d = \frac{(B_n-\Omega_d A_n)}{(1+\Omega_d^2)^{\frac{1}{2}}(A_n^2+B_n^2)^{\frac{1}{2}}}\ , \quad \cos\phi_n^d = \frac{(A_n+\Omega_d B_n)}{(1+\Omega_d^2)^{\frac{1}{2}}(A_n^2+B_n^2)^{\frac{1}{2}}}\ ,$$

$$\sin\phi_n^t = \frac{(B_n-\Omega_t A_n)}{(1+\Omega_t^2)^{\frac{1}{2}}(A_n^2+B_n^2)^{\frac{1}{2}}}\ , \quad \cos\phi_n^t = \frac{(A_n+\Omega_t B_n)}{(1+\Omega_t^2)^{\frac{1}{2}}(A_n^2+B_n^2)^{\frac{1}{2}}}\ . \tag{8.35}$$

The formulas (8.29) - (8.32) become

$$\tilde{I}_1 = I_1 k_n (1+\Omega_d^2)^{\frac{1+\xi_1}{2}}\left(\frac{X_1}{\bar{\gamma}k_n}\right)^{1+\xi_1}(A_n^2+B_n^2)^{\frac{1+\xi_1}{2}}\sin(\omega_n t+\phi_n^d)\left|\sin(\omega_n t+\phi_n^d)\right|^{\xi_1} \tag{8.36}$$

$$\tilde{I}_2 = I_2(1+\Omega_t^2)^{\frac{1}{2}}(1+\Omega_d^2)^{\frac{\xi_2}{2}}\left(\frac{X_1}{\bar{\gamma}k_n}\right)^{\xi_2}\left(\frac{\bar{\gamma}-1}{\bar{\gamma}}T_o\right)\left(\frac{X_2}{\omega_n^2}\right)(A_n^2+B_n^2)^{\frac{1+\xi_2}{2}}$$
$$\frac{d}{dt}\left\{-\cos(\omega_n t+\phi_n^t)\left|\sin(\omega_n t+\phi_n^d)\right|^{\xi_2}\right. \tag{8.37}$$

$$\tilde{I}_3 = I_3\left[\frac{(1+\Omega_d^2)^{\frac{1}{2}}X_1}{\bar{\gamma}k_n}\right]^2(A_n^2+B_n^2)\frac{d}{dt}\left\{\sin^2(\omega_n t+\phi_n^d)\right\} \tag{8.38}$$

$$\tilde{I}_4 = I_4\left[\frac{(1+\Omega_d^2)^{\frac{1}{2}}X_1}{\bar{\gamma}k_n}\right]^{2+\xi_1}(A_n^2+B_n^2)^{\frac{2+\xi_1}{2}}\frac{d}{dt}\left\{\sin^2(\omega_n t+\phi_n^d)\left|\sin(\omega_n t+\phi_n^d)\right|^{\xi_2}\right\} \tag{8.39}$$

where $\xi_1 = 2/3$, $\xi_2 = 55$ and the integrals involving the mode shapes are

$$I_1 = \frac{1}{k_n^{2+\xi_1}}\int(\nabla\psi_n)^2\left|\nabla\psi_n\right|^{\xi_1}dV \tag{8.40}$$

$$I_2 = \frac{1}{k_n^{\xi_2}}\int\psi_n^2\left|\nabla\psi_n\right|^{\xi_2}dV \tag{8.41}$$

$$I_3 = \frac{1}{k_n^2}\int \psi_n(\nabla\psi_n)^2 dV \tag{8.42}$$

$$I_4 = \frac{1}{k_n^{2+\xi_2}}\int \psi_n(\nabla\psi_n)^2\,|\nabla\psi_n|^{\xi_2} dV \tag{8.43}$$

For comparison with numerical results, these integrals will be evaluated for longitudinal modes in a uniform chamber. Then $dV = S_c dz$ and $\psi_n = \cos k_n z$ with $k_n = n\pi/L$ and $0 \le z \le L$. By making use of the periodicity of ψ_n, and with $\theta = k_n z$, one can show that the values are

$$I_1 = \frac{2nS_c}{k_n}\int_0^{\pi/2} \sin^{2+\xi_1}\theta d\theta = \frac{nS_c}{k_n} 2^{2+\xi_1} \frac{\left[\Gamma\left(\frac{3+\xi_1}{2}\right)\right]^2}{\Gamma(3+\xi_1)} = .698\left(\frac{nS_c}{k_n}\right) \tag{8.44}$$

$$I_2 = \frac{2nS_c}{k_n}\int_0^{\pi/2} \cos^2\theta\sin^{\xi_2}\theta d\theta = \frac{nS_c}{k_n}\frac{\Gamma\left(\frac{3}{2}\right)\Gamma\left(\frac{1+\xi_2}{2}\right)}{\Gamma\left(\frac{4+\xi_2}{2}\right)} = .644\left(\frac{nS_c}{k_n}\right) \tag{8.45}$$

$$I_3 = \frac{S_c}{k_n}\int_0^{n\pi} \cos\theta\sin^2\theta\, d\theta = 0 \tag{8.46}$$

$$I_4 = \frac{S_c}{k_n}\int_0^{n\pi} \cos\theta\,|\sin\theta|^{2+\xi_2} d\theta = 0 \tag{8.47}$$

To simplify writing, assume only here that $\tau_t = \tau_d$, which is very closely true in many practical cases, so $\phi_n^d = \phi_n^t = \phi_n$, and define the functions

$$\zeta_n(t) = \sin(\omega_n t+\phi_n)\,|\sin(\omega_n t+\phi_n)|^{\xi_1} \tag{8.48}$$

$$\chi_n(t) = \frac{1}{\omega_n}\frac{d}{dt}\left\{-\cos(\omega_n t+\phi_n)\,|\sin(\omega_n t+\phi_n)|^{\xi_2}\right\} \tag{8.49}$$

With all the preceding brought together, the nonlinear part of the force (8.1) is

$$\left[F_n^{(p)}\right]_{\text{nonlin}} = \omega_n\left(\frac{\kappa}{1+\kappa}\right)\left\{W_{n1}(1+\Omega_d^2)^{\frac{1}{2}}(A_n^2+B_n^2)^{\frac{1+\xi_1}{2}}\omega_n\zeta_n(t) + W_{n2}(1+\Omega_t^2)^{\frac{1}{2}}(A_n^2+B_n^2)^{\frac{1+\xi_2}{2}}\omega_n\chi_n(t)\right\} \tag{8.50}$$

where

$$W_{n1} = \frac{2}{\pi}(.698)(1+\Omega_d^2)^{\frac{\xi_1}{2}} K_1\left(\frac{\bar{a}X_1}{\bar{\gamma}\omega_n}\right)^{\xi_1}\left(\frac{X_1}{\omega_n\Omega_d}\right) , \tag{8.51}$$

$$W_{n2} = \frac{2}{\pi}(.644)(1+\Omega_d^2)^{\frac{\xi_2}{2}} (\bar{\gamma}-1)\frac{C}{\bar{C}_p} K_2\left(\frac{\bar{a}X_1}{\bar{\gamma}\omega_n}\right)^{\xi_2}\left(\frac{X_2}{\omega_n\Omega_t}\right) . \tag{8.52}$$

The time-averaging of (8.49) according to (4.14) and (4.15), with $\tau = \tau_1$ (see the remarks at the end of § 4) requires the integrals

$$I_5 = \frac{1}{\omega_n\tau_1}\int_0^{2\pi/\omega_1} \omega_n\zeta_n \begin{Bmatrix}\cos\omega_n t\\ -\sin\omega_n t\end{Bmatrix} dt = \frac{1}{2\pi}\int_0^{2\pi n} \zeta_n \begin{Bmatrix}\cos\theta\\ -\sin\theta\end{Bmatrix} d\theta$$

$$I_6 = \frac{1}{\omega_n\tau_1}\int_0^{2\pi/\omega_1} \omega_n\chi_n \begin{Bmatrix}\cos\omega_n t\\ -\sin\omega_n t\end{Bmatrix} dt = \frac{1}{2\pi}\int_0^{2\pi n} \chi_n \begin{Bmatrix}\cos\theta\\ -\sin\theta\end{Bmatrix} d\theta$$

where $\theta = \omega_n t$. With ζ_n and χ_n given by (8.48) and (8.49), the integrals are

$$I_5 = \frac{1}{2\pi}\int_0^{2\pi} \begin{Bmatrix}\cos\theta\\ -\sin\theta\end{Bmatrix} \sin(\theta+\phi_n)\left|\sin(\theta+\phi_n)\right|^{\xi_1} d\theta$$

$$I_6 = -\frac{1}{2\pi}\int_0^{2\pi} \begin{Bmatrix}\cos\theta\\ -\sin\theta\end{Bmatrix} \frac{d}{d\theta}\left\{\cos(\theta+\phi_n)\left|\sin(\theta+\phi_n)\right|^{\xi_2}\right\} d\theta$$

Because the integrands have period 2π, the limits on the integrals have been changed from $(0, 2\pi n)$ to $(0, 2\pi)$; the integrals are then multiplied by n, giving the factor $n/\omega_n\tau_1 = (2\pi)^{-1}$. Now let $\psi = \phi+\phi_n$; the limits become $(\phi, 2\pi+\phi)$ which, again because of periodicity, can be changed to $(0, 2\pi)$. Moreover, it is easy to show that the integrals over $(\pi, 2\pi)$ are equal to those over $(0, \pi)$, so one has

$$I_5 \quad \frac{1}{\pi}\int_0^{\pi} \begin{Bmatrix}\cos\psi\cos\phi_n+\sin\psi\sin\phi_n\\ -\sin\psi\cos\phi_n+\cos\psi\sin\phi_n\end{Bmatrix} \sin^{1+\xi_1}\psi\, d\psi$$

$$I_6 = -\frac{1}{\pi}\int_0^{\pi}\begin{Bmatrix}\cos\psi\cos\phi_n+\sin\psi\sin\phi_n\\ -\sin\psi\cos\phi_n+\cos\psi\sin\phi_n\end{Bmatrix}\left\{(1+\xi_2)\sin^{1+\xi_2}\psi-\xi_2\sin^{\xi_2-1}\psi\right\}d\psi$$

All integrals containing $\cos\psi$ vanish, and those containing $\sin\psi$ can be reduced further to the interval $(0, \pi/2)$, giving the results

$$I_5 = 2\begin{Bmatrix}\sin\phi_n\\ -\cos\phi_n\end{Bmatrix}\int_0^{\pi/2}\sin^{2+\xi_1}\psi\,d\psi$$

$$I_6 = \frac{2}{\pi}\begin{Bmatrix}\sin\phi_n\\ -\cos\phi_n\end{Bmatrix}\left[(1+\xi_2)\int_0^{\pi/2}\sin^{2+\xi_2}\psi d\psi - \xi_2\int_0^{\pi/2}\sin^{\xi_2}\psi\,d\psi\right]$$

For $\xi_1 = 2/3$, the integral in I_5 has the value 0.698 as in (8.44), and for $\xi_2 = 0.55$, the integrals in I_6 are

$$\int_0^{\pi/2}\sin^{2+\xi_2}\psi d\psi = 0.713\ , \qquad \int_0^{\pi/2}\sin^{\xi_2}\psi d\psi = 1.175\ .$$

Finally, then, the integrals are

$$I_5 = \frac{1.396}{\pi}\begin{Bmatrix}\sin\phi_n\\ -\cos\phi_n\end{Bmatrix} \tag{8.53}$$

$$I_6 = \frac{.918}{\pi}\begin{Bmatrix}\sin\phi_n\\ -\cos\phi_n\end{Bmatrix} \tag{8.54}$$

After $\sin\phi_n$ and $\cos\phi_n$ are replaced by their definitions (8.35), one finds for the contributions to $\dot{A}_n$ and $\dot{B}_n$, from nonlinear gas/particle interactions:

$$\frac{dA_n}{dt} = \omega_n\left(\frac{\kappa}{1+\kappa}\right)\left\{V_{n1}(B_n-\Omega_d A_n)+V_{n2}(B_n-\Omega_t A_n)\right\} \tag{8.55}$$

$$\frac{dB_n}{dt} = \omega_n\left(\frac{\kappa}{1+\kappa}\right)\left\{V_{n1}(-A_n-\Omega_d B_n)+V_{n2}(-A_n-\Omega_t B_n)\right\} \tag{8.56}$$

where

$$V_{n1} = \frac{1.396}{\pi}W_{n1}(A_n^2+B_n^2)^{.333}\ , \tag{8.57a}$$

$$V_{n2} = \frac{.918}{\pi} W_{n2}(A_n^2+B_n^2)^{.275} \quad . \tag{8.57b}$$

Note that in (8.55) and (8.56), Ω_d appears explicitly in two places, and Ω_t in two places. Actually, what arises is $\Omega = x_n \tau$ where, because of the assumption preceding (8.48), $\tau = \tau_t \approx \tau_d$. The arbitrary choice $\tau = \tau_t$ or $\tau = \tau_d$ has been made where suitable to simplify somewhat (8.55) and (8.56). The numerical errors incurred should normally be very small.

A few results have been obtained for the attenuation of a standing wave initially excited in a box of length L containing a gas/particle mixture. These have been carried out for direct comparison with the numerical results reported by Levine and Culick (1974). First, two cases will be given in some detail. The particle diameter is 2.5 microns, the particle loading is $K = 0.36$ and the frequency based on the equilibrium speed of sound $\bar{a}$ is 800 Hz in each case. The material and thermodynamic properties are listed below:

Specific heat of the gas	$C_p = 2021.8$ Joule/kgm-^oK
Specific heat of the particle material	$C_s = 0.68\ C_p$
Isentropic exponent of the gas	$\gamma = 1.23$
Prandtl number	$Pr = 0.8$
Temperature	$T = 3416\ ^oK$
Pressure	$P_o = 500$ psi
Viscosity of the gas	$\mu = 8.834 \times 10^{-4} \left(\frac{T}{3485}\right)^{.66}$ kgm/m-sec
Density of the condensed material	$\rho_s = 1766$ kgm/m^3

The only difference between the two cases is that for one, the initial amplitude is $\Delta p/p_o = 0.03$ and for the other $\Delta p/p_o = 0.15$.

Figures 8-1 and 8-2 show the waveforms obtained from the approximate and numerical analyses. The approximate results are the solutions to Equations (6.16)-(6.20); the linear coefficients α_n, θ_n are given by (8.26) and (8.27) and the additional nonlinear terms by (8.55) and (8.56). The period used to normalize the time scale is the period $2L/\bar{a}$ for linear waves based on the speed of sound of the mixture. The similarities between the waveforms and the generation and decay of the even harmonics is apparent. There is a difference in the relative phases between the even harmonics and the total waveform. This seems to arise almost entirely in the first cycle of the oscillation; it may be due to details of the numerical routines and the way in which the computations begin. This difference may therefore not reflect a genuine difference between the approximate and "exact" analyses.

A more quantitative measure of the behavior is the instantaneous value of the decay constant, α_p, calculated for successive peaks of the waveform. The histories of α_p for the two cases are shown in Figures 8-3 and 8-4. Further remarks on the behavior of α_p may be found in § 7 of the report by Levine and Culick (1974). The purpose here is only to demonstrate that the approximate analysis does give fairly reasonable results for this case. There are, however, limitations, not yet clearly defined, which arise from the approximate treatment of the nonlinear acoustics as well as the gas/particle interactions.

The linear behavior used here, described essentially by the velocity and temperature lags given by (8.18) and (8.19), is, in fact, quite restrictive. Although it is not apparent from the analyses presented here, the work reported by Levine and Culick shows that the results (8.18) and (8.19) are accurate only when $\omega \tau_d$ is small. If this condition is met, then δu_p

and δT_p are relatively small, which is consistent with the general nature of the perturbation analysis used here. For the 2.5-micron particles, $\omega\tau_d \approx .08$ at 800 Hz. The waveform and α_p for 10-micron particles at 1500 Hz ($\omega\tau_d \approx 2.4$) are shown in Figs. 8-5 and 8-6 for an initial amplitude of 3 per cent, computed with the approximate analysis. For this case, $\alpha_p \approx -530\ \text{sec}^{-1}$ when the amplitude has decreased to 1 per cent; the more exact numerical calculations give $\alpha_p \approx 870\ \text{sec}^{-1}$. Finally, in Fig. 8-7, the waveform calculated with the approximate analysis is shown for 30-micron particles at 1500 Hz ($\omega\tau_d \approx 25.8$). The value of α_p is $-70\ \text{sec}^{-1}$ at an amplitude of 1 per cent, and the numerical analysis gives $-148\ \text{sec}^{-1}$. Note that the fractional error between the approximate and numerical results for α_p increases with increasing $\omega\tau_d$. The greater amount of harmonic content present when larger particles are considered is due mostly to the reduced drag and hence reduced attenuation at the higher frequencies. The results from the approximate analysis can be improved for higher values of $\omega\tau_d$ by using different functions X_1, X_2 instead of (8.20) and (8.21).

Wave propagation in a gas/particle mixture is dispersive; the speed of propagation depends on the frequency and particle size, through the parameter $\omega\tau_d$, as well as on the amount of condensed material present. For the problems treated here, the length of the box, and hence the wavelength of the waves, is fixed. Consequently, a change in the speed of sound is reflected as a shift of frequency. The periods of the waveforms shown in Figs. 8-1, 8-2, 8-5, and 8-7 are not exactly equal to the period based on the equilibrium speed of sound. It is obvious from the figures that the frequency shift increases with $\omega\tau_d$. In §12, it is shown that to first order, the frequency shift due to linear dispersion is $\delta f = -\theta/2\pi$; here, θ is given by (8.27) for the n^{th} mode. The actual frequency change is dominated by θ_1;

TABLE 8-1

Summary of Results for Waves Attenuated in a Gas/Particle Mixture

Particle Diameter (Microns)	f_e (Hz)	f_f (Hz)	f	$\omega \tau_d$	δf (Hz)	$-\frac{\theta_1}{2\pi}$	$(\alpha_p)_{lin}$ (sec^{-1})	$(\alpha_p)_{1\%}$ (sec^{-1})
2.5								
Approximate	800	954	800	.08	1	.74	-59	-61
Numerical	800	954	801	.08	1	---	-58	-59
Approximate	1500	1788	1505	.15	5	4.8	-203	-204
Numerical	1500	1788	1504	.15	4	---	-201	-204
10								
Approximate	1500	1788	1695	2.4	195	189.9	-509	-530
Numerical	1500	1788	1740	2.8	240	---	-509	-870
30								
Approximate	1500	1788	1740	21.6	240	224.1	-67	-70
Numerical	1500	1788	1787	25.8	287	---	-69	-148

f_e frequency based on the equilibrium

f_f frequency based on the speed for the gas only, $a_g = [(\gamma-1)C_p T]^{\frac{1}{2}}$

f frequency of the calculated wave

$\delta f = f - f_e$

$(\alpha_p)_{lin}$ decay constant for linear waves, Eq. (8.76)

$(\alpha_p)_{1\%}$ decay constant for the calculated wave at approximately 1% amplitude

NOTE: Small differences arise in some quantities ($\omega \tau_d$ and $(\alpha_p)_{lin}$) which should have the same values when calculated by the approximate and numerical methods. This is due to a small difference in the value of some property, most probably the viscosity.

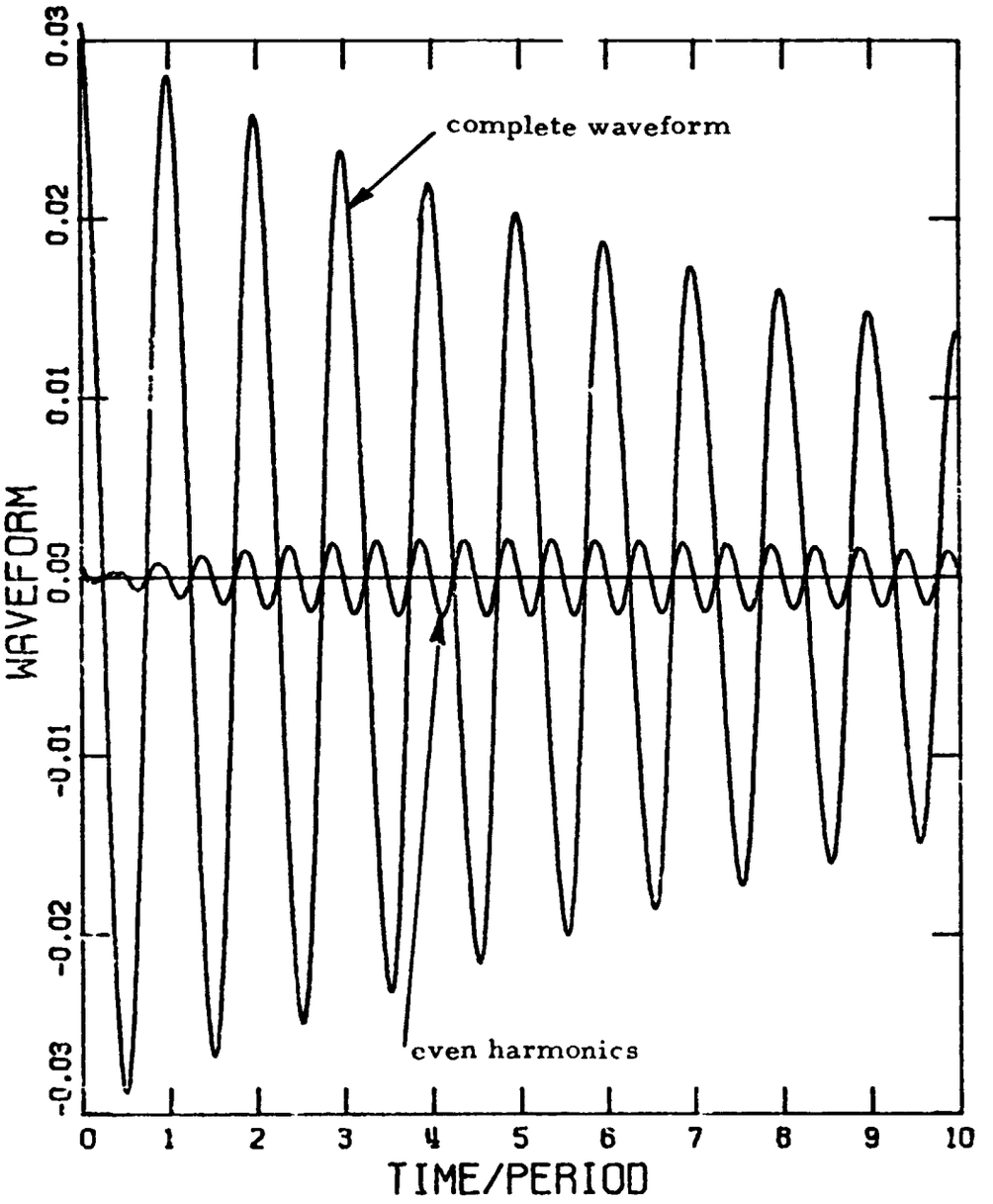

Fig. 8-1(a) Attenuation by 2.5-micron particles at 800 Hz according to the approximate analysis, $\Delta p(0)/p_o = 0.03$.

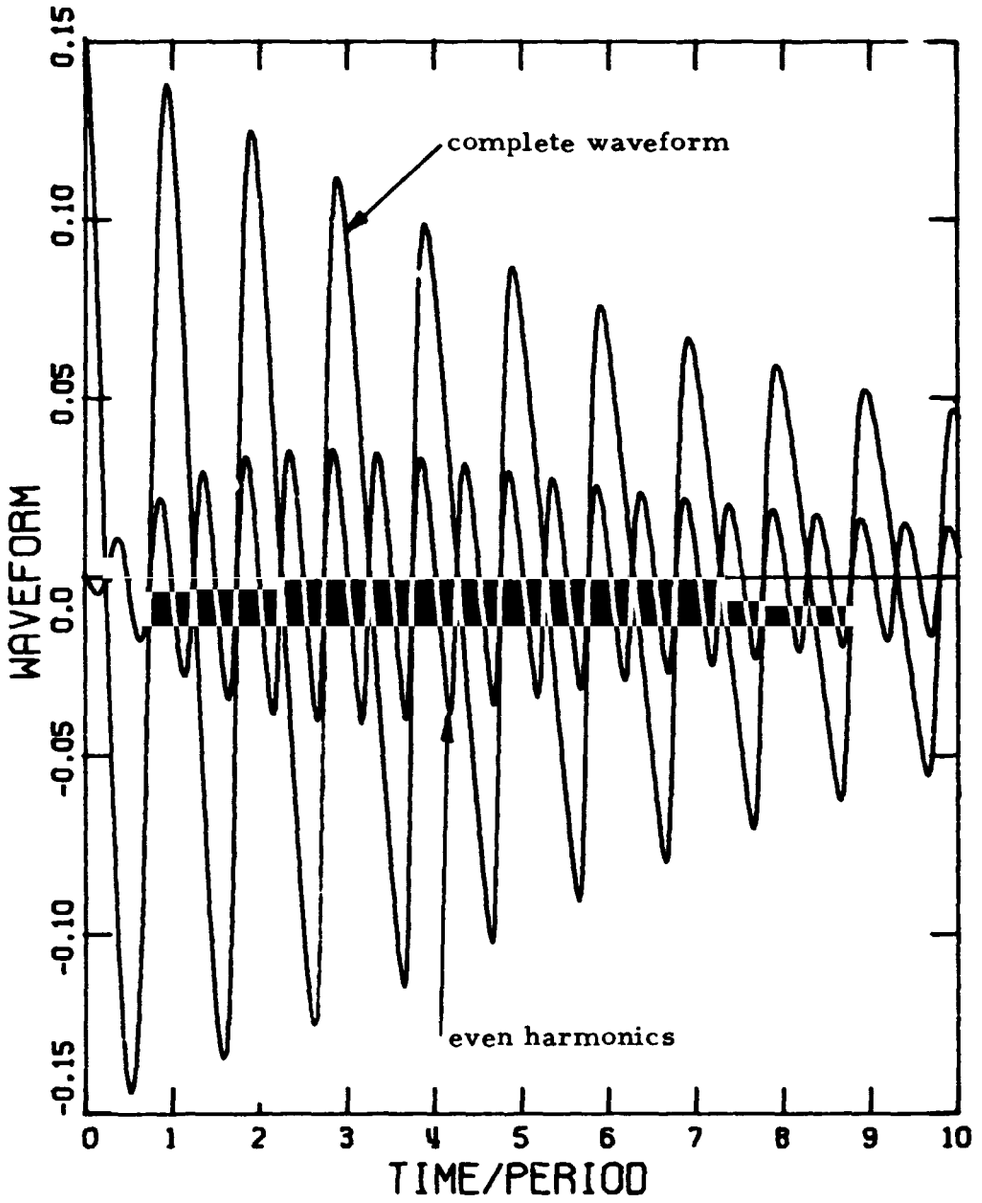

Fig. 8-1(b) Attenuation by 2.5-micron particles at 800 Hz according to the approximate analysis, $\Delta p(0)/p_o$ = 0.15.

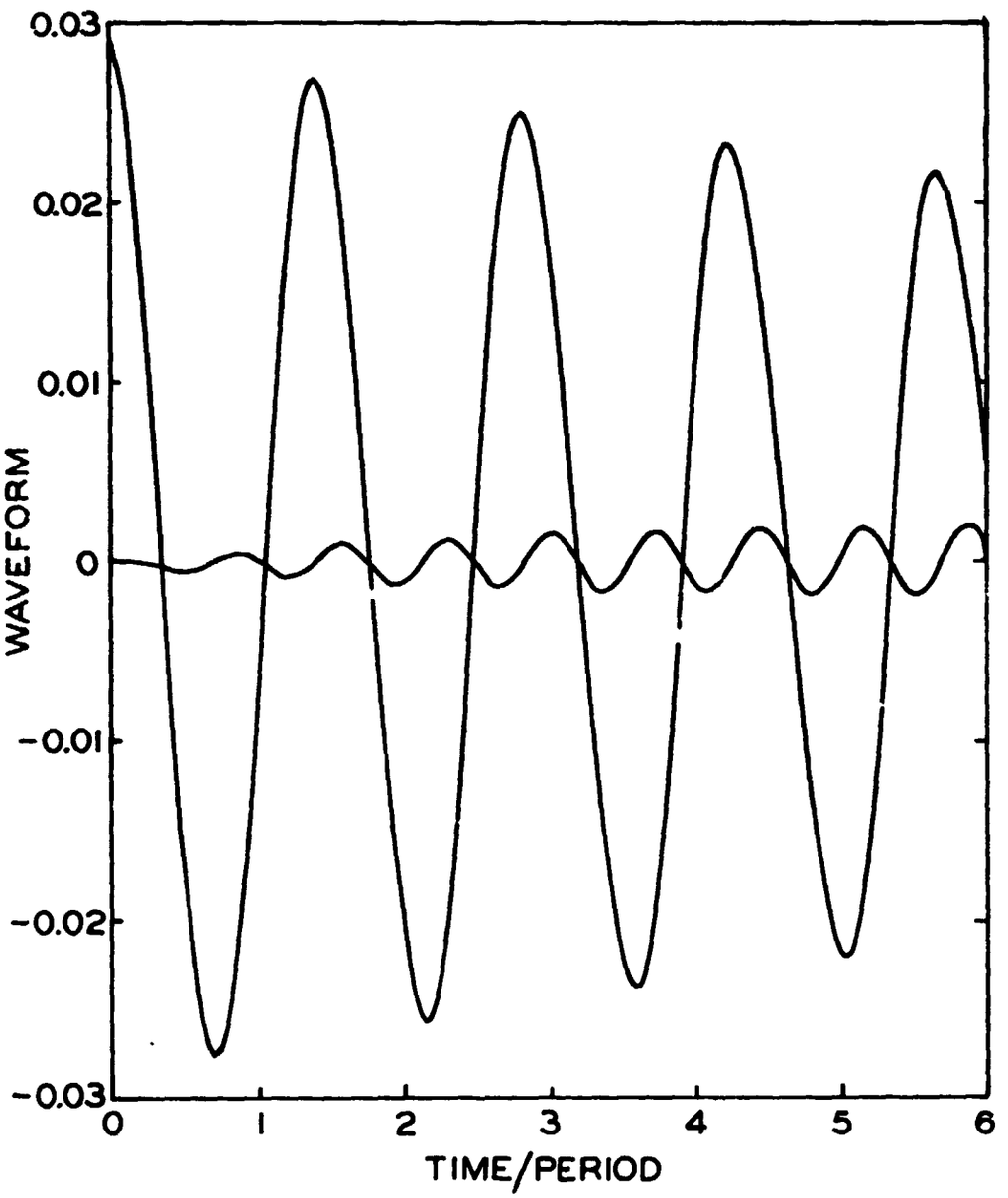

Fig. 8-2(a) Attenuation by 2.5-micron particles at 800 Hz according to the numerical analysis, $\Delta p(0)/p_o = 0.03$.

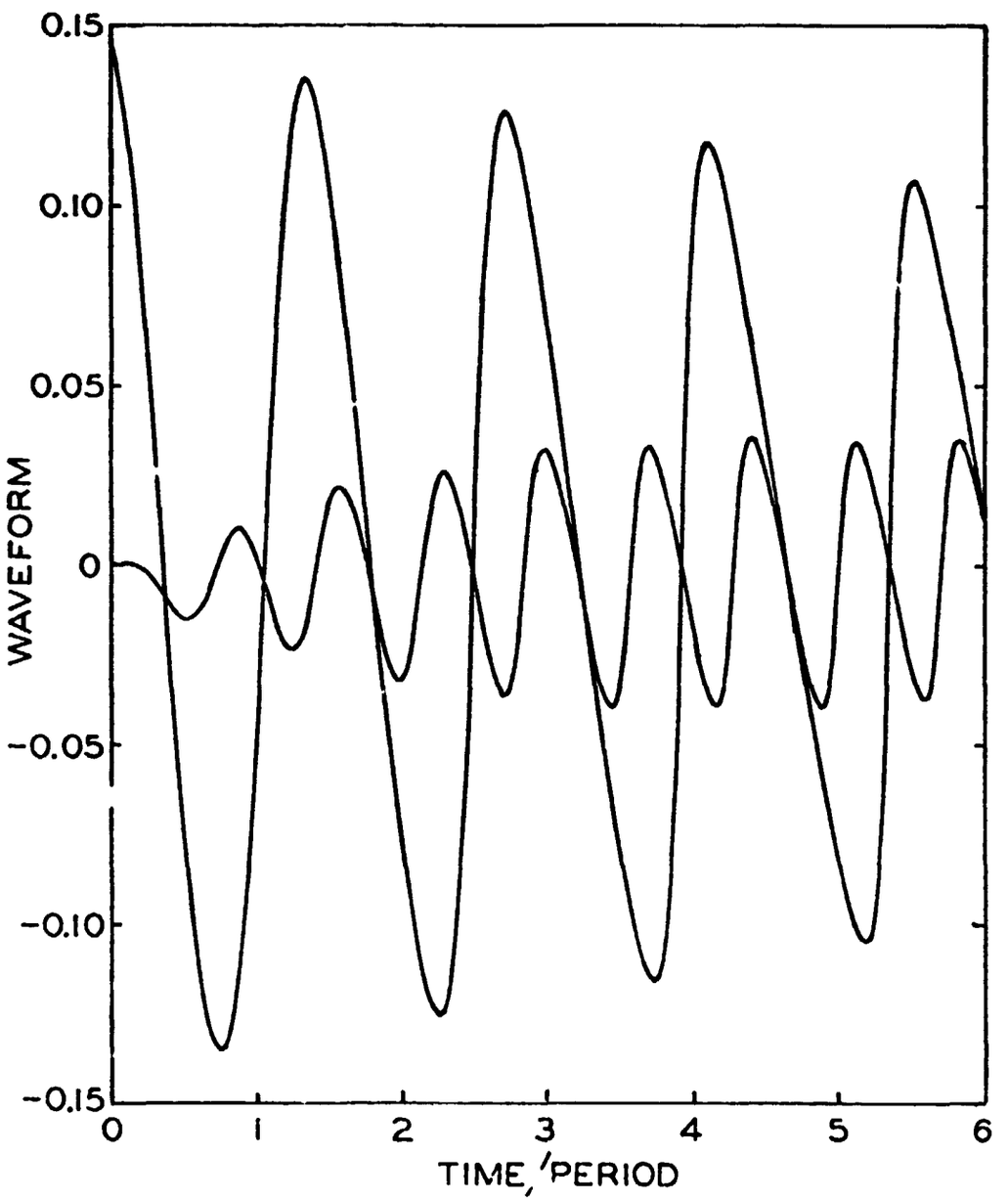

Fig. 8-2(b) Attenuation by 2.5-micron particles at 800 Hz according to the numerical analysis, $\Delta p(0)/p_o = 0.15$.

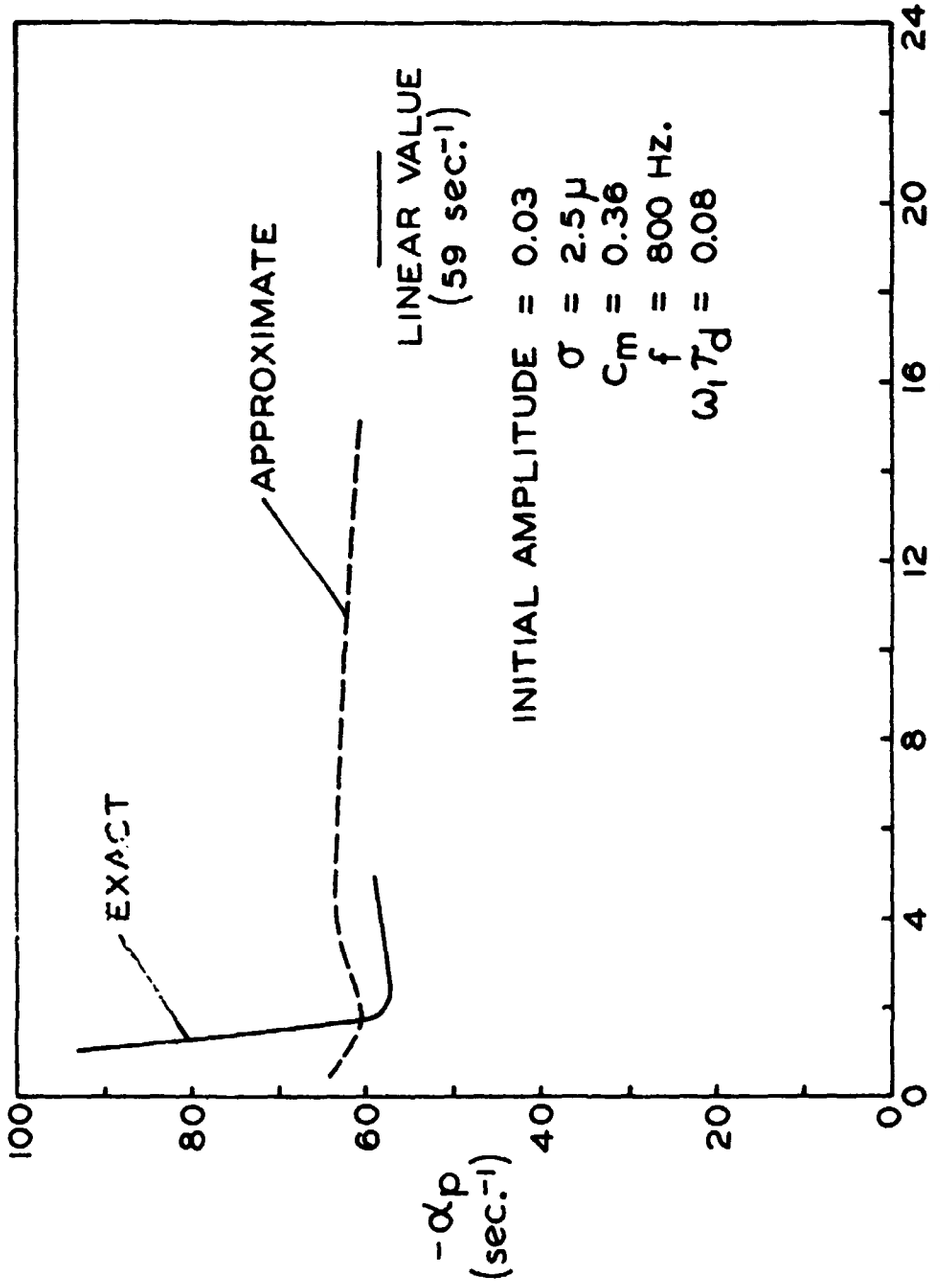

Fig. 8-3 The decay constant for the cases shown in figs. 8-1(a) and 8-2(a).

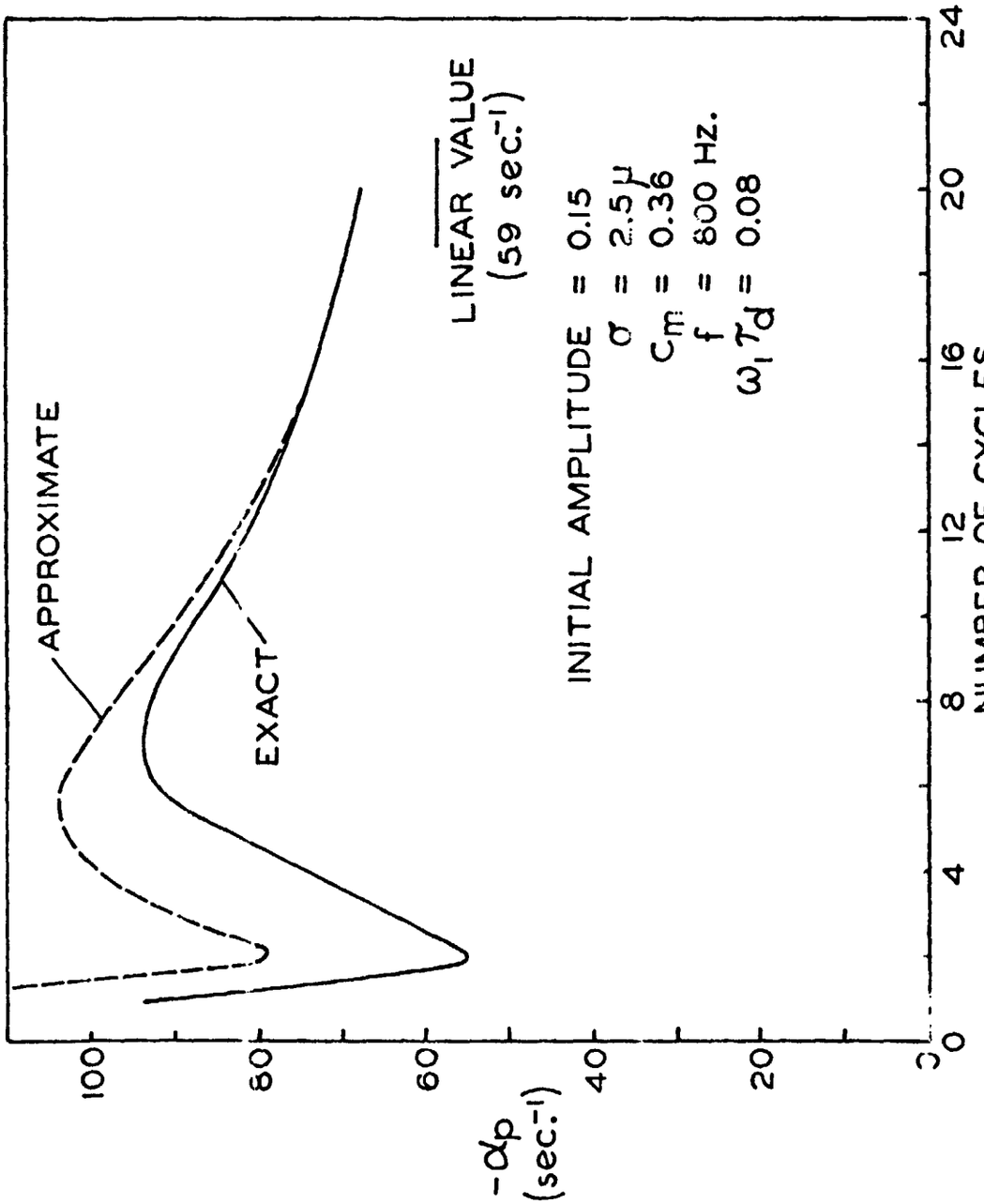

Fig. 8-4. The decay constant for the cases shown in figs. 8-1(b) and 8-2(b).

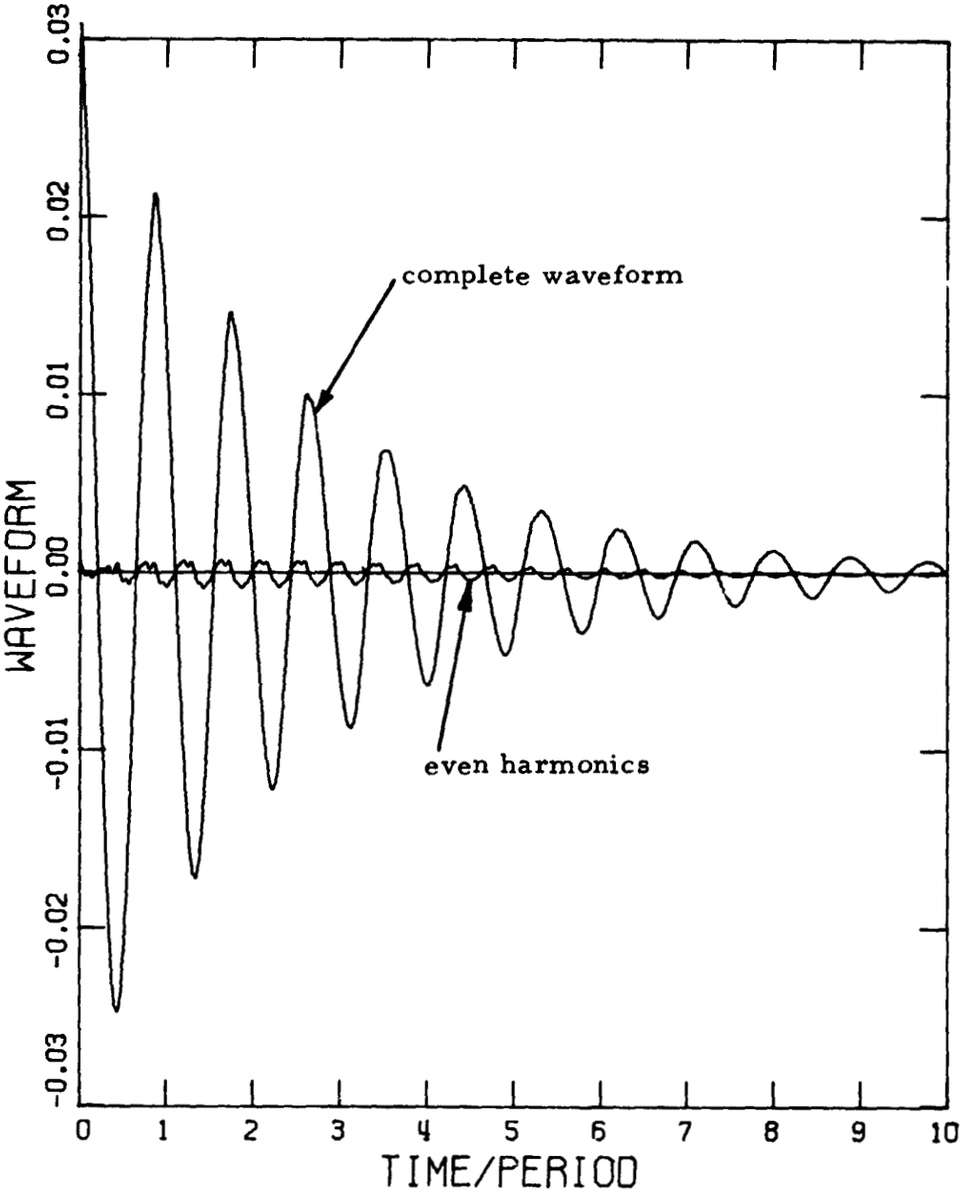

Fig. 8-5. Attenuation by 10-micron particles at 1500 Hz according to the approximate analysis, $\Delta p(0)/p_o = 0.03$.

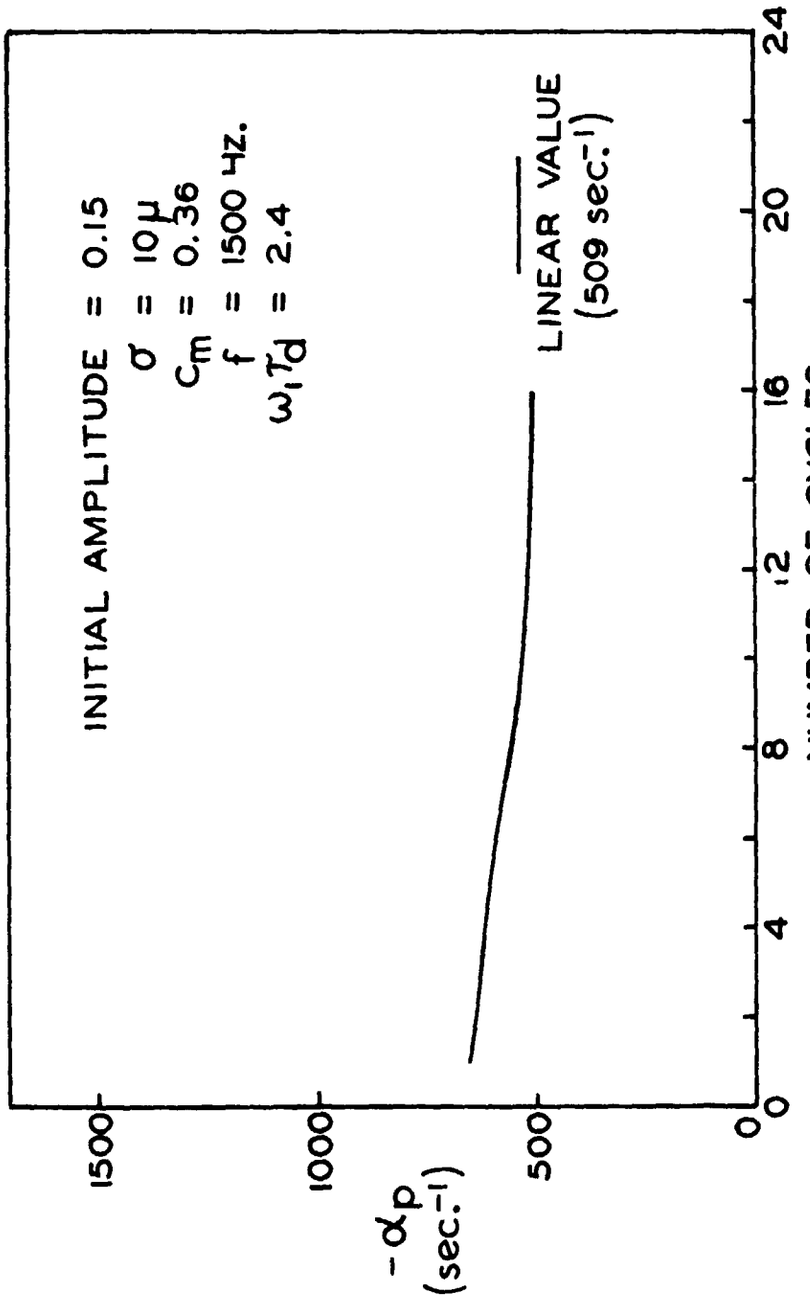

Fig. 8-6. The decay constant for the case shown in Figure 8-5.

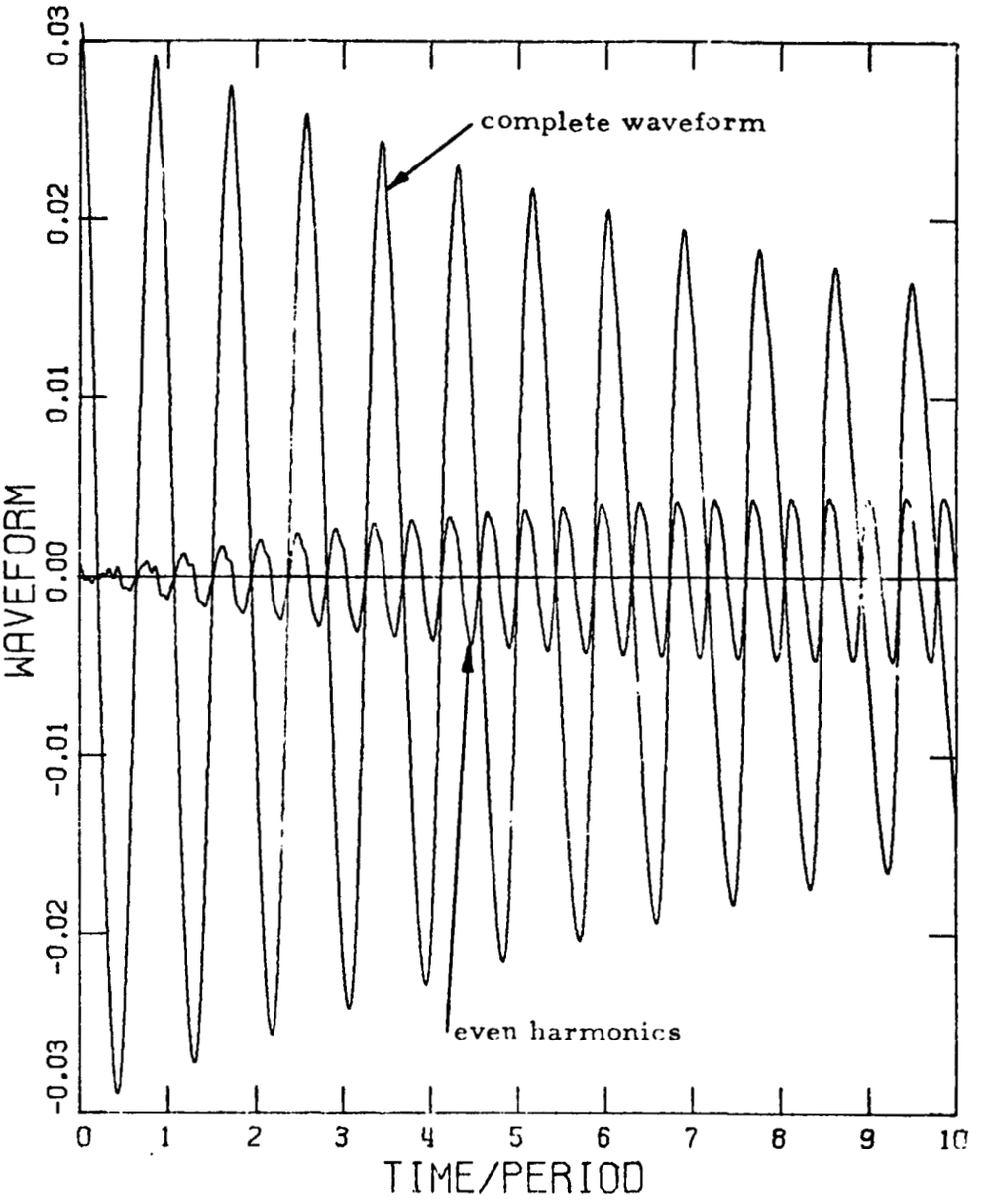

Fig. 8-7. Attenuation by 30-micron particles at 1500 Hz according to the approximate analysis; $\Delta p(0)/p_o = 0.03$.

values of θ_1 and δ_1 calculated from the waveforms are given in Table 8-1, a summary of the computations discussed here.

These results serve to demonstrate that the nonlinear generation of harmonics has substantial influence of the detailed character of the attenuation of waves. The rather close agreement between the approximate results and the numerical calculations under conditions when the approximation to the gas/particle interaction is more accurate suggests that the approximate treatment of the fluid mechanics (i.e., the terms represented by I_ε in (3.45)) is realistic, at least for moderate amplitudes.

From the point of view of reducing data for the attenuation by particle/gas interactions, it is annoying that the value of the decay constant changes so much as the waves die out (cf. Figs. 8-3, 8-4 and 8-6). It is possible that if the higher harmonics are filtered from the waveform, the behavior of α for the first harmonic alone may not be so extreme. Calculations have not been done to check this point.

Perhaps the simplest check of the fluid mechanics alone is calculation of the behavior of a wave in a box with no particles present. In this case, the wave must of course steepen, eventually forming a shock wave. Neither the exact nor approximate analyses can accommodate strong shock waves, but the initial period of development may usefully be examined. Figure 8-8 shows the exact result, and Figs. 8-9 and 8-10 show the results of the approximate analysis when five and ten modes are accounted for. Again, the qualitative agreement is quite good. As one would anticipate, the period of the wave decreases as the amplitude increases. For both the approximate and numerical analyses, obvious distortion of the peak occurs at about the fourth cycle. (The sharp jags in Fig. 8-8 may be due in part to the numerical routine.)

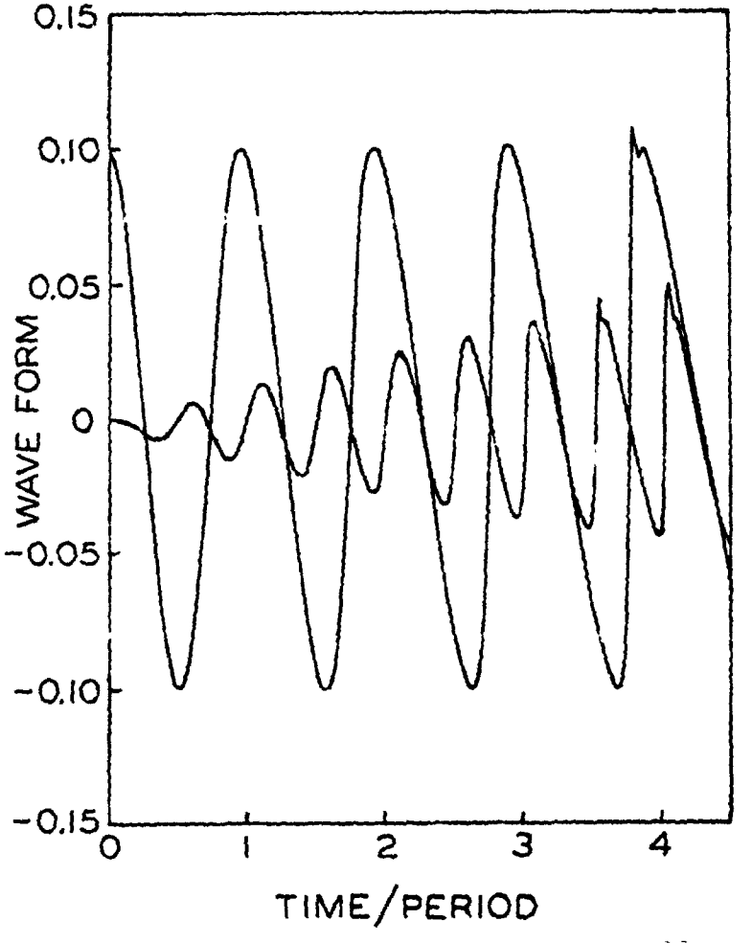

Fig. 8-8. Steepening of a standing wave in a pure gas according to the numerical analysis; f = 900 Hz.

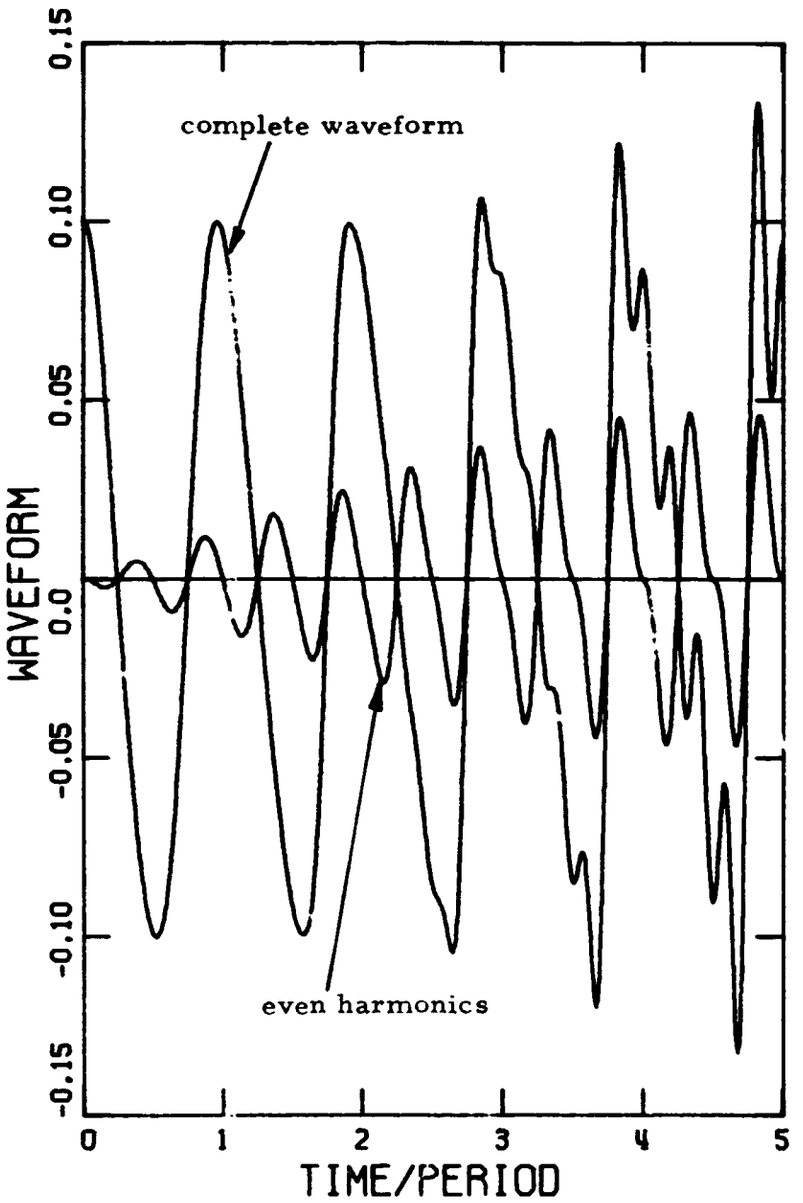

Fig. 8-9. Steepening of a standing wave in a pure gas according to the approximate analysis, with five modes accounted for; f = 900 Hz.

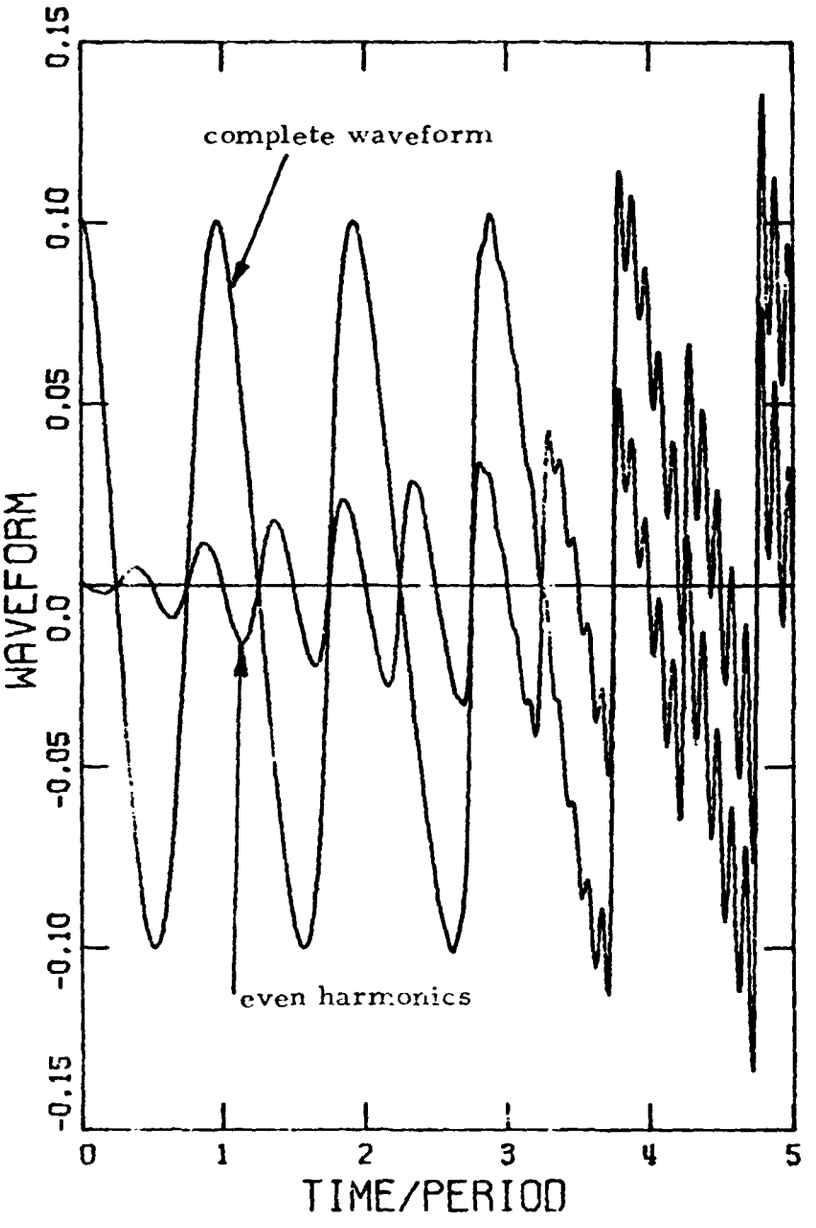

Fig. 8-10. Steepening of a standing wave in a pure gas according to the approximate analysis with ten modes accounted for; f 900 Hz.

IX. AN APPROXIMATION TO NONLINEAR VISCOUS LOSSES ON AN INERT SURFACE

There are two reasons for examining the influence of viscous stresses and heat transfer at an inert surface: these processes can be significant stabilizing influences; and in the presence of oscillations, the average heat transfer increases substantially. The second is a nonlinear effect which has on occasion caused serious structural problems, particularly in liquid rocket motors. The main purpose of this section is to show one way of incorporating some experimental results within the analysis developed earlier. As part of the argument, the more familiar linear results will also be recovered.

The viscous stresses and heat transfer at a surface are, of course, associated with a boundary layer, but they can be accommodated here by suitable interpretation of the force F and heat source Q in the equations developed in § 2 . It is only those terms which are required in this discussion, so the wave equation for the pressure fluctuation is simply

$$\frac{\partial^2 p'}{\partial t^2} - \bar{a}^2 \nabla^2 p' = \frac{\bar{R}}{\bar{C}_v} \frac{\partial Q'}{\partial t} - \bar{a}^2 \nabla \cdot \vec{F}' \quad . \tag{9.1}$$

The boundary condition is

$$\hat{n} \cdot \nabla p' = \hat{n} \cdot \vec{F}' \tag{9.2}$$

For this problem, then, the equation for the amplitude of the n^{th} harmonic is

$$\ddot{\eta}_a + \omega_n^2 \eta_n = \frac{\bar{\gamma}}{\rho_o \bar{a}^2 E_n^2} \left\{ \frac{\bar{R}}{\bar{C}_v} \frac{d}{dt} \int Q' \psi_n \, dV - \bar{a}^2 \int \vec{F}' \cdot \nabla \psi_n \, dV \right\} \tag{9.3}$$

The heat source Q' is taken here to be associated with the heat flux vector $\vec{q}'$, and the force $\vec{F}$ with the viscous stress tensor $\vec{\vec{\tau}}$:

$$Q' = \nabla \cdot \vec{q}' \qquad \vec{F}' = \nabla \cdot \vec{\tau}' \tag{9.4}$$

Both $\vec{q}'$ and $\vec{\tau}'$ are significantly non-zero only in thin regions near the boundary. Then if y denotes the coordinate normal to the wall, measured positive inward, dv = dydS and

$$Q' = \frac{\partial q_y'}{\partial y} \qquad \vec{F}' = \frac{\partial \vec{\tau}_y'}{\partial y} \tag{9.5}$$

The conventions used here are that q_y', the component of $\vec{q}'$ normal to the surface, is positive for heat transfer to the wall, and $\vec{F}'$, being parallel to the surface, is positive when the force tends to accelerate the gas. In the volume integrals of (9.3), ψ_n and $\nabla\psi_n$ are essentially independent of y, so one can write

$$\int Q' \psi_n \, dv \approx \iint dS \, \psi_n \int_o^\infty \frac{\partial q_y'}{dy} \, dy = - \iint q_w' \psi_n \, dS \tag{9.6}$$

$$\int \vec{F}' \cdot \nabla \psi_n \, dv \approx \iint dS \, \nabla\psi_n \cdot \int_o^\infty \frac{\partial \vec{\tau}_y'}{\partial y} \, dy = - \iint \vec{\tau}_w' \cdot \nabla\psi_n \, dS \tag{9.7}$$

Here, the surface stress is $\vec{\tau}_w' = - \mu(\partial \vec{u}'/\partial y)_w$, where $\vec{u}'$ is the velocity fluctuation parallel to the surface, so

$$- \iint \vec{\tau}_w' \cdot \nabla \psi_n \, dS = \iint (\mu \frac{\partial \vec{u}'}{\partial y})_w \cdot \nabla \psi_n \, dS \tag{9.8}$$

Only the linear stress will be treated, but both linear and nonlinear contributions to the heat transfer will be accommodated by writing

$$q_w' = (k \frac{\partial T'}{dy})_w + \bar{h}(T_\infty' - T_w') \tag{9.9}$$

Owing to the thermal inertia of the wall, $T_w' \approx 0$; the temperature fluctuation T_∞' far from the wall is that associated with the acoustic field. The average heat transfer coefficient, $\bar{h}$, will be assumed in a manner described below, to depend on the amplitude of the acoustic field.

Equation (9.3) can now be written

$$\ddot{\eta}_n + \omega_n^2 \eta_n = -\frac{\bar{\gamma}}{\rho_o E_n^2} \iint (\mu \frac{\partial \vec{u}'}{\partial y})_w \cdot \nabla \psi_n dS - \frac{\bar{R}/\bar{C}_v}{p_o E_n^2} \frac{d}{dt} \iint (k \frac{\partial T'}{dy})_w \psi_n dS$$

$$- \frac{\bar{R}/\bar{C}_v}{p_o E_n^2} \frac{d}{dt} \iint \bar{h} T'_\infty \psi_n dS \qquad (9.10)$$

First, calculation of the linear parts will be outlined. The known solutions for the velocity and temperature fluctuations in a sinusoidal acoustic field are

$$u' = \hat{u} [1 - e^{-\lambda y}] e^{i\omega t}$$
$$T' = \hat{T} [1 - e^{-(Pr)^{\frac{1}{2}} \lambda y}] e^{i\omega t} \qquad (9.11)$$

where $\hat{u}$, $\hat{T}$ are the amplitudes far from the wall, and

$$\lambda = \frac{1}{\delta}(1+i) \qquad \delta = \sqrt{2\bar{\nu}/\omega} \qquad (9.12)$$

Thus, for purely harmonic oscillations,

$$(\mu \frac{\partial u'}{\partial y})_w = \frac{\mu}{\delta}(1+i)\hat{u} e^{i\omega t}$$
$$(k \frac{\partial T'}{\partial y})_w = \frac{k}{\delta}(Pr)^{\frac{1}{2}}(1+i)\hat{T} e^{i\omega t}$$

As in the preceding section, the replacement $i \rightarrow \omega \partial/\partial t$ is made, and for the n^{th} harmonic one has

$$\left(\mu \frac{\partial u'}{\partial y}\right)_w = \frac{\mu}{\delta}\left(\frac{1}{\bar{\gamma} k_n^2}\right)(\dot{\eta}_n - \omega_n \eta_n)(\nabla \psi_n)_{\parallel}$$
$$\left(k \frac{\partial T'}{\partial y}\right)_w = \frac{k}{\delta}(Pr)^{\frac{1}{2}}\left(\frac{\bar{\gamma}-1}{\bar{\gamma}}\right) T_o \left(\eta_n + \frac{1}{\omega_n}\dot{\eta}_n\right) \psi_n$$

where $(\nabla \psi_n)_{\parallel}$ is the component of $\nabla \psi_n$ parallel to $\vec{u}'$ at the surface. Substitution into (9.10), and some rearrangement leads to

$$\dot{\eta}_n + \omega_n^2 \eta_n = -2\alpha_n^{(v)}(\dot{\eta}_n - \omega_n \eta_n) - \frac{\bar{R}/\bar{G}_v}{p_o E_n^2}\left(\frac{\bar{\gamma}-1}{\bar{\gamma}}\right) T_o \frac{d}{dt} \iint \bar{h}\, \eta_n\, \psi_n^2\, dS \qquad (9.13)$$

where

$$\alpha_n^{(v)} = \frac{(\omega_n \bar{\nu}/2)^{\frac{1}{2}}}{2(1+c_m)} \frac{1}{E_n^2} \iint \left[\left(\frac{\nabla \psi_n}{k_n}\right)^2 + \frac{\bar{\gamma}-1}{\sqrt{Pr}} \iint \psi_n^2\, dS \qquad (9.14)$$

it has been assumed that the motion far from the wall is isentropic, so $\Gamma'_\infty = (\bar{\gamma}-1)(T_o p'/\bar{\gamma} p_o)$. For a longitudinal mode in a straight cylindrical tube,

$$\iint \left(\frac{\nabla \gamma_n}{kn}\right)^2 dS = \iint \psi_n^2\, dS = \pi DL/2$$

and with $C_m = 0$, (9.14) becomes the familiar result for the decay constant for a standing longitudinal wave:

$$\alpha_n^{(v)} = \frac{2}{D}\sqrt{\frac{\omega_n \bar{\nu}}{2}}\left(1 + \frac{\bar{\gamma}-1}{\sqrt{Pr}}\right) .$$

The treatment of the remaining term in (9.13) rests on appeal to some recent experimental results. Perry and Culick (1974) have reported measurements of the time- and space-averaged values of the heat transfer coefficient in a T-burner with propellant discs at the ends. Denote this coefficient by $\langle \bar{h} \rangle$. The data could be quite well represented by the expression

$$\frac{\langle \bar{h} \rangle \delta}{k} = 0.044\, Re_a^{\frac{1}{2}} \qquad (9.15)$$

where

$$Re_a = \frac{|\hat{p}|_m \delta}{\mu \bar{a}} \qquad (9.16)$$

The symbol $|\hat{p}|_m$ represents the maximum amplitude of the pressure fluctuation, namely that measured at the end of the T-burner; this is equal to $p_o|\eta_n|$ for the n^{th} mode.

In the absence of any other information, two assumptions will be made. First, it is reasonable to assume that the local time-averaged heat

ransfe- coefficient is also proportional to the square root of the pressure amplitude, as (9.15) shows for the space-averaged value. Hence, for the n^{th} mode,

$$\bar{h} = K_n |\psi_n \eta_n|^{\frac{1}{2}} \tag{9.17}$$

where K_n is a constant to be determined. The second assumption is that (9.17) is valid for all modes. From the definitions of $\bar{h}$ and $\langle \bar{h} \rangle$,

$$\langle \bar{h} \rangle = \frac{1}{S} \iint \bar{h} \, dS = \frac{1}{L} \int_o^L \bar{h} \, dz \tag{9.18}$$

for a cylinder. It follows from (9.15)-(9.18) that the constant K_n is given as

$$K_n = 0.044 \frac{k\sqrt{p_o}}{\sqrt{\mu \bar{a}}} \left(\frac{\omega_n}{2\bar{\nu}}\right)^{\frac{1}{4}} \left[\frac{1}{L} \int_o^L |\psi_n|^{\frac{1}{2}} \, dz\right]^{-1}$$

The integral has the value

$$\frac{1}{L} \int_o^L |\psi_n|^{\frac{1}{2}} \, dz = \frac{1}{L} \int_o^L |\cos k_n z|^{\frac{1}{2}} \, dz = .765$$

so

$$K_n = 0.0575 \frac{k\sqrt{p_o}}{\sqrt{\mu \bar{a}}} \left(\frac{\omega_n}{2\bar{\nu}}\right)^{\frac{1}{4}} \tag{9.19}$$

Note that the mode shape cos $(k_n z)$ is used to obtain (9.19) because the data was taken in a uniform tube. The assumptions introduced above imply that the result is supposed to be valid for a local surface element whatever may be the mode in the chamber.

With (9.17), the last term of (9.13) is

$$\frac{\bar{R}}{\bar{c}_v} \left(\frac{\bar{\gamma}-1}{\bar{\gamma}}\right) \frac{T_o}{p_o} \frac{K_n}{E_n^2} \iint \psi_n^2 |\psi_n|^{\frac{1}{2}} \, dS \, \frac{d}{dt} (\eta_n |\eta_n|^{\frac{1}{2}})$$

The constants can be combined as

$$H_n = 0.0575 \, \pi^{\frac{1}{4}} \frac{\bar{\gamma}-1}{Pr \, \bar{\gamma}^{\frac{1}{2}}} (\bar{\nu} f_n \bar{a}^{-2})^{\frac{1}{4}} J_n \tag{9.20}$$

$$J_n = \frac{1}{E_n^2} \iint \psi_n^2 |\psi_n|^{\frac{1}{2}} dS \tag{9.21}$$

Equation (9.13) is now

$$\ddot{\eta}_n + \omega_n^2 \eta_n = -2\alpha_n^{(v)} (\dot{\eta}_n - \omega_n \eta_n) - H_n \frac{d}{dt} (\eta_n |\eta_n|^{\frac{1}{2}}) \tag{9.22}$$

When substituted into the formulas (6.1) and (6.2) obtained with the method of averaging, the linear terms give

$$\frac{1}{2\pi n} \int_0^{2\pi/\omega_1} (\dot{\eta}_n - \omega_n \eta_n) \begin{Bmatrix} \cos \omega_n t \\ -\sin \omega_n t \end{Bmatrix} dt = \frac{1}{2} \begin{Bmatrix} A_n - B_n \\ A_n + B_n \end{Bmatrix} \tag{9.23}$$

Define the angle φ_n as

$$\sin\varphi_n = \frac{B_n}{\sqrt{A_n^2 + B_n^2}} \qquad \cos\varphi_n = \frac{A_n}{\sqrt{A_n^2 + B_n^2}} \tag{9.24}$$

and one can write

$$\eta_n |\eta_n|^{\frac{1}{2}} = (A_n^2 + B_n^2)^{3/4} \sin(\omega_n + \varphi_n) |\sin(\omega_n t + \varphi_n)|^{\frac{1}{2}}$$

The integrals (6.1) and (6.2) arising from application of the method of averaging to the nonlinear term are

$$\frac{1}{2\pi n} \int_0^{2\pi\omega_1} \begin{Bmatrix} \cos \omega_n t \\ \sin \omega_n t \end{Bmatrix} \frac{d}{dt} (\eta_n |\eta_n|^{\frac{1}{2}}) dt$$

$$= \frac{(A_n^2 + B_n^2)^{3/4}}{2\pi n} \int_0^{2\pi n} \begin{Bmatrix} \cos\theta \\ -\sin\theta \end{Bmatrix} \frac{d}{d\theta} [\sin(\theta + \varphi_n) |\sin(\theta + \varphi_n)|^{\frac{1}{2}}] d\theta$$

where $\theta = \omega_n t$. The integrals can be reduced in much the same way as those in § 8 to give

$$6 \frac{(A_n^2 + B_n^2)^{3/4}}{2\pi} \begin{Bmatrix} \cos\varphi_n \\ \sin\varphi_n \end{Bmatrix} \int_0^{\pi/2} \cos^2\psi \sin^{\frac{1}{2}}\psi d\psi$$

The integral has value .478 and the final result for the nonlinear term in (9.22) is

$$\frac{1}{2\pi}\int_0^{2\pi/\omega_1} H_n \frac{d}{dt}(\eta_n|\eta_n|^{\frac{1}{2}})\begin{Bmatrix}\cos\omega_n t\\ -\sin\omega_n t\end{Bmatrix} dt = H_n\left(\frac{1.434}{\pi}\right)\begin{Bmatrix}A_n(A_n^2+B_n^2)^{\frac{1}{4}}\\ B_n(A_n^2+B_n^2)^{\frac{1}{4}}\end{Bmatrix} \quad (9.25)$$

The equations for A_n and B_n, with only the viscous losses shown are therefore

$$\frac{dA_n}{dt} = -\alpha_n^{(v)}(A_n-B_n) - .457\, H_n\, A_n(A_n^2+B_n^2)^{\frac{1}{4}} \quad (9.26)$$

$$\frac{dB_n}{dt} = -\alpha_n^{(v)}(A_n+B_n) - .457\, H_n\, B_n(A_n^2+B_n^2)^{\frac{1}{4}} \quad (9.27)$$

In the special circumstance when these equations are applied to waves in a cylindrical chamber with an inert lateral boundary,

$$J_n = \frac{1.836}{R_c}$$

where R_c is the radius of the chamber. Then the coefficient in (9.26) and (9.27) can be written

$$.457\, H_n = \frac{1.143}{R_c}\,\frac{\bar{\gamma}-1}{Pr\,\bar{\gamma}^{\frac{1}{2}}}\left[\left(\frac{\bar{\nu}}{10^{-4}}\right)\left(\frac{f_n}{1000}\right)\left(\frac{\bar{a}}{1000}\right)^2\right]^{\frac{1}{4}} \quad (9.28)$$

where the units are: R_c, meters; $\bar{\nu}$, (meters)^2/sec ; f_n, Hz; and $\bar{a}$, meters/sec.

X. CHANGE OF AVERAGE PRESSURE ASSOCIATED WITH UNSTEADY WAVE MOTIONS

There are often circumstances, particularly in solid propellant motors, when a substantial increase of the mean pressure may accompany unstable oscillations. This can become a serious practical problem, but it will be treated here only to the extent that one aspect is related to the analysis developed in the preceding sections. It should be remarked in passing that the likely cause of large DC shifts of chamber pressure in motors is usually a change in the burning rate of the propellant, perhaps associated with the erosive action of unsteady motions parallel to the burning surface. That subject will not be discussed here.

The main point of this section is that the zeroth term in the expansion (1.6) represents a DC shift of pressure; the corresponding frequency and mode shape are $\omega_o = 0$, $\psi_o = 1$. In all the preceding discussion, and in other works as well, the influence of a small average change of pressure has been ignored. All the formalism developed in sections 2 and 3 is valid and can be used to compute the change of average pressure due to the unsteady motions, as well as its influence on the wave motions. From (4.1) and (4.2), the equation for η_o is found to be

$$\frac{d^2\eta_o}{dt^2} = -\sum_{i=0}^{\infty}(D_{oi}\dot{\eta}_i+E_{oi}\eta_i)-\sum_{i=0}^{\infty}\sum_{j=0}^{\infty}[A_{oij}\dot{\eta}_i\dot{\eta}_j+B_{oij}\eta_i\eta_j] . \qquad (10.1)$$

The values of the coefficients D_{oi}, E_{oi} depend on the processes considered. For example, with D_{ni} given by (3.41), one can easily determine the results

$$D_{oo} = \frac{\bar{\gamma}-1}{v}\int \frac{\bar{w}}{\bar{\rho}_g}\frac{p}{} \, dv \qquad (10.2)$$

$$D_{oi} = \frac{\bar{\gamma}-1}{v} \int \psi_i \frac{\bar{w}_p}{\bar{\rho}_g} \, dv \tag{10.3}$$

$$D_{no} = -\frac{1}{E_n^2} \left\{ \int \vec{\bar{u}} \cdot \nabla \psi_n dv + (\bar{\gamma}-1) \int \psi_n \frac{\bar{w}_p}{\bar{\rho}_g} \, dv \right. \tag{10.4}$$

where the factor v arises from $E_o^2 = v$. It is interesting also to examine the term arising from surface combustion; this can also be interpreted to represent other sorts of processes as well. The term in question on the right hand side of (3.40) is

$$\frac{\bar{\gamma}}{\rho_o} \frac{\partial}{\partial t} \iint \mathcal{R} \psi_n \, dS \ . \tag{10.5}$$

For purposes of illustration, the fluctuation of the gases leaving the surface is assumed to be simply related to the pressure, and $\mathcal{R}$ is approximated by (7.7),

$$\mathcal{R} \approx \rho_o \bar{u}_b \sum_{i=0}^{\infty}{}' \left[\mathcal{R}_i^{(r)} + \frac{1}{\omega_i} \mathcal{R}_i^{(i)} \frac{\partial}{\partial t} \right] \eta_i \psi_i \ . \tag{10.6}$$

Equations (10.5) and (10.6) give

$$\bar{\gamma} \bar{u}_b \sum_{i=0}^{\infty} \iint \left[\mathcal{R}_i^{(r)} \dot{\eta}_i - \omega_i \mathcal{R}_i^{(i)} \eta_i \right] \psi_i \psi_n dS \tag{10.7}$$

in which the approximation $\ddot{\eta}_i \approx -\omega_i^2 \eta_i$ has again been used. Comparison with (3.40) shows that the corresponding additional terms on the right hand side of (10.1) are

$$\frac{\bar{\gamma} \bar{u}_b}{v} \sum_{i=0}^{\infty} \iint \left[\mathcal{R}_i^{(r)} \dot{\eta}_i - \omega_i \mathcal{R}_i^{(i)} \eta_i \right] \psi_i dS$$

$$\equiv \frac{\bar{\gamma} \bar{u}_b}{v} \iint \mathcal{R}_o^{(r)}{}_{(\omega=0)} \dot{\eta}_o dS + \frac{\bar{\gamma} \bar{u}_b}{v} \sum_{i=1}^{\infty} \iint \left[\mathcal{R}_i^{(r)} \dot{\eta}_i - \omega_i \mathcal{R}_i^{(i)} \eta_i \right] \psi_i dS \ . \tag{10.8}$$

The first term represents the contribution to the change of average pressure in the chamber (really the second time derivative) because the surface

combustion itself responds to the average change of pressure.

Suppose, for example, that all other terms are ignored and that the response $\mathcal{R}_o^{(r)}$ is uniform over the surface. Then (10.7) and (10.1) give

$$\frac{d^2\eta_o}{dt^2} = \frac{\overline{\gamma}\,\overline{u}_b}{v}\,\mathcal{R}_o^{(r)}{}_{(\omega=0)}\,\frac{d\eta_o}{dt}\,S_b \tag{10.9}$$

where S_b is the total area of burning surface. According to the discussion in § 7, see eq. (7.4) and following remarks, $\mathcal{R}_o^{(r)}$ may be approximated by the value of $R_b^{(r)}$ at $\omega = 0$; thus, $\mathcal{R}_o^{(r)}{}_{(\omega=0)} \approx n$, and (10.9) is

$$\frac{d^2\eta_o}{dt^2} = \frac{\overline{\gamma}\,\overline{u}_b}{v}\,n\,\frac{d\eta_o}{dt}\,S_b \ .$$

The first integral is

$$\frac{dp'_o}{dt} = \overline{\gamma}\,n\,\overline{u}_b\,\frac{S_b}{v}\,p'_o \tag{10.10}$$

where p'_o is the change of average pressure; the constant of integration has been set equal to zero which merely sets an acceptable initial condition. Now (10.10) is simply an expression of the change of pressure in a closed chamber due to mass addition. To see this, note that conservation of mass provides

$$\frac{d}{dt}(\rho v) = \rho_c\,r\,S_b$$

where ρ_c is the density of solid and r is the linear burning rate. The perturbation of this equation combined with the isentropic relation $p \sim \rho^{\gamma}$ gives

$$\frac{\rho_o v}{p_o}\,\frac{dp'_o}{dt} = \overline{\gamma}\,\rho_c\,r'S_b \ .$$

But $r' \approx n(p'/p_o)\overline{r}$ and $\rho_c\overline{r} = \rho_o\overline{u}_b$, so the last equation becomes (10.10). The point of this elementary example is that the elaborate formalism de-

veloped for unsteady motions does indeed contain familiar quasi-steady behavior. A term representing the influence of erosion can also be incorporated in this analysis, but it will not be considered here.

It may be noted that the remaining terms in (10.7) sometimes contribute nothing. For the case of longitudinal modes with a burning surface extending the entire length of the chamber, for example, the integrals of ψ_i over the surface vanish. Interactions between the wave motions and surface combustion then contribute nothing to the average pressure in the chamber.

The nonlinear terms contained in I_ε, eq. (3.45), also contribute to the average pressure in the chamber. Only the parts containing p' as a factor are involved, and it is not difficult to use the results (3.58) and (3.59) to determine the following formulas for the coefficients:

$$B_{oii} = \frac{\bar{\gamma}-1}{\bar{\gamma}} \left(\frac{E_i^2}{v} \right) \omega_i^2 \tag{10.11}$$

$$B_{non} = \frac{\bar{\gamma}-1}{\bar{\gamma}} \omega_n^2 \tag{10.12}$$

All others vanish; there are no non-zero values of A_{nij} for n, i, or j equal to zero. According to (10.1), the nonlinear interactions produce a negative contribution to the second time derivative of the average pressure:

$$\left(\frac{d^2 \eta_o}{dt^2} \right)_{nonlinear} = -\left(\frac{\bar{\gamma}-1}{\bar{\gamma}} \right) \sum_{i=1}^{\infty} \omega_i^2 \left(\frac{E_i^2}{v} \right) \eta_i^2 \quad . \tag{10.13}$$

It is perhaps surprising that the sign is negative. Because in some sense the processes involved represent a dissipation of energy from the wave motions to the average state, one might have anticipated a positive sign corresponding to a tendency to increase the pressure. The interpretation is not, however, clear at this time.

The influence of changing average pressure will not be considered further in this report.

XI. APPLICATION TO THE STABILITY OF LONGITUDINAL MODES IN MOTORS AND T-BURNERS

It has been shown in §6 that the nonlinear terms simplify considerably for the case of longitudinal modes. This situation will be treated here for several examples. Some preliminary results were reported by Levine and Culick (1974). Application to large motors was examined by Culick and Kumar (1974). The discussion here is to demonstrate how the approximate analysis can be used to study practical configurations and to provide a limited comparison with the more exact numerical results reported elsewhere.

For all the calculations reported in this section, the following material and thermodynamic properties are used:

specific heat of the gas	$C_p = 2021.8 \frac{\text{Joule}}{\text{kgm-}^\circ\text{K}}$
specific heat of the particle material	$C_s = 0.68\, C_p$
thermal diffusivity of the propellant	$\kappa = 10^{-7}\ \text{m}^2/\text{sec}^2$
Prandtl number of the gas	$Pr = 0.8$
viscosity of the gas	$\mu = 8.834\times10^{-4}(T/3485)^{.66}\ \frac{\text{kgm}}{\text{m-sec}}$
isentropic exponent of the gas	$\gamma = 1.23$
linear burning rate of the propellant	$\bar{r} = 0.00812(p_o/500)^{.3}\ \text{m/sec}$
density of the propellant	$\rho_c = 4000\ \text{kgm/m}^3$
density of the condensed material	$\rho_s = 1766\ \text{kgm/m}^3$

11.1 Application to a Small Cylindrical Motor

Because the nonlinear acoustics terms represented by I_ϵ, eq.(3.45), are given explicitly, the first step in the analysis consists in evaluating the contributions to the linear coefficients α_n and θ_n. Four contributions to linear stability are included; arising from the nozzle, the condensed ma-

terial in the gas phase, the surface combustion processes, and the one dimensional approximation to inelastic acceleration of flow issuing from the lateral surface ("flow turning"). The formulas for the corresponding values of α_n are

Nozzle

$$\alpha_n = -\bar{a}\left(\frac{J}{\bar{L}}\right)\left(\frac{2}{\bar{\gamma}+1}\right)^{\frac{3-\bar{\gamma}}{2(\bar{\gamma}-1)}} \tag{11.1}$$

Particles

$$\alpha_n = -\frac{1}{2}\left(\frac{\kappa}{1+\kappa}\right)\left[X_1+(\bar{\gamma}-1)\frac{C}{\bar{C}_p}X_2\right]_{x=x_n} \tag{11.2}$$

Flow Turning

$$\alpha_n = -\tfrac{1}{2}\bar{u}_b\left(\frac{S_b}{V}\right) \tag{11.3}$$

Combustion

$$\alpha_n = \tfrac{1}{2}\bar{\gamma}\bar{u}_b\left(\frac{S_b}{V}\right)R_b^{(r)} \tag{11.4}$$

The formula (11.1) is based on quasi-steady behavior; the velocity fluctuations are in-phase with pressure fluctuations at the nozzle entrance. Hence, the response function has no imaginary part and, as shown by eq. (7.10), the value of θ_n for the nozzle is zero. The term representing flow-turning is the last one in (3.41); there is no corresponding E_{ni}, so θ_n is also zero for flow turning. The only non-zero values are for the gas/particle interactions and combustion; the first is given by (8.27) and the second by use of (7.10) and (11.4):

Particles

$$\theta_n = \frac{1}{2}\left(\frac{\kappa}{1+\kappa}\right)\left[\frac{\Omega_d^2}{1+\Omega_d^2}+(\bar{\gamma}-1)\frac{C}{\bar{C}_p}\frac{\Omega_t^2}{1+\Omega_t^2}\right]_{x=x_n} \tag{11.5}$$

Combustion

$$\theta_n = -\tfrac{1}{2}\overline{\gamma}\,\overline{u}_b\left(\frac{S_b}{V}\right)R_b^{(i)} \qquad (11.6)$$

The two examples treated here were discussed in §7.4 of Culick and Levine (1974), where the result of the numerical analysis is given. Each is for a motor having a cylindrical bore and length 23.5 inches. The mean pressure, port area, and throat area differ and are given below:

	(a)	(b)
Length (in.)	23.5	23.5
Port Area (in^2)	3.33	4.73
Throat Area (in^2)	.439	.562
Pressure (psia)	1568	1412

These are the first and last cases given in Table 7-3 by Culick and Levine (1974). The fundamental frequency is 900 Hz.

For both cases, the particle diameter is assumed to be 2.0 microns and the mass fraction is $\varkappa = 0.36$. The combustion response is taken to be the representation (7.4) given above, with A = 6.0 and B = 0.56. Because the pressures are different, so are the flame temperatures in the two cases; for (a), $T_f = 3525^{\circ}K$ and for (b), $T_f = 3515^{\circ}K$. The small difference has only minor influence on the results.

With the above values, and the formulas (11.1) - (11.4), waves for case (a) are found to be stable. The values of the decay constants for the first five modes are given in Table 11-1 below. The numerical calculations produced an unstable wave which, with an initial amplitude of 5 per cent (fundamental mode) eventually reached a limiting amplitude of 4.2 per cent. In view of the successful comparison for the cases treated in § 8 for attenuation by particle damping, and because the representation of the

TABLE II-1. Values of α_n and θ_n for Three Cases of Unsteady Motions in a Small Motor.

	Case (a)	Case (aa)	Case (b)
α_1	-18.5 (sec^{-1})	8.0 (sec^{-1})	-9.1 (sec^{-1})
α_2	-359.3	-342.8	-334.8
α_3	-610.1	-583.6	-566.5
α_4	-915.9	-889.4	-871.4
α_5	-1239.2	-1262.7	-1244.0
θ_1	12.9	12.9	64.0
θ_2	46.8	46.8	34.9
θ_3	-29.3	-29.3	-35.6
θ_4	-131.0	-131.0	-135.0
θ_5	-280.0	-280.0	-283.0

combustion response is the same in the approximate and numerical analysis, a likely source of the difference in the results is the behavior of the nozzle.

In the numerical analysis, the calculations for the entire two-phase flow were carried out to the nozzle throat. The influence of the nozzle is buried in the results and its contribution to attenuation cannot be determined. For the approximate analysis, the influence of the nozzle is represented as a surface admittance function evaluated at the nozzle entrance. The result (11.1) is strictly valid for quasi-steady behavior of a gas only; it has been extended to the case of two-phase flow by using the value of $\bar{\gamma}$ for the mixture. The point is that there is reason to expect that the contribution of the nozzle is different in the two analyses.

As a means of comparing the analyses, the value of the attenuation constant associated with the nozzle is chosen to obtain the same limiting amplitude as found in the numerical analysis. This procedure rests on the observation, elaborated upon further in §12, that the values of the limiting amplitudes are quite sensitive to the values of the linear coefficients α_n, θ_n.

Not a very large change is required. Equation (11.1) gives $\alpha_n = -153.25\ \text{sec}^{-1}$. If this is changed to $-126.75\ \text{sec}^{-1}$, then $\alpha_1 = 8.00$ and the limiting amplitude is about 4.2 per cent. The values of the α_n and θ_n for five modes are given in Table 11-1, for the case denoted (aa). Figure 11-1 shows the amplitudes of the five harmonics considered; the functions A_n and B_n are shown in Figure 11-2 and 11-3, and a few cycles of the wave at limiting amplitude are given in Figure 11-4.

The attenuation by the nozzle is assumed to vary linearly with the ratio J of throat area to port area, having the value $-126.75\ \text{sec}^{-1}$ when J

has the value (. 132) for case (a). Then with the other required data given above, the approximate analysis applied to case (b) produces the results shown in the last column of Table 11-1. The initial disturbance is stable, the decay constant for the first harmonic being $\alpha_1 = -9.12\ \text{sec}^{-1}$. After twenty cycles (. 02222 sec) the amplitude is roughly 3. 5 per cent according to the approximate analysis. The numerical analysis gave an amplitude of 3. 02 per cent after twenty cycles. It appeared that the wave may have stabilized at a limiting amplitude, but the calculation was not carried further. In view of the slow decay found with the approximate analysis, it may be that the conclusion based on the numerical analysis, for only twenty cycles, is incorrect, based on incomplete results. If a true limit was indeed reached, then of course the approximate analysis gives the wrong result. A limit of 3 per cent would be reached only if α_1 is positive, having a value less than 8. 00 .

That nonlinear influences are in fact active, even at such relatively small amplitudes, is easily established. Consider a wave having a decay constant equal to $-9.12\ \text{sec}^{-1}$ and a frequency of 900 Hz. According to linear behavior, the amplitude would be 4. 08 per cent after twenty cycles if the initial amplitude is 5 per cent. The more rapid decay shown by the nonlinear analysis is evidently due to the transfer of energy, through the nonlinear processes, from the fundamental oscillation to higher harmonics which are then attenuated much more rapidly. Nonlinear particle damping was included in the approximate analysis but, as one should expect for the small amplitudes arising in these examples, its influence is negligibly small.

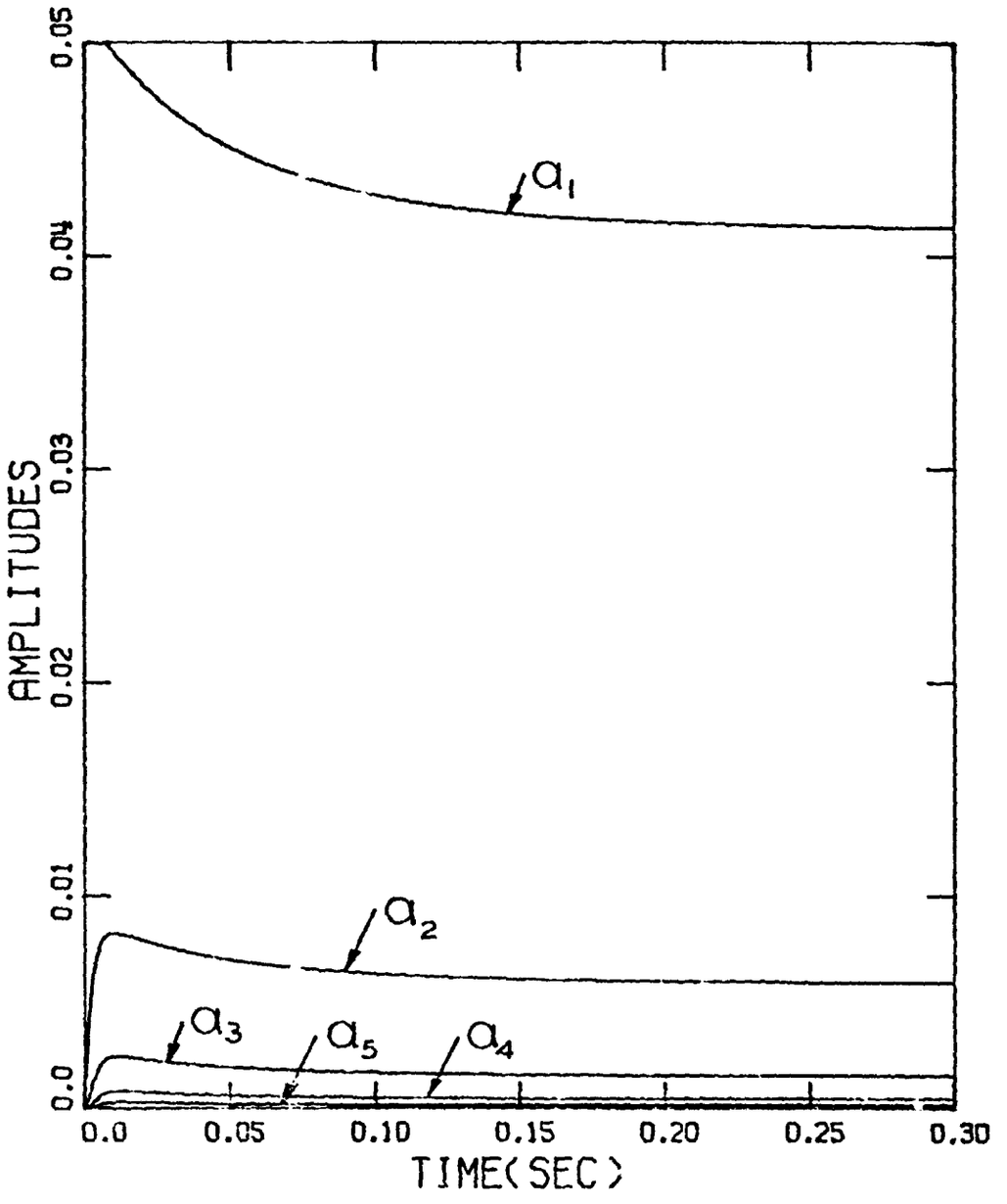

Figure 11-1. Amplitudes for unstable oscillations in a motor, case (aa) of Table 11-1.

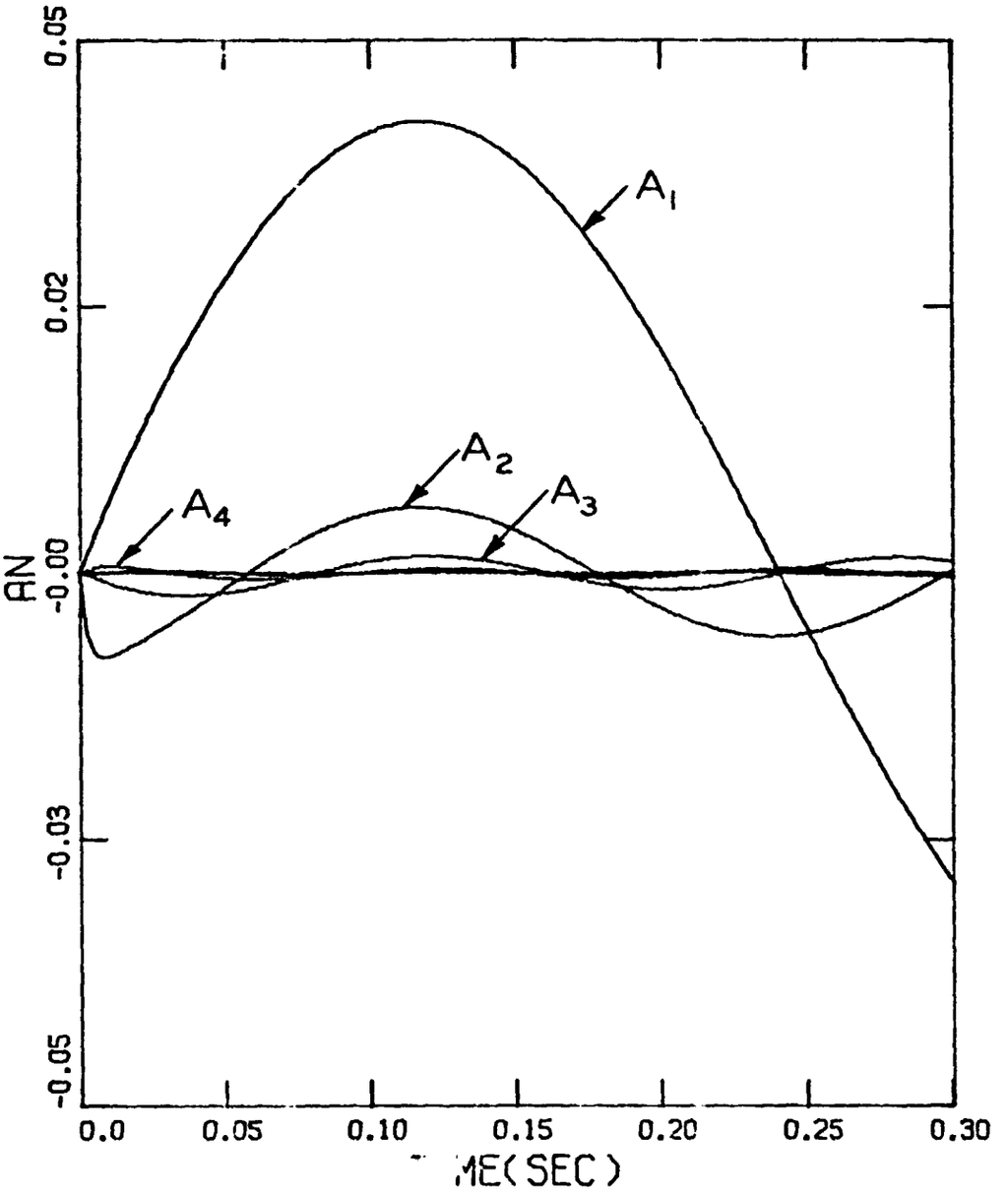

Figure 11-2. The functions $A_n(t)$ for case (aa) of Table 11-1.

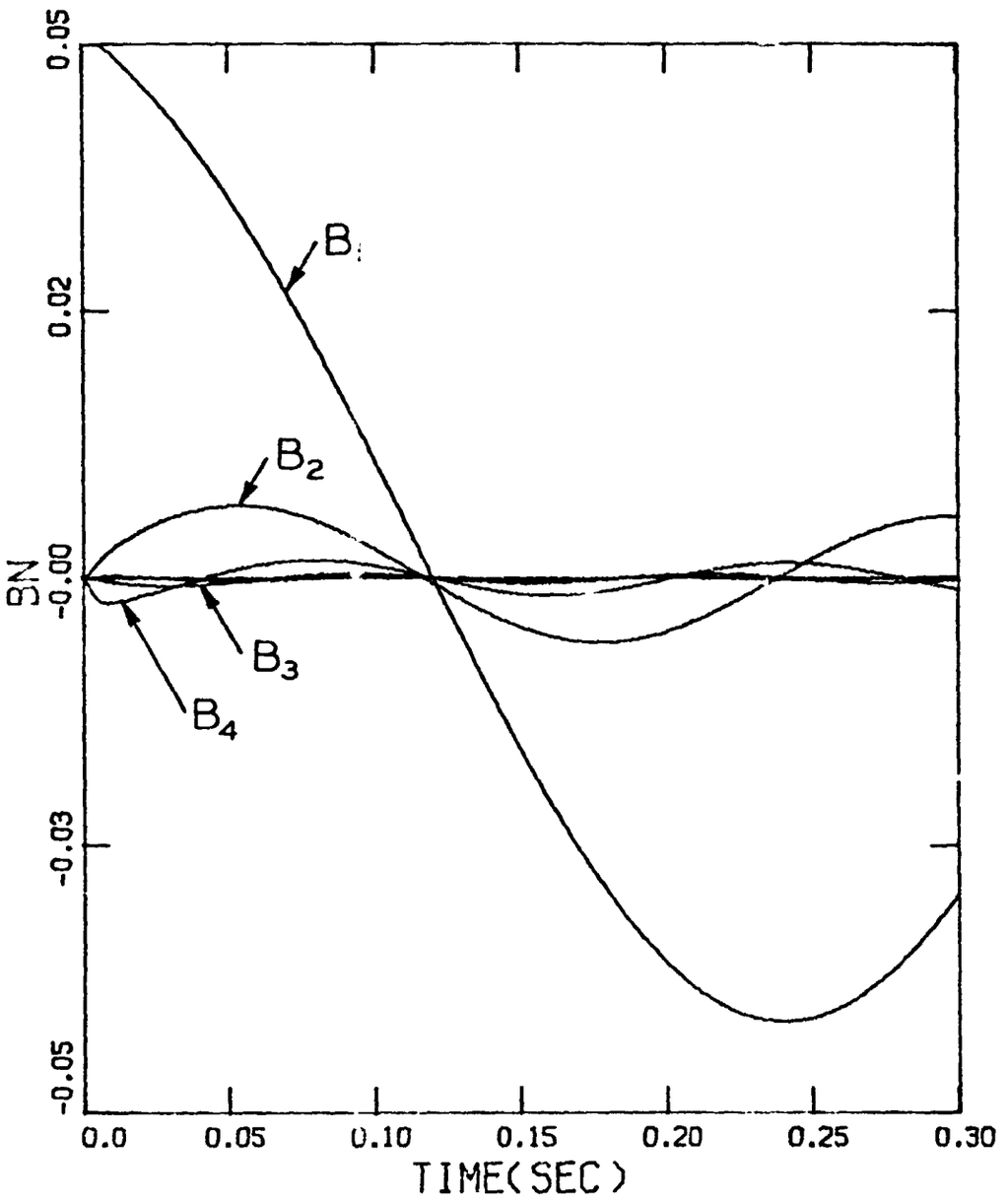

Figure 11-3. The functions $B_n(t)$ for case (aa) of Table 11-1.

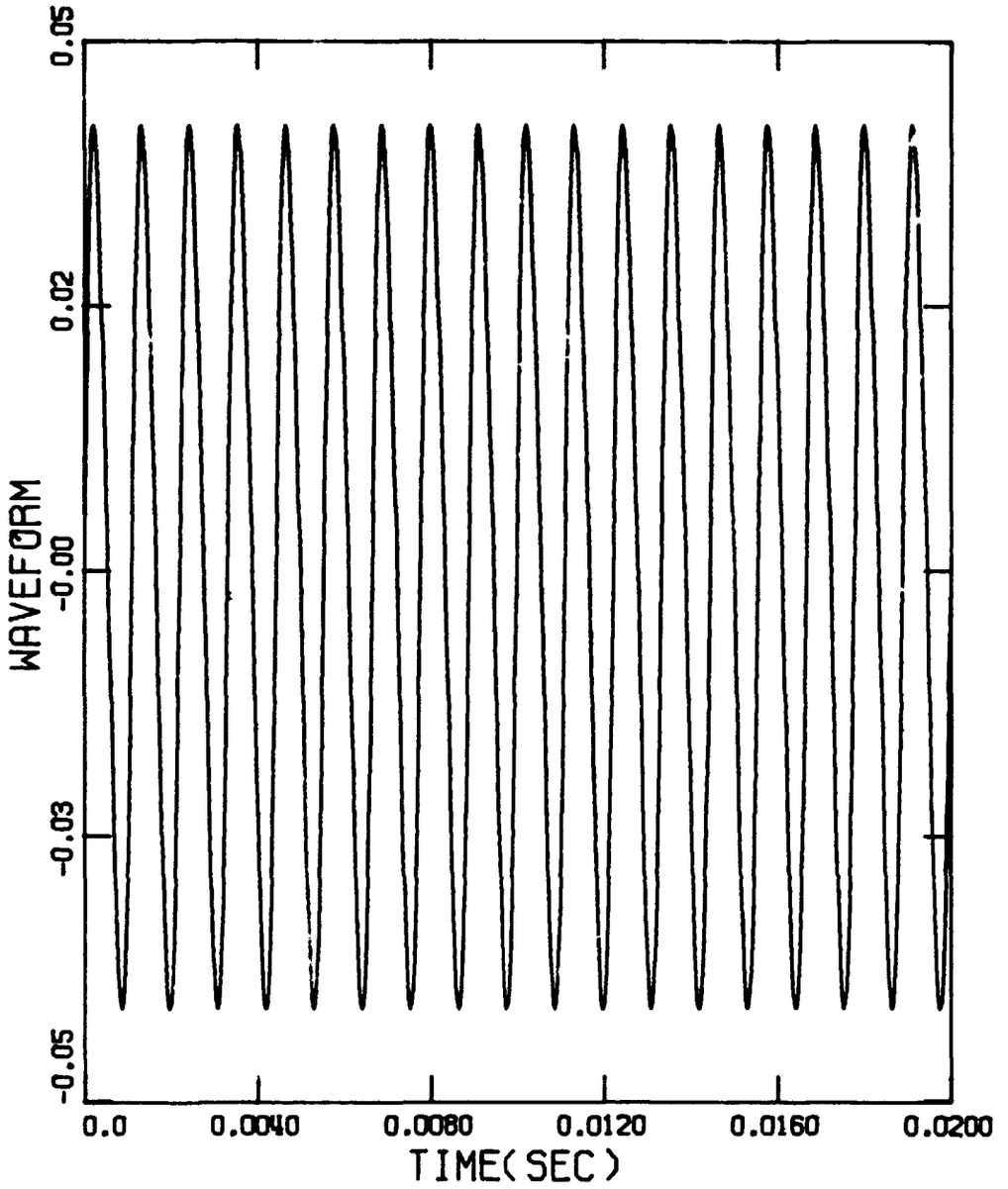

Fig. 11-4 Waveform at limiting amplitude for the example shown in Fig. 11-1.

11.2 Application to a T-Burner

The numerical analysis has also been used to analyze a T-burner. Both the calculation and the data are for flush cylindrical grains. Data of course can be obtained only approximately at that flush condition.

Most of the properties used are the same as those listed above, with the following exceptions. The flame temperature is 3264^{o}K, the particle diameter is 3.0 microns, and the parameters in the combustion response are $A = 8.8$, $B = 0.67$.

The T-burner differs from a motor most importantly in two respects: the vent is in the center, and there are substantial areas of inert surface. Apart from possible interactions between the non-uniform mean flow and acoustic velocity, one expects that the center vent should have very little influence on the fundamental mode. Indeed, all odd modes, which have pressure nodes at the center, should not be much affected. Indeed, all odd modes, which have pressure nodes at the center, should not be much affected. In the calculations discussed here, the vent is assumed to have no effect on the odd modes.

Because the even modes have pressure anti-nodes at the center of the burner, they will be influenced by the vent. For comparison with the numerical results given by Levine and Culick (1974), the flow in the vent is assumed to be subsonic and to respond as a plug flow. If the plug has effective length ℓ_v , and the pressure downstream is essentially constant, the vent exhausting into a surge tank, then the equation of motion for the plug is

$$\rho_o \ell_v \frac{du'}{dt} = p' \ , \tag{11.7}$$

where u' is positive outward from the burner. For harmonic motions, the

amplitude of the motion is

$$\hat{u} = -\frac{i}{\rho_o \omega \ell_v} \hat{p} \tag{11.8}$$

The admittance function for the ℓ^{th} mode is therefore given by the formula

$$A_v \equiv \left(\frac{\hat{u}/\bar{a}}{\hat{p}/\gamma \rho_o} \right)_\ell = -\frac{i}{\rho_o \omega \ell \ell_v} . \tag{11.9}$$

Because the velocity fluctuation of the plug is ninety degrees out of phase with the pressure, the admittance function has no real part and there will be no contribution to the linear decay constant. The representation of the vent as linearized inviscid plug flow introduces no losses. If viscous effects or radiation to the surroundings are included, the phase between the velocity and pressure fluctuations is changed and there are then associated energy losses.

The influence of the vent is accommodated in the nonlinear formulation by the term containing $\mathcal{R}$ in (3.40), where $\mathcal{R}$ is defined by (3.42). Let F_v denote that term so that, if only the effect of the vent is considered, the equation for the amplitude of the n^{th} mode is

$$\ddot{\eta}_n + \omega_n^2 \eta_n = F_v \tag{11.10}$$

$$F_v = -\frac{\bar{\gamma}}{\rho_o E_n^2} \iint \mathcal{R}_v \psi_n dS \tag{11.11}$$

$$\mathcal{R}_v = -\left(\rho_o u_v' + \bar{u}_v \frac{p'}{\rho_o \bar{a}^2} \right) \tag{11.12}^*$$

The argument used in §7 will again be used here to adapt the admittance function (11.9), defined only for harmonic motions, to the general case of unsteady motions. Then F_v can be written

---

*Note the negative sign in $\mathcal{R}_v$ to account for the fact that both u_v' and $\bar{u}_v$ are positive outward.

$$F_v = -\frac{\bar{\gamma}}{E_n^2}\frac{d}{dt}\iint \psi_n^2\left[\frac{\bar{a}}{\bar{\gamma}}\left(A_v^{(r)}\eta_n + \frac{1}{\omega_n}A_v^{(i)}\dot{\eta}_n\right) + \frac{\bar{u}_v}{\rho_o \bar{a}^2}\dot{\eta}_n p_o\right]dS \quad .$$

The integrand is nearly constant over the vent, and with $E_n^2 = S_c L/2$

$$F_v \equiv -E_{nn}\eta_n - D_{nn}\dot{\eta}_n - \left[2\omega_n\left(\frac{\bar{a}}{\bar{L}}\right)\left(\frac{S_v}{S_c}\right)A_v^{(i)}\right]\eta_n$$

$$-\left[2\bar{\gamma}\left(\frac{\bar{a}}{\bar{L}}\right)\left\{\left(\frac{S_v}{S_c}\right)A_v^{(i)} + 2\bar{M}_b\left(\frac{S_b}{S_c}\right)\right\}\right]\dot{\eta}_n \qquad (11.13)^*$$

According to the rule (6.10), the linear coefficients for the n^{th} mode are

$$\alpha_n = -\tfrac{1}{2}D_{nn} = \bar{\gamma}\left(\frac{\bar{a}}{\bar{L}}\right)\left\{\left(\frac{S_v}{S_c}\right)A_v^{(r)} + 2\bar{M}_b\frac{S_b}{S_c}\right\} \qquad (11.14)$$

$$\theta_n = -\frac{1}{2}\frac{E_{nn}}{\omega_n} = \left(\frac{\bar{a}}{\bar{L}}\right)\left(\frac{S_v}{S_c}\right)A_v^{(i)} \qquad (11.15)$$

If the mean flow term (proportional to $\bar{M}_b$ in (11.14)) is neglected, and the admittance function is purely imaginary, as for (11.9), then only the coefficients θ_n for the even modes are affected by the oscillating plug flow.

It is not difficult to work out the formulas for the linear coefficients arising from combustion, particle/gas interactions, flow-turning, and heat losses on the lateral boundary. They are given here for the case of cylindrical grains of length L_b extending from the ends.

Combustion

$$\alpha_n = \bar{\gamma}\left(\frac{\bar{u}_b}{\bar{L}}\right)\left(\frac{2\pi R_c L_b}{S_c}\right)\left(1 + \frac{\sin 2k_n L_b}{2k_n L_b}\right)R_b^{(r)} \qquad (11.16)$$

$$\theta_n = -\frac{R_b^{(i)}}{R_b^{(r)}}\alpha_n \qquad (11.17)$$

---

*Here, $S_c = \pi R_c^2$ is the cross-sectional area of the burner, S_v is the cross-sectional area of the vent, and S_b is the area of burning surface in one half of the burner.

Particles

$$\alpha_n = -\frac{1}{2}\left(\frac{\kappa}{1+\kappa}\right)\left[X_1 + (\bar{\gamma}-1)\frac{C}{\bar{C}_p}X_2\right]_{\omega=\omega_n} \tag{11.18}$$

$$\theta_n = \frac{\omega_n}{2}\left(\frac{\kappa}{1+\kappa}\right)\left[\frac{\Omega_d^2}{1+\Omega_d^2} + (\bar{\gamma}-1)\frac{C}{\bar{C}_p}\frac{\Omega_t^2}{1+\Omega_t^2}\right]_{\omega=\omega_n} \tag{11.19}$$

Flow Turning

$$\alpha_n = 2\left(\frac{\bar{u}_b}{r_c}\right)\left(\frac{L_b}{L}\right)\left[1 - \frac{\sin 2k_r L_b}{2k_n L_b}\right] \tag{11.20}$$

$$\theta_n = 0 \tag{11.21}$$

Linear Heat Losses

$$\alpha_n = -\frac{1}{R_c}\sqrt{\frac{a_n \nu}{2}}\left\{\left(1 + \frac{\bar{\gamma}-1}{\sqrt{Pr}}\right)\left(1 - 2\frac{L_b}{L}\right) + 2\frac{L_b}{L}\left(1 - \frac{\bar{\gamma}-1}{\sqrt{Pr}}\right)\frac{\sin 2k_n L_b}{2k_n L_b}\right\} \tag{11.22}$$

$$\theta_n = -\alpha_n \tag{11.23}$$

Once again, the combustion response is assumed to be given by (7.4) for pressure coupling only.

Both nonlinea particle damping and nonlinear heat losses are included in the calculations. The first has already been discussed; the formulas are the same as those used in § 8. Nonlinear heat losses are handled approximately by using the formulas worked out for a tube, in § 9, but weighted by the proportion of lateral surface which is inert. Thus, the coefficient given by (9.38) is multiplied by $(L-2L_b)/L$. Although nonlinear heat transfer may be important in setting the values of limiting amplitudes, particularly for tests with unmetallized propellants, very little is known at the present time. No extensive numerical results have been obtained specifically to determine its influence.

Calculations have been done for an example treated numerically by Levine and Culick (1974). The propellant is the same as that used in the examples discussed in §11.1. Owing to heat losses, the temperature in the chamber is assumed to be somewhat lower, $T_f \approx 3264^{\circ}K$, roughly in accord with observations. Also, the particle diameter is assumed to be 3.0 microns, and the parameters in the combustion response are A = 8.8, B = 0.67; these values were chosen somewhat arbitrarily to produce the correct growth rate of unstable waves, and should not be taken as representing the actual behavior of the propellant. The computed results will depend quite heavily on the combustion response. The main purpose here is to compare the approximate and numerical analyses.

With the data given above, and with L = 23.5 inches, R_c = 0.75 inches, the values of the constants α_n and θ_n are listed below in Table 11-2 for two values of S_b/S_c. For S_b/S_{co} = 7.06, two cases are shown: in case (a), there is no influence of the vent; and in case (b), the unsteady flow in the vent is treated as a plug flow, as described above. The values of the α_n and θ_n are listed in Table 11-2. The values for α_1 computed with heat transfer neglected agree almost exactly with those deduced from the unstable waveforms produced by the numerical analysis. The amplitudes of the first five harmonics, for the case S_b/S_c = 7.06 and with no influence of the vent, are shown in Figure 11-5. In Figures 11-6 and 11-7 the functions A_n and B_n are shown. These should be compared with the results for the example for behavior in a motor covered in § 11.1. For that case, all harmonics reached finite limiting amplitudes when the functions A_n and B_n oscillate with fixed amplitudes and frequencies. Here, the first harmonic grows without limit, and although the amplitudes of the higher harmonics show a

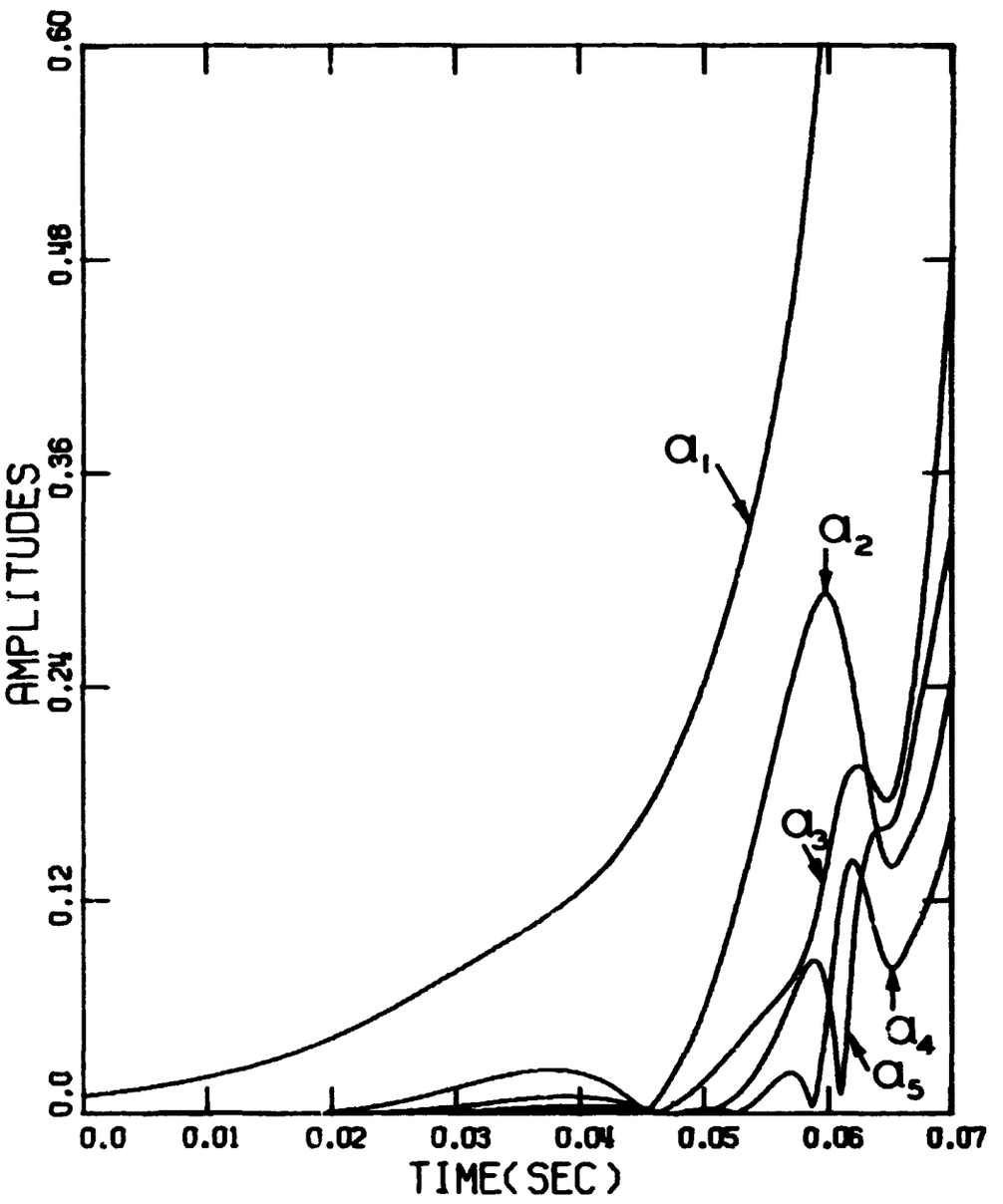

Figure 11-5. Amplitudes for unstable oscillations in a T-burner, case (a) of Table 11-2 (no influence of the vent).

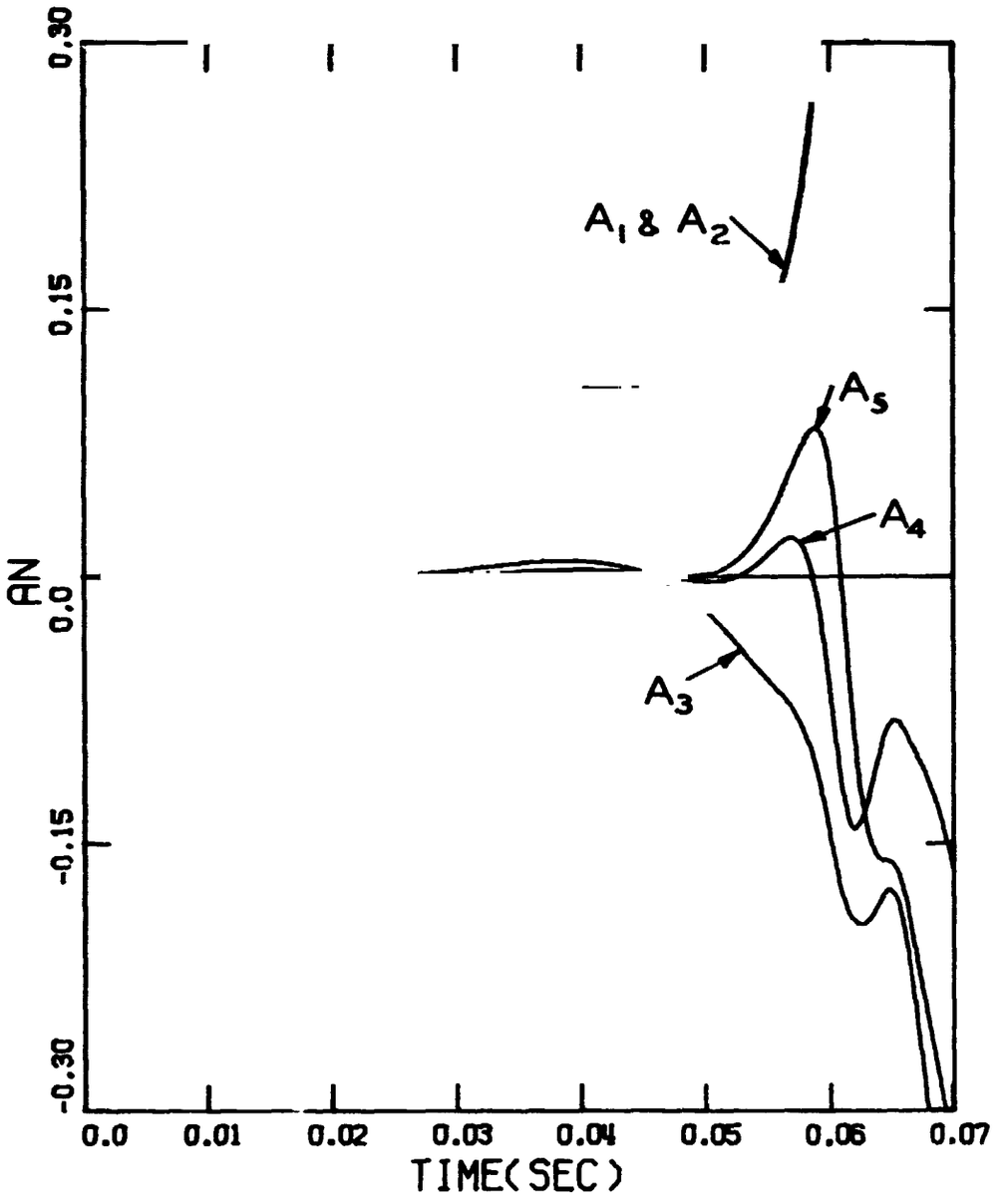

Figure 11-6. The functions $A_n(t)$ for case (a) of Table 11-2.

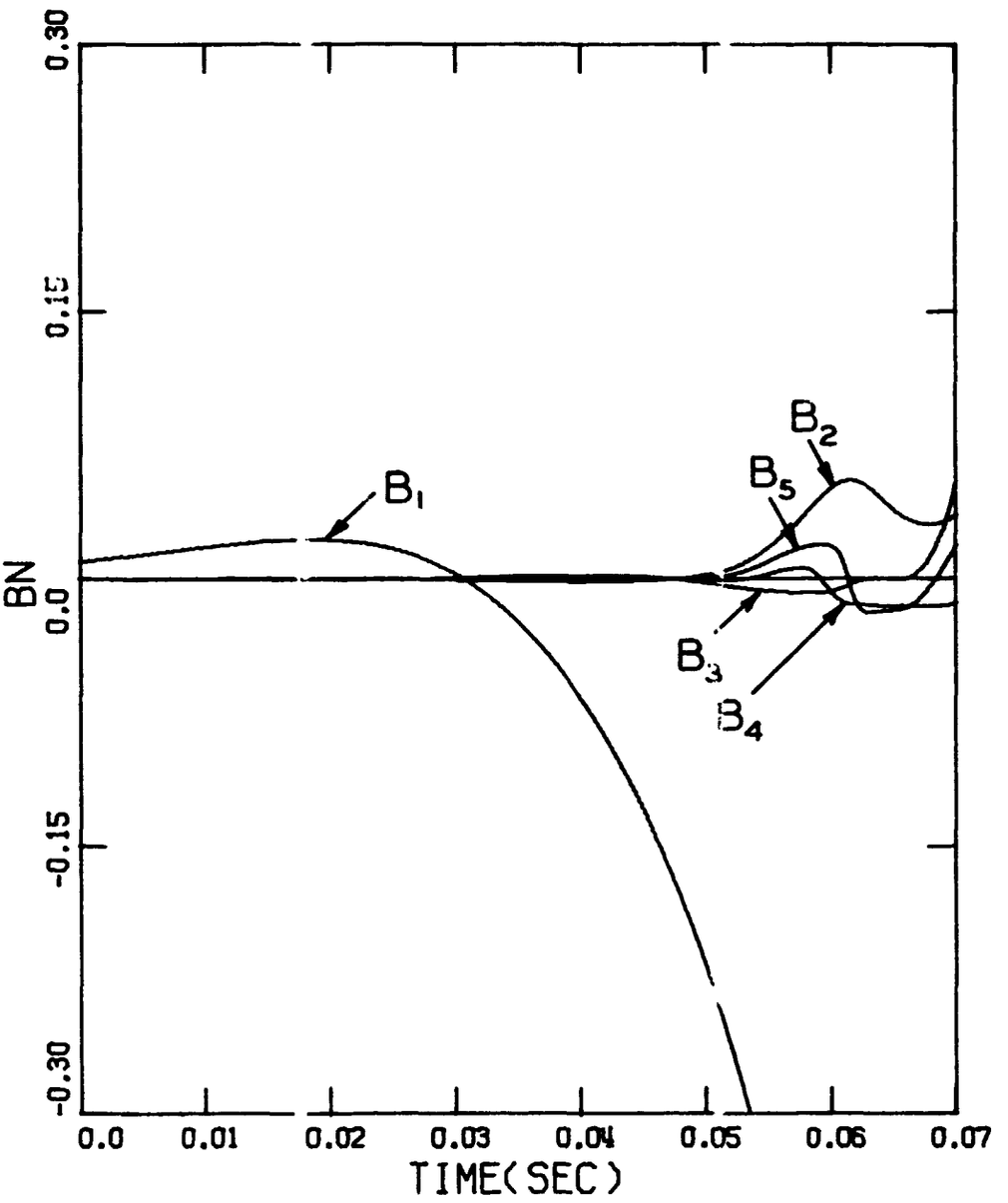

Figure 11-7. The functions $B_n(t)$ for case (a) of Table 11-2.

TABLE 11-2.

Values of α_n and θ_n for Two Cases of Unstable Motions in a T-Burner.

	Case (a)	Case (b)
α_1	73.9 (sec^{-1})	73.9 (sec^{-1})
α_2	-319.2	-319.2
α_3	-725.7	-725.7
α_4	-1195.0	-1195.0
α_5	-1691.1	-1691.1
θ_1	49.2	49.2
θ_2	7.5	-1560.0
θ_3	-186.0	-186.0
θ_4	-490.5	-1275.0
θ_5	-915.0	-915.0

decay period after about 0.05 seconds, they too eventually grow without limit. It is a curious result that the functions $A_1(t)$ and $A_2(t)$ are almost identical; note that $B_1(t)$ and $B_2(t)$ are considerably different. Why this occurs in this special case is an unanswered question.

The amplitudes and the functions $A_n(t)$, $B_n(t)$ are shown in Figures 11-8, 11-9, and 11-10 for the case (b) of Table 11-2. Comparison with the results for case (a) shows the influence of the plug flow. As noted above, this treatment of the vent provides no losses, but there is a change in the relative phases of the harmonics, because the values of θ_2 and θ_4 are quite considerably affected. The most notable feature is the decrease of the amplitude of the first harmonic in the period .05 - .09 sec., after which it again grows without limit. The values are unrealistically high, much

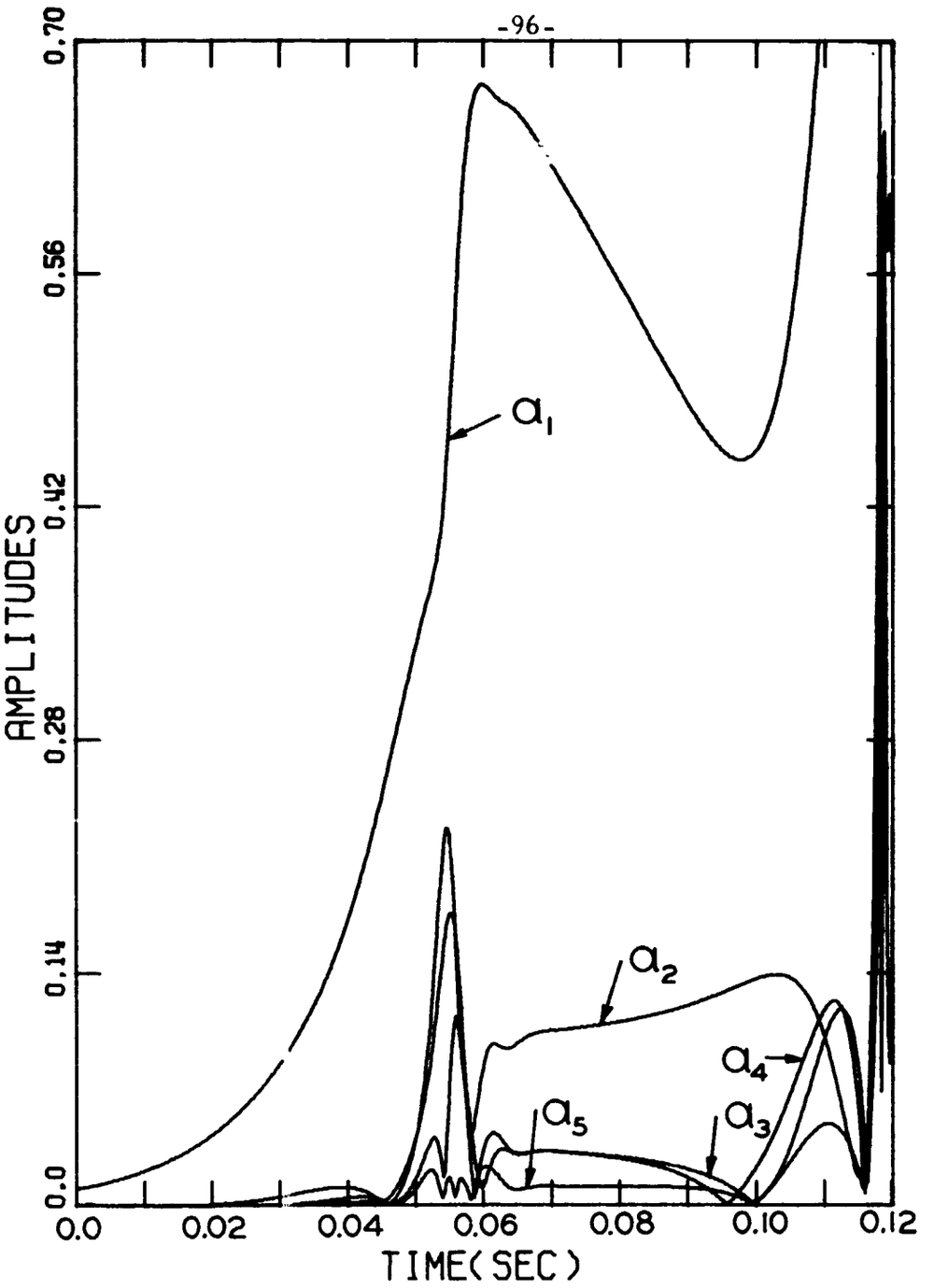

Figure 11-8. Amplitudes for unstable oscillations in a T-burner, case (b) of Table 11-2 (unsteady flow in the vent treated as a plug flow).

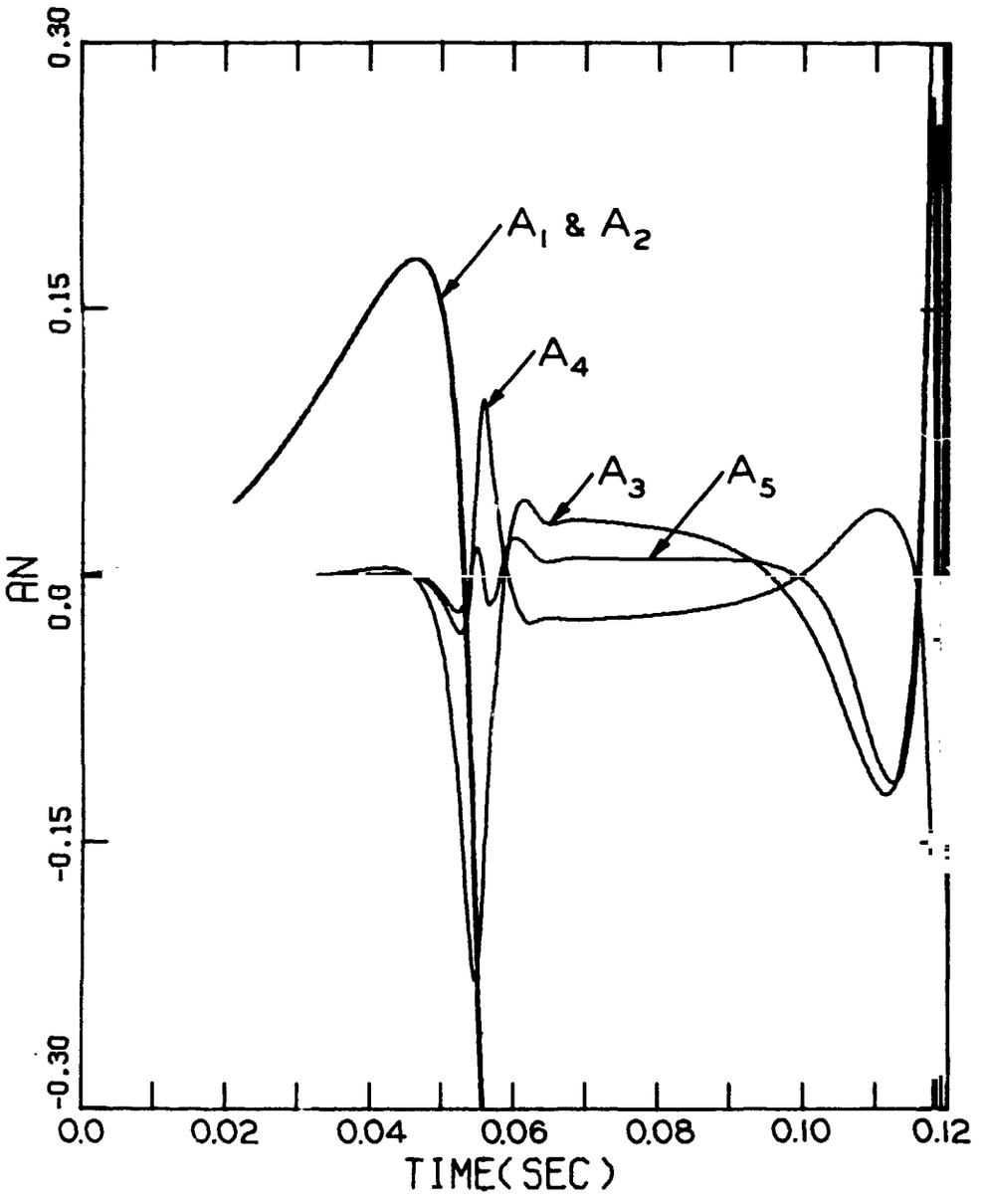

Figure 11-9. The functions $A_n(t)$ for case (b) of Table 11-2.

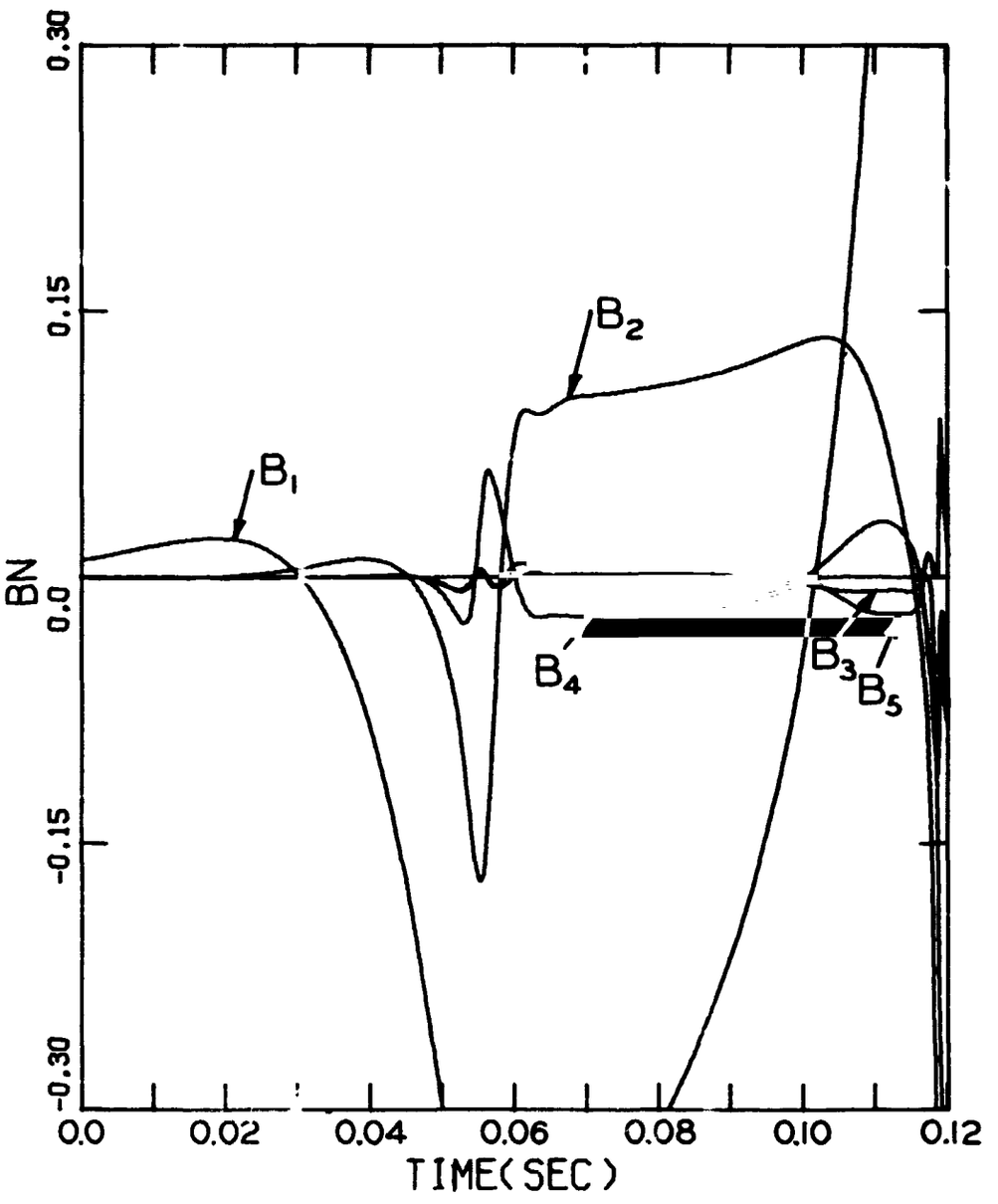

Figure 11-10. The Functions $B_n(t)$ for Case (b) of Table 11-2.

larger than those observed for the tests which were the basis of these calculations.

It is a puzzling difficulty at the present time that for apparently realistic values of the data required, the calculated amplitudes for motions in a T-burner are much too large and may even grow without limiting. This has been the case with other examples not included here. A similar difficulty was encountered in the numerical calculations. For the case (b), the numerical results seemed to indicate that the amplitude was limiting, at a value of roughly .37, at approximately .08 seconds; after this time, the amplitude of the fundamental mode according to Figure 11-8 begins to grow again. The numerical results were not carried out further.

Thus, for the examples treated here, limiting behavior has not been obtained for the unstable motions in a T-burner. Even with the growth constant for the fundamental mode arbitrarily reduced, the amplitude grows without limit; as α_1 tends to zero, a longer time is required for the amplitude to reach unity. This is a striking contrast with the results obtained for a motor. In both cases, reasonable values of the required data have been used. But as shown by Tables 11-1 and 11-2, the relative values of the α_n, θ_n for the various harmonics are considerably different. This is clearly the origin of the difference in nonlinear behavior, but the details are not known, and no generalizations can be offered.

The difference between cases of limited and unlimited growth appears strikingly in the functions $A_n(t)$ and $B_n(t)$. If the value of θ_n is non-zero, both functions oscillate (see §12.2) when the amplitudes limit. Otherwise, the behavior has no obvious pattern. The contrast may be seen by comparing the results of §11.1 with those shown here. This question is remarked upon further in §12.2, but a general answer is yet to be found.

XII. THE CONNECTION WITH LINEAR STABILITY ANALYSIS AND THE BEHAVIOR OF APPROXIMATE NONLINEAR SOLUTIONS

Most problems of combustion instability in solid propellant rockets, liquid propellant rockets, and in thrust augmentors have been studied by using linear stability analysis. It has been emphasized in the formal construction of the analysis given here, and in the examples covered in §§ 8 and 11, that the linear coefficient α_n is exactly the familiar decay or growth constant for the n^{th} harmonic. One of the appealing features of the results (cf. eqns. (4.18), (4.19), and (6.10) - (6.12)) is that the correspondence is so readily established and obvious. In practice, this means that the numerical results obtained from linear stability analysis may be used directly in the approximate nonlinear analysis. Indeed, for the examples given in § 11, the cost of doing the necessary linear calculations was comparable to that of the numerical solution to the nonlinear equations. In § 12.1, the relation between the present analysis and the more familiar linear stability analysis is elaborated upon further.

One of the interesting questions which arises in connection with the nonlinear analysis is: under what conditions will the motions reach a limiting amplitude? Put another way, for what ranges of the linear coefficients $\{\alpha_n, \theta_n\}$ will the system of coupled nonlinear oscillators execute a limit cycle? At the present time, the answer to this question is not known, and therefore it is also not possible to offer any generalizations about the values of limiting amplitude, and how they depend on the linear coefficients. A few remarks on this subject, which merits further work, are given in § 12.2.

12.1 The Connection with Linear Stability Analysis

All analyses of linear stability are ultimately related in one way or other to the inhomogeneous wave equation with inhomogeneous boundary conditions, having the form

$$\frac{1}{\bar{a}^2}\frac{\partial^2 p'}{\partial t^2} - \nabla^2 p' = -h \quad , \tag{12.1}$$

$$\hat{n} \cdot \nabla p' = -f \quad . \tag{12.2}$$

For the formulation given earlier, h stands for the sum of h_μ and the linear part of h_v in eq. (3.8); f represents f_s, f_μ and the linear part of f_v in (3.9).

The linear stability of normal modes is studied by assuming that p' has the form

$$p'(\vec{r}, t) = \hat{p}(\vec{r}) e^{i\bar{a}kt} \quad , \tag{12.3}$$

and the problem comes down to determining the mode shape $\hat{p}(\vec{r})$ and the complex wave number k :

$$k = \frac{1}{\bar{a}}(\omega - i\alpha_n) \tag{12.4}$$

where α_n is the growth constant for the perturbed n^{th} mode. Because h and f are linear in perturbations (they both contain the velocity $\vec{u}'$ as well as p'), they may be written in the form

$$h(r, t) = \hat{h}(\vec{r}) e^{i\bar{a}kt} \quad , \quad f(\vec{r}, t) = \hat{f} e^{i\bar{a}kt} \quad . \tag{12.5}$$

Then (12.1) and (12.2) become

$$\nabla^2 \hat{p} + k^2 \hat{p} = h \tag{12.6a}$$

$$\hat{n} \cdot \nabla \hat{p} = -\hat{f} \tag{12.6b}$$

The functions $\hat{h}$ and $\hat{f}$ are of first order in the Mach number of the mean flow, assumed to be small. It is then a relatively simple matter to deduce a formula for k^2, valid to first order in the Mach number (Culick 1975, for example):

$$k^2 = k_n^2 + \frac{1}{E_n^2}\left\{\int \psi_n \hat{h}\, dV + \oiint \psi_n \hat{f}\, dS\right\} \tag{12.7}$$

Equation (12.7) is based on an iterative procedure; this first approximation requires substitution of the unperturbed mode shape (ψ_n) for the acoustic quantities appearing in $\hat{h}$ and $\hat{f}$.

Because $\alpha_n/\omega \ll 1$, the real and imaginary parts of (12.7) can be written

$$\omega^2 - \omega_n^2 = \frac{\bar{a}^2}{p_o E_n^2}\, \mathrm{Re}\left\{\int \psi_n \hat{h}\, dV + \oiint \psi_n \hat{f}\, dS\right\} . \tag{12.8}$$

$$\alpha_n = -\frac{\bar{a}^2}{2p_o \omega E_n^2}\, \mathrm{Im}\left\{\int \psi_n \hat{h}\, dV + \oiint \psi_n \hat{f}\, dS\right\} . \tag{12.9}$$

It is helpful to make the discussion more specific by considering only one term for a specific problem. For this purpose, the contribution from surface combustion in a cylindrical motor serves quite nicely. Then according to eq. (3.4),

$$f = \rho_o \frac{\partial \vec{u}'}{\partial t} \cdot \hat{n} , \tag{12.10}$$

so

$$\hat{f} = i\bar{a}k\rho_o \hat{\vec{u}} \cdot \hat{n} . \tag{12.11}$$

Then with the definitions introduced in § 7.6, and if non-isentropic temperature fluctuations are ignored, (12.11) can be expressed in terms of the response function:

$$\hat{f} = -i\bar{a}k\rho_o \bar{u}_b \left(R_b^{(r)} + iR_b^{(i)}\right) \frac{\hat{p}}{p_o} . \tag{12.12}$$

Substitution into (12.8) and (12.9) gives

$$\omega^2 - \omega_n^2 = \gamma \bar{u}_b \left(\frac{2}{R_c}\right)(2\omega_n) R_b^{(i)} , \tag{12.13}$$

$$\alpha_n = \gamma \bar{u}_b \left(\frac{2}{R_c} \right) R_b^{(r)} \qquad (12.14)$$

Now because it is a requirement, in order for the calculation to be valid, that the perturbations be small, ω must not differ much from ω_n, so (12.13) can be written

$$\delta\omega_n = \omega - \omega_n \approx \gamma \bar{u}_b \left(\frac{2}{R_c} \right) R_b \quad . \qquad (12.15)$$

More generally, (12.8) gives

$$-\theta_n = \frac{\omega^2 - \omega_n^2}{2\omega_n} \approx \omega - \omega_n \approx \frac{\bar{a}^2}{2 p_o \omega_n E_n^2} \mathrm{Re}\left\{ \int \psi_n \hat{h}\, dV + \oint\!\!\!\oint \psi_n f\, dS \right\} \quad . \qquad (12.16)$$

For most work in the past dealing with combustion instability, the frequency shift due to perturbations has been ignored. It is normally too small to be distinguished in experimental work. However, it happens, as the example in § 11.2 suggests, that the nonlinear behavior -- in particular the limiting amplitude -- may be quite sensitive to those characteristics which cause a linear frequency shift. The reason is that the phase relationships between the various harmonics are affected.

The formal connection between the linear stability analysis and the nonlinear analysis based on the method of averaging may be seen most quickly by comparing eqs. (12.14) and (12.13) or (12.15) with eqs. (7.9) and (7.10), which for a cylindrical grain become (11.4) and (11.5). For this special case, the values of α_n are the same, and

$$\theta_n = -\delta\omega_n \quad . \qquad (12.17)$$

The fact that the linear coefficient θ_n is the negative of the frequency shift can be shown quite easily by starting with the definition of η_n:

$$\eta_n = G_n \sin(\omega_n t + \phi_n) = A_n \sin(\omega_n t) + B_n \cos(\omega_n t) \quad . \qquad (12.18)$$

The frequency of the actual wave (i.e., when perturbed from the mode

having frequency ω_n) is

$$\omega = \frac{d}{dt}(\omega_n t + \phi_n) = \omega_n + \dot{\phi}_n \ ,$$

so

$$\delta\omega_n = \dot{\phi}_n \quad . \tag{12.19}$$

Now $\tan\phi_n = B_n/A_n$, and differentiation with respect to time gives

$$\dot{\phi}_n = \frac{B_n}{A_n}\left(\frac{\dot{B}_n}{B_n} - \frac{\dot{A}_n}{A_n}\right)\frac{A_n^2}{A_n^2+B_n^2} \quad . \tag{12.20}$$

The linear parts of the equations for A_n and B_n are, from (4.18) and (4.19),

$$\frac{dA_n}{dt} = \alpha_n A_n + \theta_n B_n \ , \tag{12.21a}$$

$$\frac{dB_n}{dt} = \alpha_n B_n - \theta_n A_n \quad . \tag{12.21b}$$

From these it follows that

$$\frac{\dot{B}_n}{B_n} - \frac{\dot{A}_n}{A_n} = -\theta_n\left(\frac{A_n^2+B_n^2}{A_n B_n}\right) \ ,$$

and substitution into (12.20) gives the result

$$\delta\omega_n = \dot{\phi}_n = -\theta_n \ . \tag{12.22}$$

This relation has been referred to in § 8; numerical results for the shift of frequency (or dispersion) associated with gas/particle interactions are given in Table 8-1.

The main point here is that numerical results obtained with the approximate nonlinear analysis have shown that the nonlinear behavior may be quite sensitive to the quantity $\theta_n = -\delta\omega_n$, which has largely been ignored in linear stability analysis.

It should be clear that the relation $\theta_n = -\delta\omega_n$ is true in general, and not just a special result for surface combustion. This can be seen di-

rectly by returning to eq. (3.15) for η_n, and retaining only the linear terms incorporated in h and f used above:

$$\ddot{\eta}_n + \omega_n^2 \eta_n = -\frac{\bar{a}^2}{p_o E_n^2} \{ \int \psi_n h dV + \iint \psi_n f dS \} \quad . \tag{12.23}$$

For harmonic motions, $\eta_n = \hat{\eta}_n \exp(i\bar{a}kt)$ and because both $\hat{h}$ and $\hat{f}$ are proportional to $\hat{\eta}_n$, the factor can be dropped, so that (12.18) becomes

$$-(\omega - i\alpha)^2 + \omega_n^2 = -\frac{\bar{a}^2}{p_o E_n^2} \{ \int \psi \hat{h} dV + \iint \psi_n \hat{f} dS \} \quad .$$

The real and imaginary parts are once again (12.8) and (12.9)

When the method of averaging is applied to (12.18), the right hand side is expressed as a combination of terms depending on η_i or $\dot{\eta}_i$, eqns. (4.1) and (4.2); with only the linear terms retained, (12.18) is

$$\ddot{\eta}_n + \omega_n^2 \eta_n = -D_{nn}\dot{\eta}_n - E_{nn}\eta_n - \sum_{i \neq n} [D_{ni}\dot{\eta}_i + E_{ni}\eta_i] \quad . \tag{12.24}$$

The analysis developed in §4 leads to the first order differential equations (4.18) and (4.19) for A_n and B_n. Those equations show that in general there are terms representing linear coupling between the modes providing, of course, that the coefficients E_{ni}, E_{ni} don't vanish. These terms do not arise in the usual linear stability analysis because the restriction is enforced from the beginning that the motion consists only of a wave having a single frequency. If all the D_{ni} and E_{ni} are zero, or for the case of longitudinal modes, the equations for the A_n and B_n are eventually found to be (12.21a, b), with

$$\alpha_n = -\frac{D_{nn}}{2} \quad , \quad \theta_n = -\frac{E_{nn}}{2} \quad . \tag{12.25}$$

The only remaining point to establish is that the α_n and θ_n are the same as defined by eqns. (12.9) and (12.16). This is easily shown in

special cases. To see that the equalities are true in general, begin with the two expressions (12.23) and (12.24) for the right hand sides, and $D_{ni} = E_{ni} = 0$:

$$D_{nn}\dot{\eta}_n + E_{nn}\eta_n = \frac{\bar{a}^2}{p_o E_n^2}\left\{\int \psi_n h dV + \iint \psi_n f dS\right\} . \qquad (12.26)$$

Now the same argument is used for the left hand side of (12.26) as that introduced first in the paragraph preceding eq. (7.7). Namely, the approximation is made for harmonic motions, $\dot{\eta}_n \approx i\omega_n \eta_n$. Put another way, because the D_{nn}, E_{nn} are already small quantities, and real, then for harmonic motions,

$$D_{nn}\dot{\eta}_n \approx i\omega_n D_{nn}\hat{\eta}_n e^{i\omega_n t} .$$

The real and imaginary parts of (12.26) are then

$$D_{nn} \approx \frac{\bar{a}^2}{p_o \omega_n E_n^2}\, \mathrm{Im}\left\{\int \psi_n \hat{h} dV + \iint \psi_n \hat{f} dS\right\} , \qquad (12.27)$$

$$E_{nn} \approx -\frac{\bar{a}^2}{p_o E_n^2}\, \mathrm{Re}\left\{\int \psi_n \hat{h} dV + \iint \psi_n \hat{f} dS\right\} . \qquad (12.28)$$

Comparison with (12.8) and (12.16) shows immediately that $\alpha_n = -D_{nn}/2$ and $\theta_n = -E_{nn}/2\omega_n$ as required.

12.2 Remarks on the Behavior of Solutions Obtained with the Approximate Nonlinear Analysis

For the example given in §11.1, in which all amplitudes reach limiting values, the functions $A_n(t)$ and $B_n(t)$ both oscillate, with the same amplitude and a phase difference of $\pi/2$ after the limit condition has been reached. This sort of behavior has been most commonly found in cases for which the motion eventually executes a limit cycle. There are examples, as shown below, in which the A_n and B_n as well as the amplitudes

$\sqrt{A_n^2+B_n^2}$ tend in the limit to constant values. If a limit cycle does not exist, there seems to be a wide variety of possible behavior. One example has been given in §11.2; several more will be included in this section.

According to the discussion in §12.1, the linear behavior of the functions $A_n(t)$ and $B_n(t)$ is oscillatory with exponential growth or decay. The frequency of the oscillation is θ_n, the negative shift of the normal frequency ω_n. To see this explicitly, note that by definition,

$$\begin{aligned} A_n(t) &= G_n \cos \phi_n \\ B_n(t) &= G_n \sin \phi_n \end{aligned} \tag{12.29}$$

According to (12.22), $\dot{\phi}_n = -\theta_n$, so ϕ_n is a constant minus $\theta_n t$. Hence, A_n and B_n both oscillate at the frequency θ_n. Another way of establishing this result, and at the same time incorporating the nonlinear influences, may be had by combining the equations for A_n and B_n; write these in the form

$$\frac{dA_n}{dt} = \alpha_n A_n + \theta_n B_n + f_n \tag{12.30}$$

$$\frac{dB_n}{dt} = \alpha_n B_n - \theta_n B_n + g_n \tag{12.31}$$

where f_n, g_n stand for nonlinear terms and, in the general case, for linear coupling terms as well.

Differentiate (12.30) with respect to time and then use the two equations to eliminate B_n and $\dot{B}_n$. A similar procedure can be applied to (12.31). The two second-order equations for A_n and B_n are produced:

$$\frac{d^2A_n}{dt^2} - 2\alpha_n \frac{dA_n}{dt} + (\alpha_n^2+\theta_n^2)A_n = \dot{f}_n - \alpha_n f_n + \theta_n g_n , \tag{12.32}$$

$$\frac{d^2B_n}{dt^2} - 2\alpha_n \frac{dB_n}{dt} + (\alpha_n^2+\theta_n^2)B_n = \dot{g}_n - \alpha_n g_n - \theta_n f_n . \tag{12.33}$$

These equations represent two coupled nonlinear oscillators associated with each of the normal modes. The homogeneous solutions for the linear operators are

$$A_n, B_n \sim e^{\alpha_n t} e^{i\theta_n t}, \tag{12.34}$$

so that for an unstable mode, the A_n, B_n exhibit oscillatory growth or decay. For cases in which the amplitudes A_n, B_n show the limiting behavior noted above, the nonlinear terms on the right hand side must be taken into account. If they have relatively small influence on the frequency, then in the limit cycle, both A_n and B_n oscillate with frequency θ_n, the negative of the frequency shift of the frequency for the primary oscillators represented by the η_n.

But if the motion does go into a limit cycle, the nonlinear terms on the right hand sides of (12.32) and (12.33) must have some influence. A purely oscillatory behavior would be produced by (12.32) if the term $-2\alpha_n \dot{A}_n$ is exactly compensated and if the remainder of the right hand side contributes a term proportional to $\dot{A}_n$. It would be interesting and quite likely very useful to determine the general conditions under which solutions of that type do or do not exist.

Equation (12.34) shows that if $\theta_n = 0$, the functions A_n and B_n do not oscillate when the motion is linear. There are cases in which that behavior persists when nonlinear influences are accounted for (see case (ii) below); and there are conditions under which the A_n and B_n are not purely oscillatory even though $\theta_n \neq 0$ (case (iii) below). Again, quantitative generalizations would probably be very useful for practical applications.

One way of attacking this problem would be to use the method of averaging to solve (12.32) and (12.33). This would not give general results

covering all possibilities, but it might yield information at least in respect to the conditions for oscillatory behavior of $A_n(t)$ and $B_n(t)$.

No formal results have been obtained for the general behavior of the solutions. The practical importance of pursuing the problem lies in the possibility for defining the ranges of values of the linear coefficients, α_n and θ_n, for which limit cycles exist; and for determining the dependence of the limit amplitudes on those parameters.

In the absence of general results, the problem has been studied in a very modest way simply by carrying out calculations for special cases. Seven examples are included here; the values of α_n and θ_n are listed in Table 12-1. Case (i) has been chosen as the reference because it exhibits the relatively nice oscillatory behavior of the functions $A_n(t)$ and $B_n(t)$. For each case, the results are shown for the amplitudes and for the $A_n(t)$; the $B_n(t)$ behave qualitatively like the $A_n(t)$ in all cases. The calculations were done for five modes, but to make the figures a bit less crowded, only the curves for the first three modes are shown in Figures 12-4 to 12-7.

Note that in the reference case, Figure 12-1, the first mode is unstable and all higher modes are rather heavily damped with $\alpha_n = -100\ \text{sec}^{-1}$. Case (ii), Figure 12-2, shows the change to non-oscillatory growth of the $A_n(t)$ when $\theta_n = 0$. Cases (iii) through (vi), Figures 12-3 to 12-6, show the influence of making each of the higher modes neutrally stable. The results reflect at least partly the strength of the coupling between the first and each of the higher modes. Evidently the higher odd modes are more strongly coupled to the fundamental than are the higher even modes. With α_3 or α_5 equal to zero, the motions grow without limit; but when α_2 or α_4 are zero, the motion does reach limit cycles, although they differ in detail. Even the qualitative aspects are not obvious from the equations

(6.16) - (6.20) which have been solved.

Figure 12-7 for case (vii) is included as an illustration of somewhat more erratic behavior which often ensues if more than one mode is unstable. Still more extreme cases have been encountered, but nothing can be accomplished by mustering all the results which have been obtained.

TABLE 12-1. Values of α_n and θ_n for Figures 12-1 to 12-7.

Case	α_1	α_2	α_3	α_4	α_5	θ_1	θ_2	θ_3	θ_4	θ_5
(i)	16	-100	-100	-100	-100	-16	-50	-50	-50	-50
(ii)	16	-100	-100	-100	-100	0	0	0	0	0
(iii)	16	0	-100	-100	-100	-16	-50	-50	-50	-50
(iv)	16	-100	0	-100	-100	-16	-50	-50	-50	-50
(v)	16	-100	-100	0	-100	-16	-50	-50	-50	-50
(vi)	16	-100	-100	-100	0	-16	-50	-50	-50	-50
(vii)	16	0	16	-100	-100	-16	-50	-50	-50	-50

For all cases: f = 800 Hz

$$\beta = \left(\frac{\bar{\gamma} + 1}{8\bar{\gamma}}\right) \omega_1 = 1140 \text{ sec}^{-1}$$

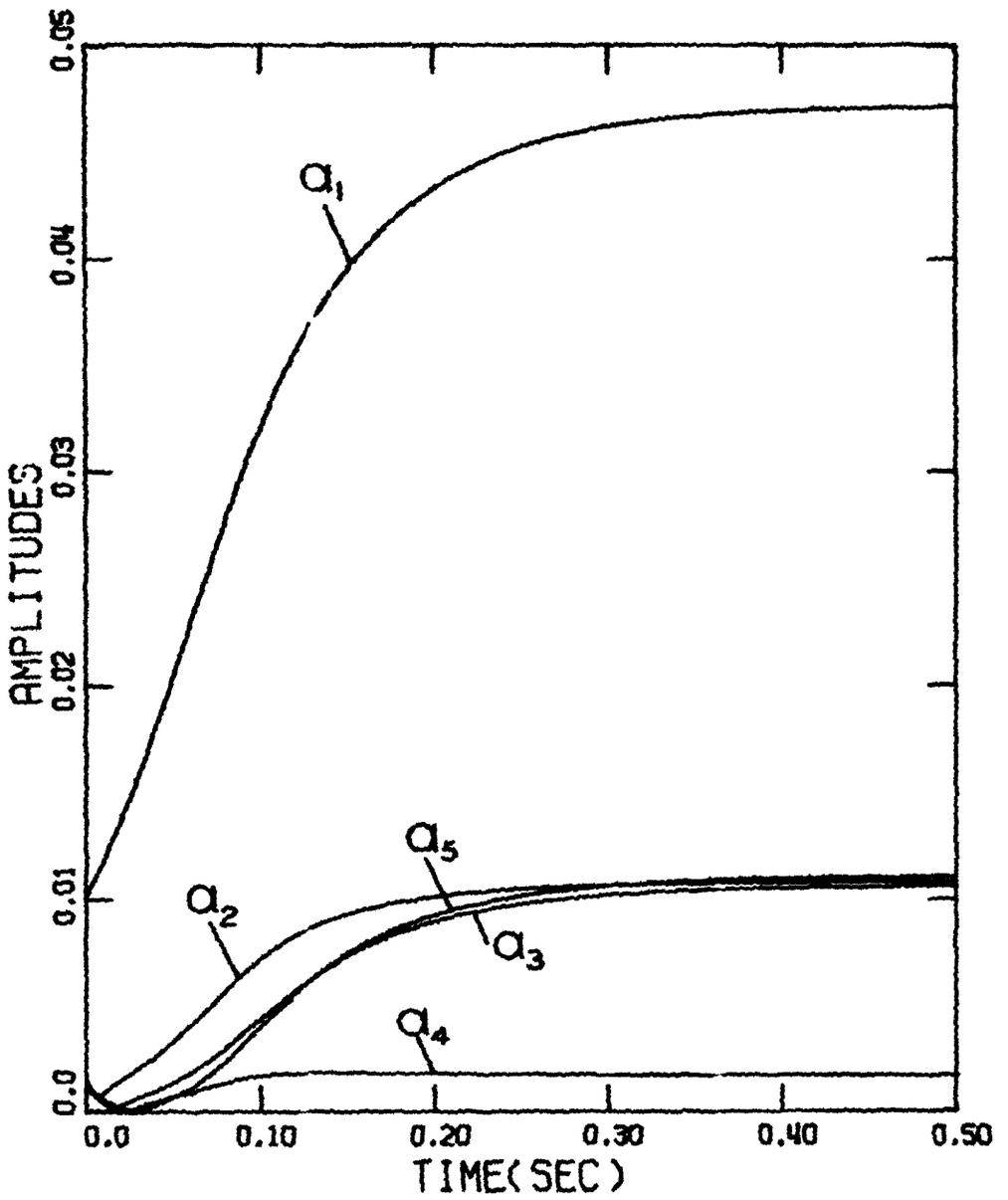

Fig. 12-2(a) Amplitudes for case (ii); values of α_n same as for case (i) but θ_n 0 for all modes.

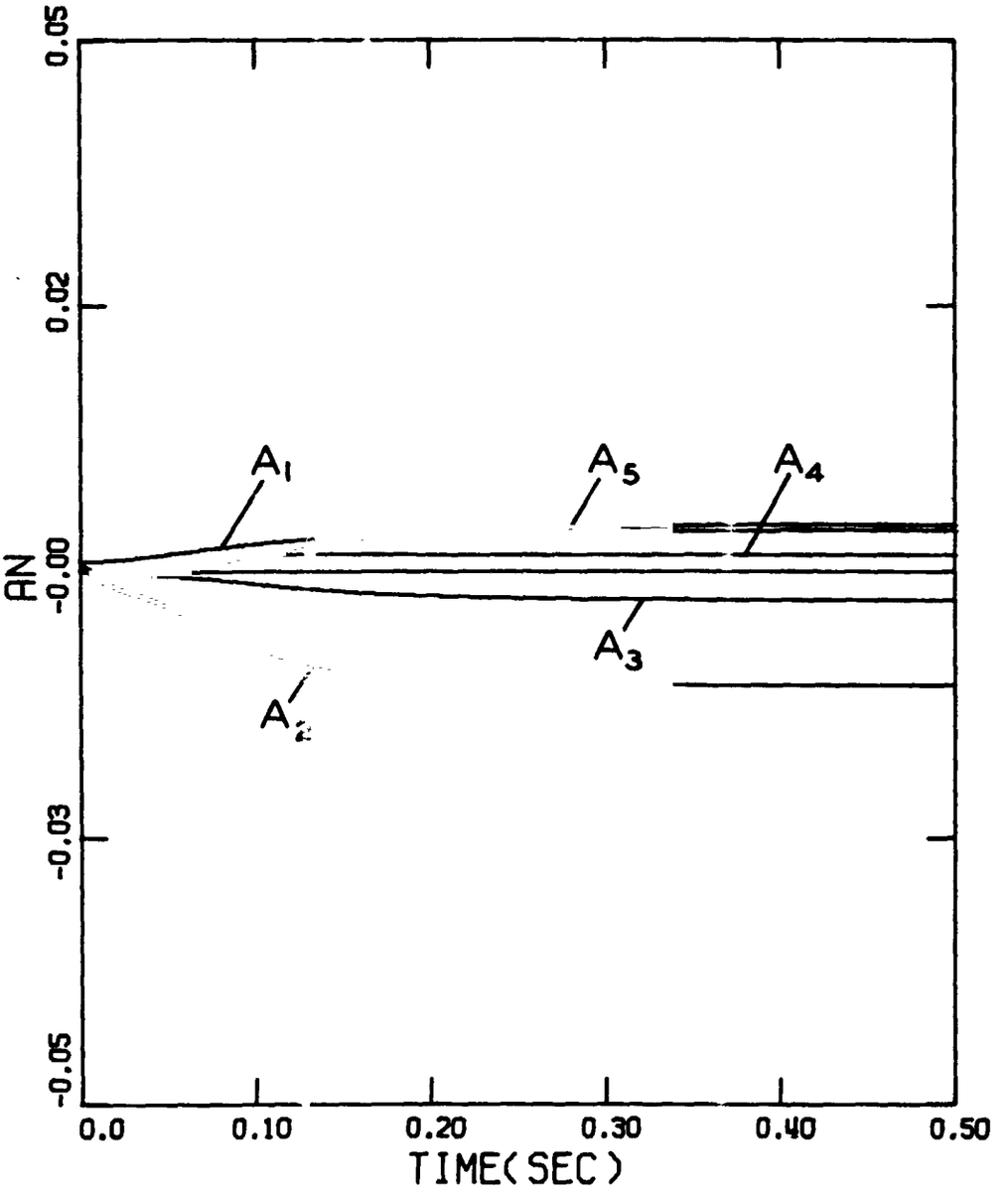

Fig. 12-2(b) The functions $A_n(t)$ for case (ii).

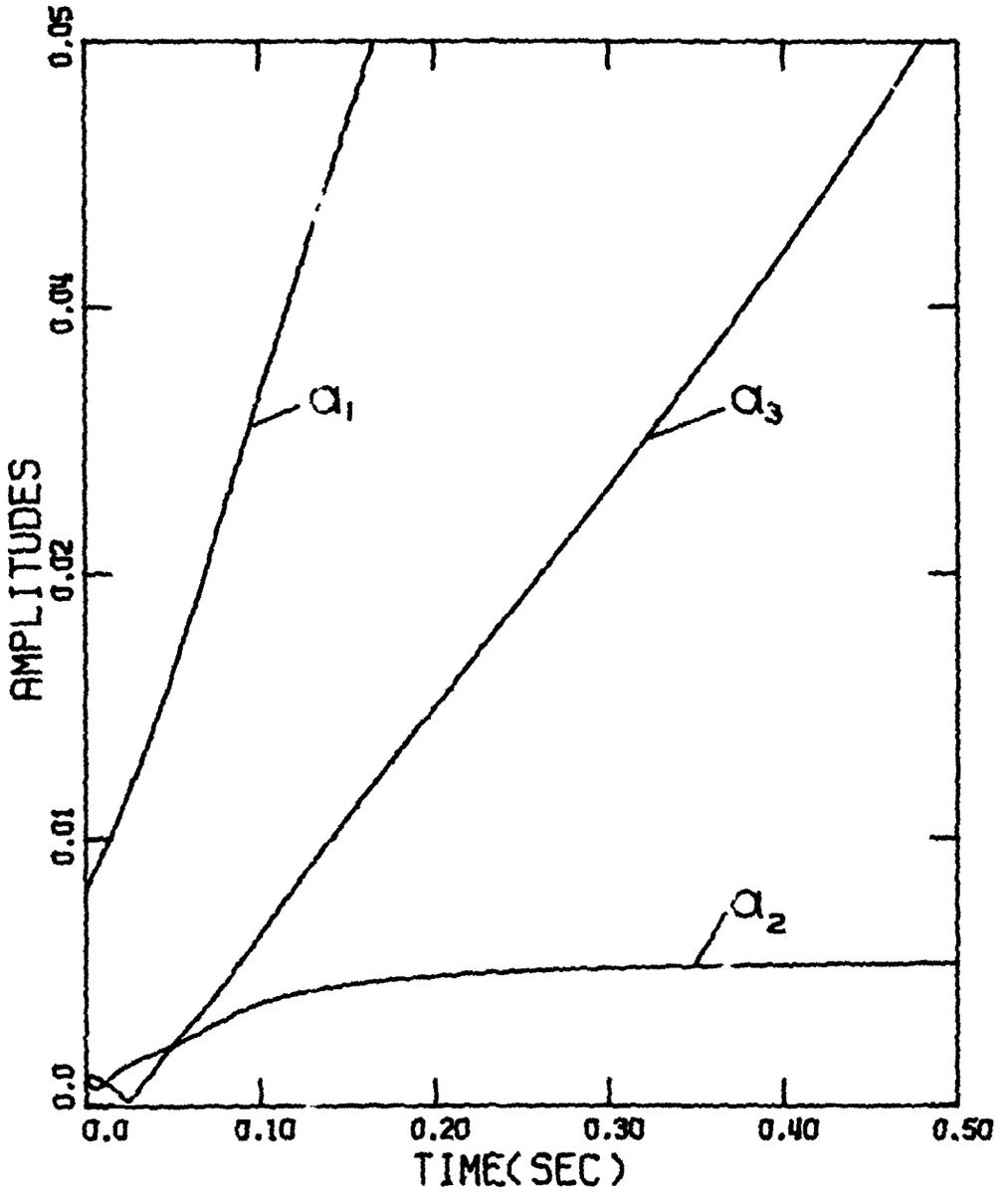

Fig. 12-4(a) Amplitudes for case (iv); values of θ_n and α_n same as case (i), except $\alpha_3 = 0$.

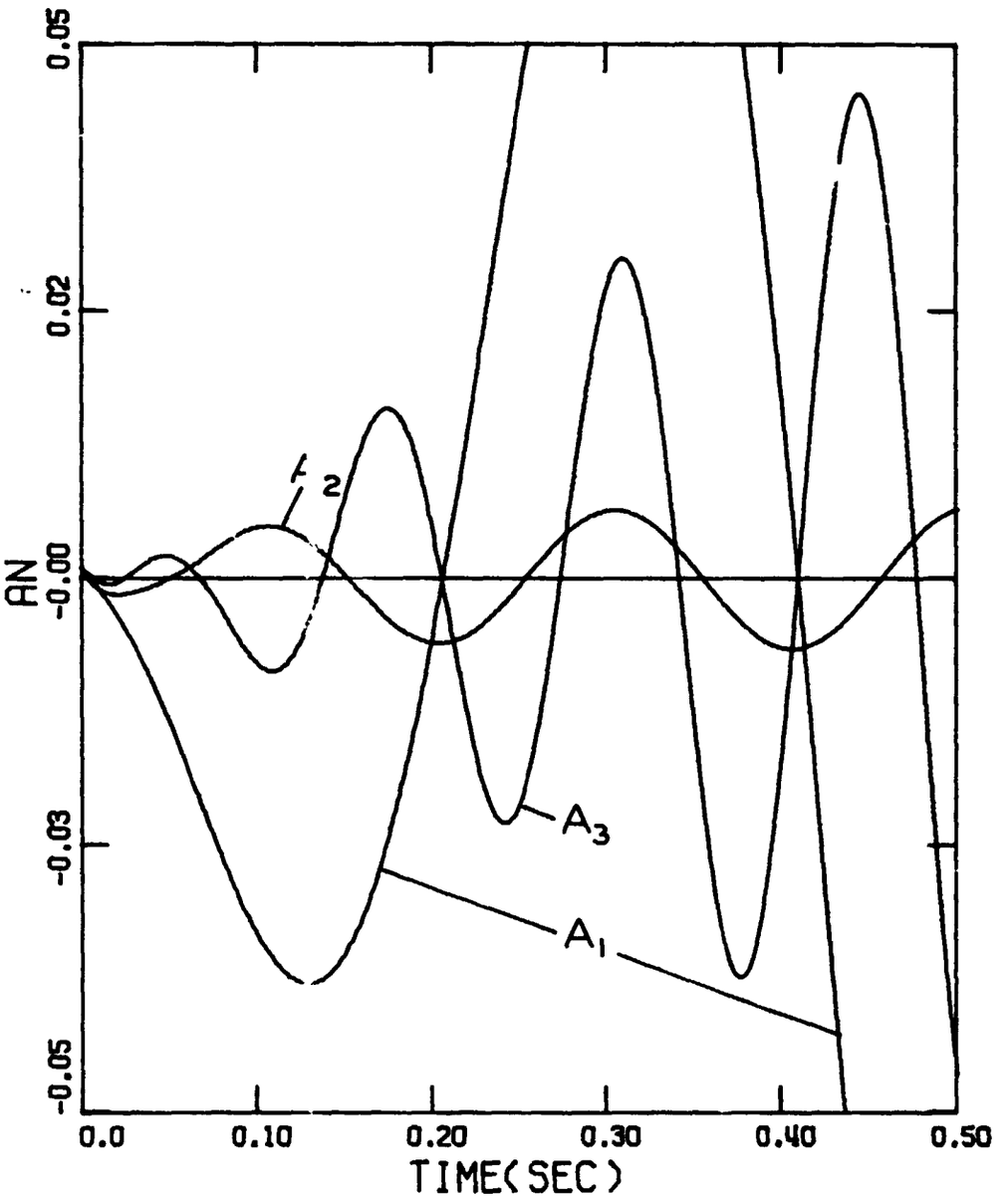

Fig. 12-4(b) The functions $A_n(t)$ for case (iv).

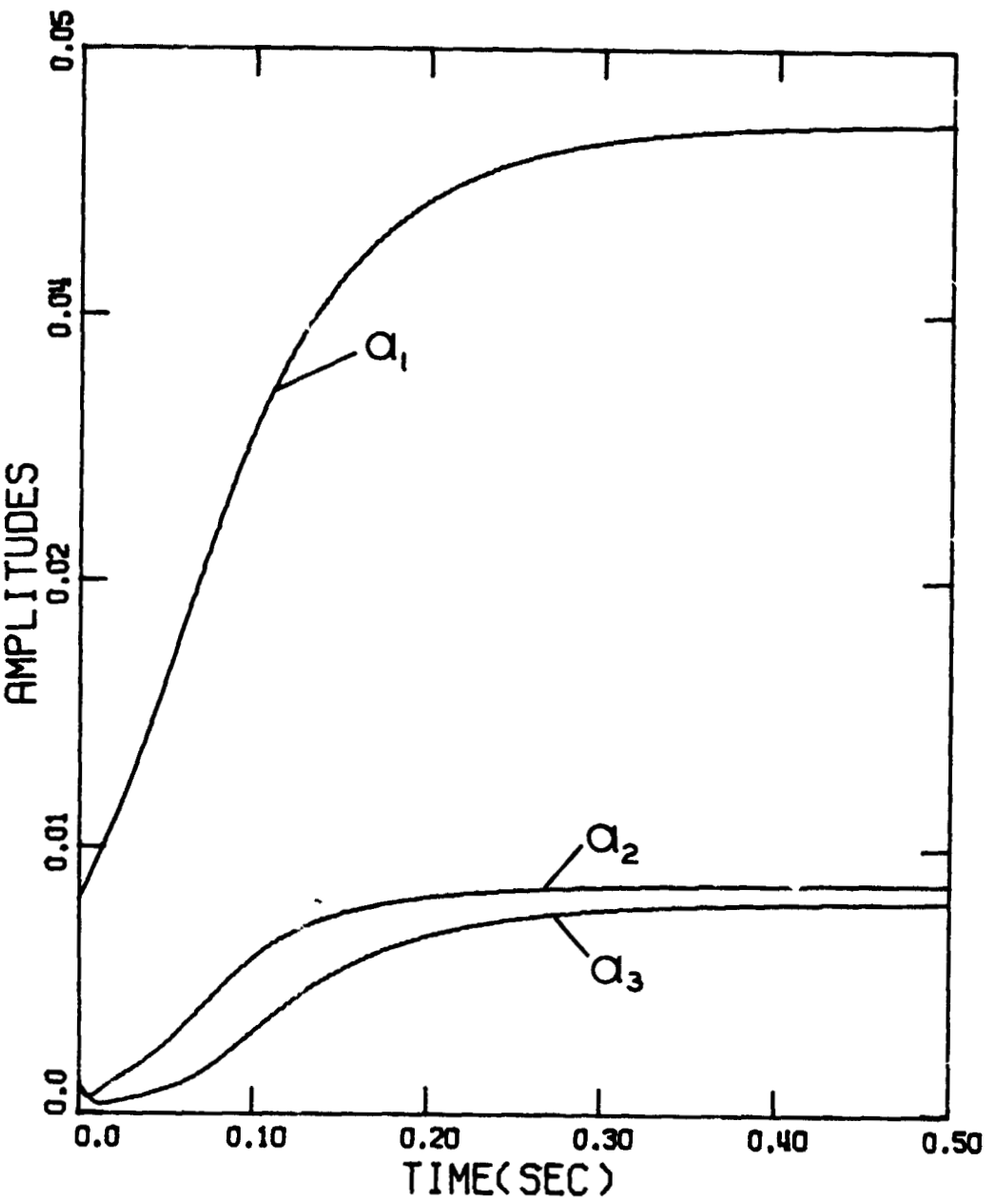

Fig. 12-5(a) Amplitudes for case (v); values of θ_n and α_n same as for case (i) except $\alpha_4 = 0$.

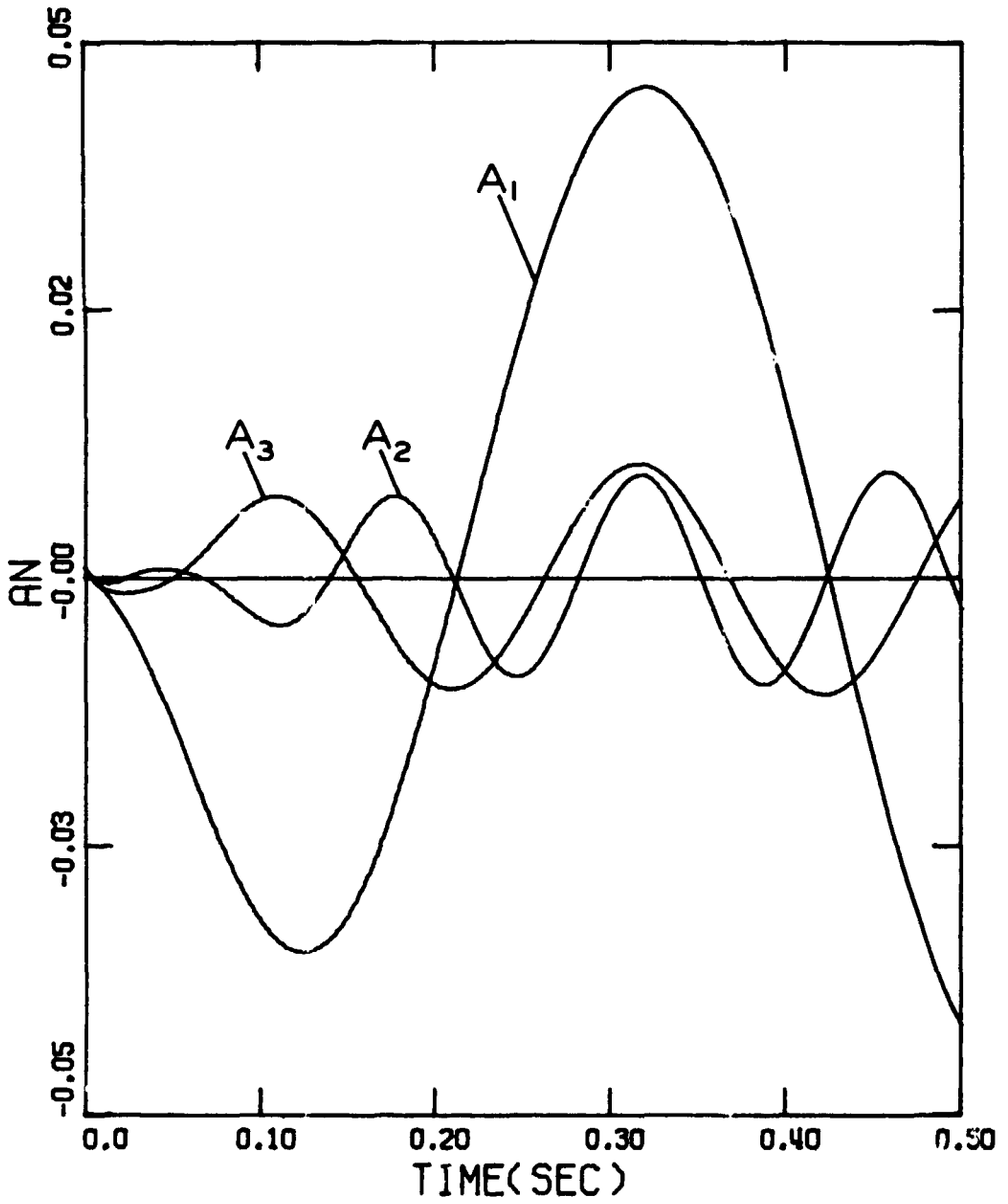

Fig. 12-5(b) The functions $A_n(t)$ for case (vi).

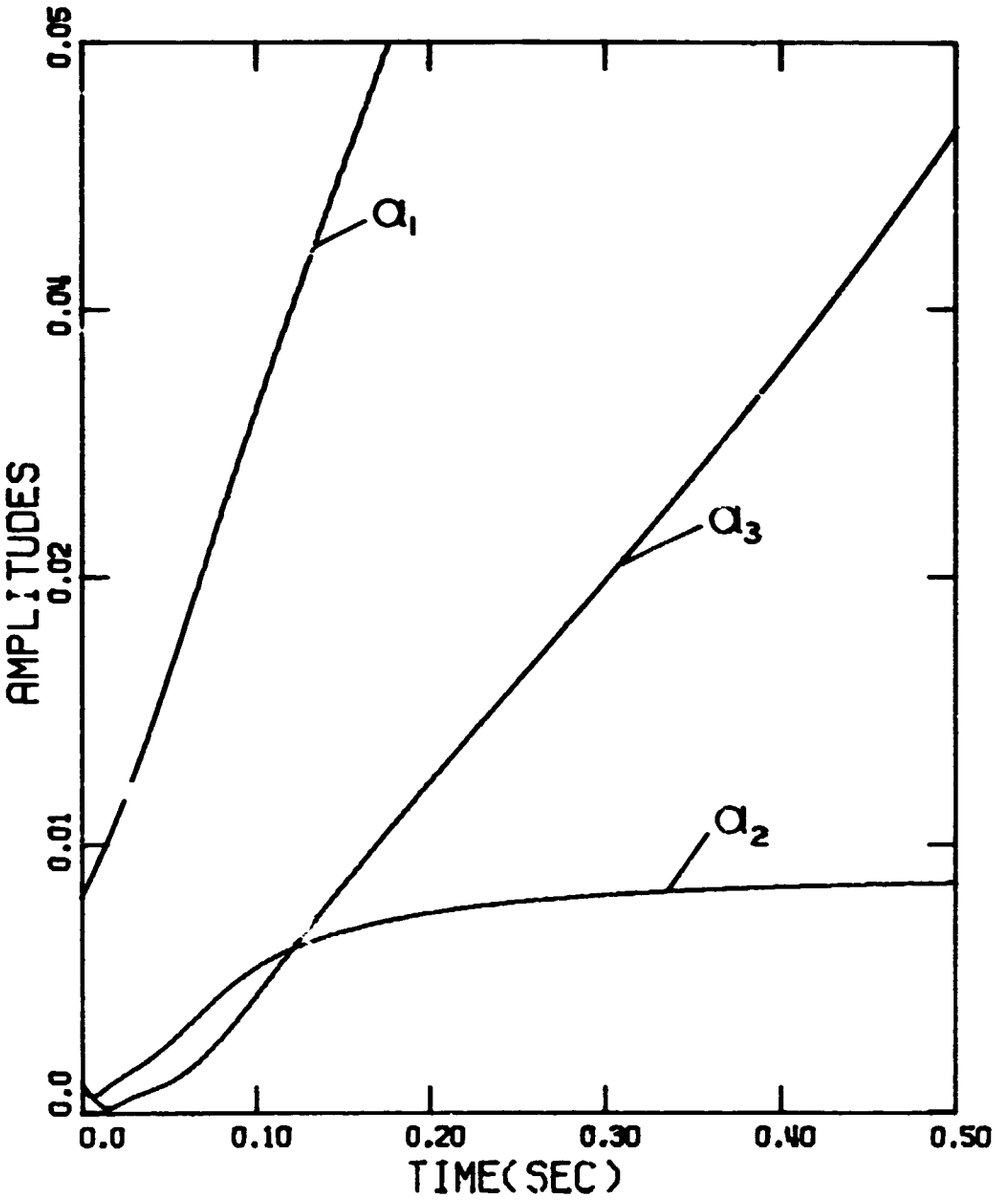

Fig. 12-6(a) Amplitudes for case (vi); values of θ_n and α_n same as case (i) except $\alpha_5 = 0$.

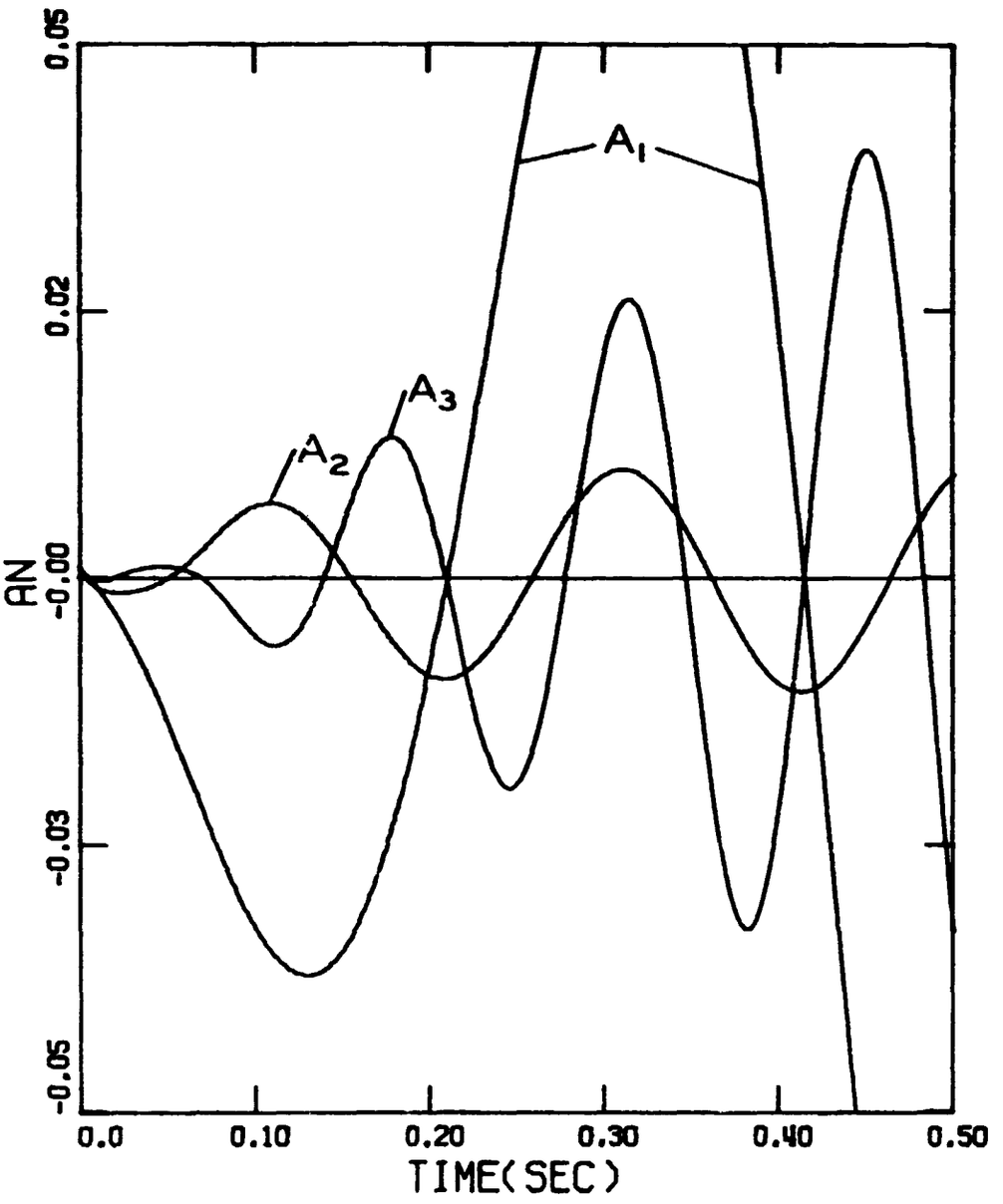

Fig. 12-6(b) The functions $A_n(t)$ for case (vi).

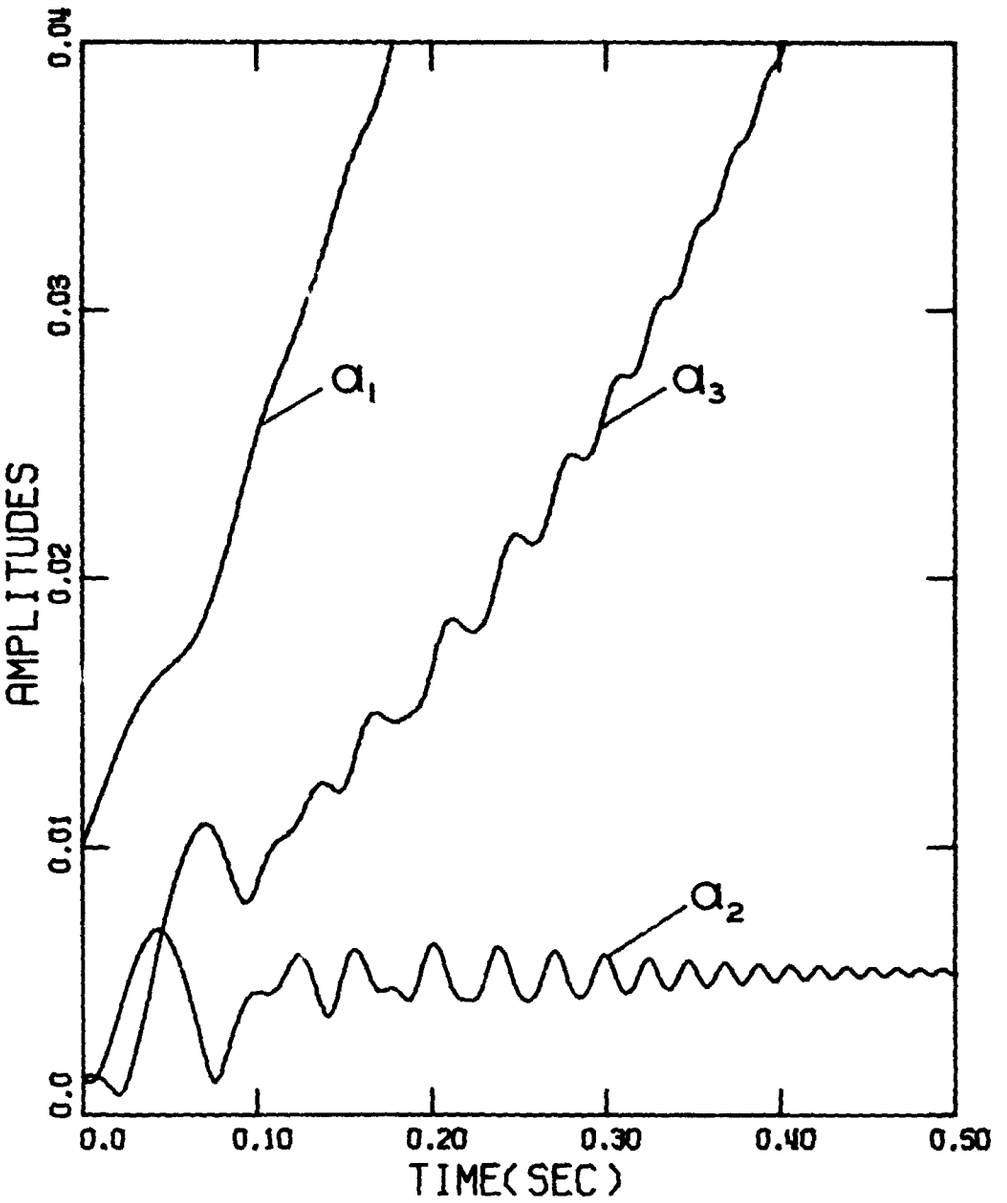

Fig. 12-7(a) Amplitudes for case (vii); values of θ_n and α_n same as for case (i) except $\alpha_2 = 0$ and $\alpha_3 = 16$.

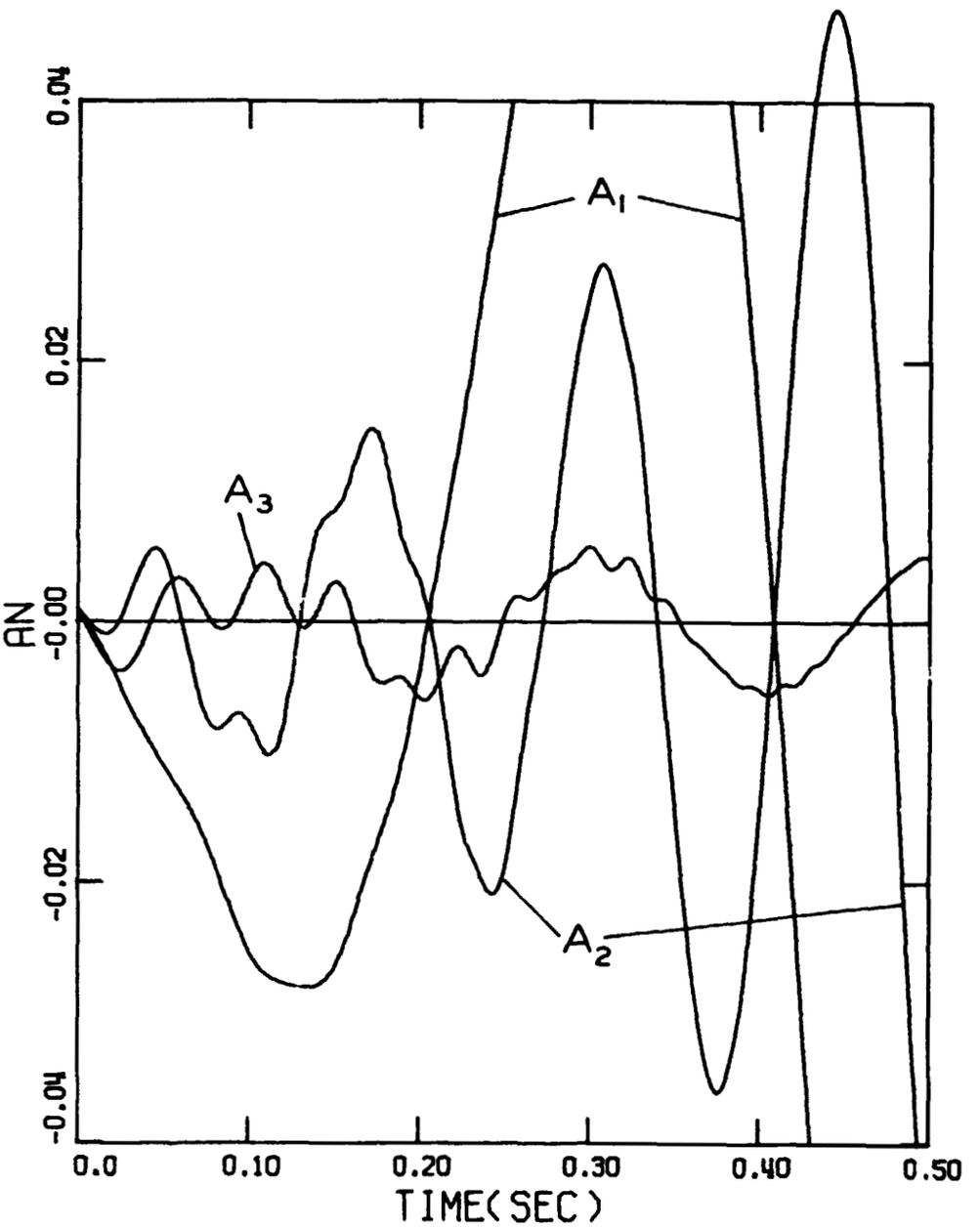

Fig. 12-7(b) The Functions $A_n(t)$ for case (vii).

REFERENCES

Bogoliubov, N. N. and Mitropolsky, Yu. A. (1961) Asymptotic Methods in the Theory of Nonlinear Oscillations, Hindustan Publishing Co., Delhi, India.

Chester, W. (1964) "Resonant Oscillations in Closed Tubes," J. Fluid Mechanics, V. 18, p. 44.

Culick, F. E. C. (1971) "Nonlinear Growth and Limiting Amplitude of Acoustic Waves in Combustion Chambers," Comb. Sci. and Tech., V. 3, no. 1, p. 16.

Culick, F. E. C. (1973) "Stability of One-Dimensional Motion in a Rocket Motor," Comb. Sci. and Tech., V. 7, no. 4, p. 165.

Culick, F. E. C. (1975) "Stability of Three-Dimensional Motions in a Combustion Chamber," Comb. Sci. and Tech. (in press).

Culick, F. E. C. and Kumar, R. N. (1974) "Combustion Instability in Large Solid Rocket Motors," 10th JANNAF Combustion Meeting, Newport, Rhode Island.

Culick, F. E. C. and Levine, J. N. (1974) "Comparison of Approximate and Numerical Analyses of Nonlinear Combustion Instability," AIAA 12th Aerospace Sciences Meeting, Washington, D. C. AIAA Paper No. 74-201.

Krylov, N. and Bobollubov, N. (1947) Introduction to Nonlinear Mechanics, Princeton University Press, Princeton, N. J.

Levine, J. N. and Culick, F. E. C. (1972) "Numerical Analysis of Nonlinear Longitudinal Combustion Instability in Metallized Propellant Solid Rocket Motors," Ultrasystems, Inc., Irvine, Calif. Technical Report AFRPL-TR-72-88.

Levine, J. N. and Culick, F. E. C. (1974) "Nonlinear Analysis of Solid Rocket Combustion Instability," Ultrasystems, Inc., Irvine, Calif. Technical Report AFRPL-74-45.

Lores, M. E. and Zinn, B. T. (1973) "Nonlinear Combustion Instability in Rocket Motors," AIAA 11th Aerospace Sciences Meeting, Washington, D. C. AIAA Paper No. 73-217.

Perry, E. H. and Culick, F. E. C. (1974) "Measurement of Wall Heat Transfer in the Presence of Large-Amplitude Combustion-Driven Oscillations," Comb. Sci. and Tech., V. 9, p. 49.

Zinn, B. T. and Powell, E. A. (1970) "Application of the Galerkin Method in the Solution of Combustion-Instability Problems," XIXth International Astronautical Congress, V. 3. Propulsion Re-Entry Physics, Pergamon Press.